



TÉCNICO
LISBOA

Development of a Cost Model for Novel Aircraft Configurations

Pedro Miguel Panão Carvalho

Thesis to obtain the Master of Science Degree in

Aerospace Engineering

Supervisors: Prof. Inês Esteves Ribeiro
Dr. Frederico José Prata Rente Reis Afonso

Examination Committee

Chairperson: Prof. Filipe Szolnoky Ramos Pinto Cunha
Supervisor: Prof. Inês Esteves Ribeiro
Members of the Committee: Dr. Bruno Alexandre Rodrigues Simões Soares
Prof. Paulo Miguel Nogueira Peças

July 2018

Acknowledgments

Firstly, I would like to acknowledge my supervisors, Prof. Inês Esteves Ribeiro, Dr. Frederico Afonso and Prof. Fernando Lau, of Técnico Lisboa at Universidade de Lisboa, who gave me the pleasure to work in this master thesis, for all their support, either in research or writing, and for always guiding me through the work. I would also like to thank them for all the knowledge shared with me and the motivation and enthusiasm showed about my work.

Furthermore, I would also want to express my gratitude to Dr. Bruno Soares for all the support and experienced advices, and for the availability to answer all my questions.

To all my family, especially my mother and sister, I would like to thank them very much for all the love and support over this period, for their belief in me and for kept me going through the most difficult times. A special acknowledgement to my father who always encouraged me to achieve more, and unfortunately is not able to physically see me conclude this journey. I hope you are proud.

Finally, I would like to thank my friends, who have shown me great friendship and support since the beginning. Thank you Conversa de Café, Risco ao Meio, Agrupamento 1224 - Marinha das Ondas, Francisco, Isabel, Rodrigo, João, Tiago, Pedro e Afonso, for keep challenging me and making me happy.

Resumo

No sector aeroespacial existe uma crescente procura de novas configurações e de novos materiais para aeronaves. A configuração mais utilizada actualmente encontra-se numa fase em que apenas pequenas melhorias podem ser realizadas. Além disso, os materiais compósitos são cada vez mais procurados como substitutos do alumínio, verificando-se um aumento da sua implementação neste sector.

O desenvolvimento de novas configurações é então uma realidade necessária, assim como uma estimativa de custos numa fase preliminar do design das mesmas, para que possam ser tomadas decisões sobre a viabilidade financeira do investimento. Aquando do desenvolvimento de uma aeronave convencional, os parâmetros utilizados na sua estimativa de custos provém de dados históricos. No caso de novas configurações, estes parâmetros não existem, havendo necessidade de um novo método para se estimar os custos.

Assim, desenvolve-se um modelo de custos baseado no processo de produção ATL (Automated Tape Laying) para diferentes configurações de aeronaves, capaz de estimar os custos de produção, tendo por dados de entrada a geometria das peças. Pode ainda adaptar-se o modelo a diferentes volumes de produção anuais ou à capacidade do número de máquinas existentes numa fábrica.

Nesta tese são ainda analisados casos de estudo relativamente à fase de produção e aquisição de uma aeronave convencional e de um joined wing. Os custos de produção de ambas as aeronaves são obtidos pelo modelo acima referido e, posteriormente, comparados entre si. Estes dados são ainda utilizados numa análise de sensibilidade relativamente à quantidade de material e numa análise de investimentos.

Palavras-chave: Modelo de custo, ATL, Materiais compósitos, Custos de produção, Novas configurações de aeronaves

Abstract

In the aerospace sector there is a growing demand for new aircraft configurations and new materials. Nowadays, only minor improvements can be made to the most used aircraft configuration. Moreover, composite materials are increasingly sought after as substitutes for aluminium and, therefore, their implementation in this sector is growing.

Consequently, the development of novel configurations is a necessary reality, as well as costs estimate at a preliminary design stage, so that decisions can be made on the financial viability of the investment. When developing a conventional aircraft, the parameters used in its cost estimate come from historical data. However, in the case of novel configurations, these parameters do not exist, requiring a new method for estimating costs.

Thus, a process based cost model of automated tape laying (ATL) manufacturing is developed for different aircraft configurations considering relevant data of aircraft parts (geometry). In this way, the estimate of the production costs is possible. The model can also be adapted to different annual production volumes or to the capacity of the existing machines in a plant.

In this thesis, a conventional aircraft and a joined wing are also analysed in relation to their production and acquisition phases. The production costs of both aircraft are obtained by the above mentioned model and then compared to each other. These data are still used in a sensitivity analysis with respect to the amount of material used, and in an investment appraisal.

Keywords: Cost model, ATL, Composites, Production Costs, Novel aircraft configurations

Contents

- Acknowledgments iii
- Resumo v
- Abstract vii
- List of Tables xi
- List of Figures xiii
- Nomenclature xv
- Glossary xvii

- 1 Introduction 1**
- 1.1 Topic Overview 2
- 1.2 Objectives 2
- 1.3 Thesis Outline 3

- 2 Background 5**
- 2.1 Life Cycle Costing 5
 - 2.1.1 Design phase 6
 - 2.1.2 Production phase 8
 - 2.1.3 Utilization phase 9
 - 2.1.4 Disposal phase 10
- 2.2 Design for Cost 12
- 2.3 Cost Estimation Techniques 13
- 2.4 Composites 14
- 2.5 Production Methods of Composites 16
 - 2.5.1 Hand Lay-up 17
 - 2.5.2 Automated Tape Laying 17
 - 2.5.3 Automated Fiber Placement 18
- 2.6 Novel Aircraft Configurations 18
 - 2.6.1 Blended Wing Body 19
 - 2.6.2 Joined Wing 20
 - 2.6.3 Strut/Truss Braced Wing 20
- 2.7 Investment Appraisal 21

3	Cost Model Development	23
3.1	Process Based Cost Model	23
3.2	Processes	24
3.3	Inputs	25
3.3.1	Exogenous Data	26
3.3.2	Material Data	26
3.3.3	Process Data	27
3.3.4	Part Data	30
3.4	Intermediate Calculations	36
3.4.1	Material	36
3.4.2	Time	37
3.5	Costs	40
3.5.1	Variable Costs	41
3.5.2	Fixed Costs	42
4	Test Cases and Results	45
4.1	Part Data	45
4.2	Exogenous Data	49
4.3	Material Data	49
4.4	Processes Data	50
4.4.1	Reception, Check and Storage	50
4.4.2	Application of copper, glass fiber and dry carbon fiber	51
4.4.3	ATL	52
4.4.4	Application of glass fiber, dry carbon fiber and vacuum bagging	53
4.4.5	Autoclave	54
4.4.6	Demolding, Finishing and Adjusting	55
4.4.7	Non-Destructive Tests	56
4.5	Costs	56
4.5.1	Production costs considering the production at maximum capacity	57
4.5.2	Production costs considering an annual production volume of 50 aircraft	60
4.6	Sensitivity Analysis	64
4.7	Investment Appraisal	68
5	Conclusions and Future work	71
	Bibliography	73
A	Cycle Times and Allocations	79
B	Weights	85

List of Tables

2.1	End-of-life strategies.	10
3.1	Exogenous Data.	26
3.2	Material Data.	26
3.3	Manufacturing Process Data.	27
3.4	Infrastructure-related Process Data.	28
3.5	Consumables data.	29
3.6	Geometry Data.	30
4.1	Geometry inputs for conventional aircraft	46
4.2	Geometry inputs for joined wing	47
4.3	Thicknesses, perimeters and areas of skins of conventional aircraft	47
4.4	Thicknesses, perimeters and areas of spars of conventional aircraft	48
4.5	Thicknesses, perimeters and areas of skins of joined wing	48
4.6	Thicknesses, perimeters and areas of spars of joined wing	48
4.7	Exogenous Data.	49
4.8	Material Data.	50
4.9	Reception, check and storage data.	51
4.10	Application of copper, glass fiber and dry carbon fiber data.	51
4.11	ATL Data.	52
4.12	Percentages of technical scrap according to different tape orientations.	53
4.13	Consumables Data.	53
4.14	Application of glass fiber, dry carbon fiber and vacuum bagging data.	54
4.15	Autoclave data.	54
4.16	Demolding, adjusting and finishing data.	55
4.17	Non-destructive tests data.	56
4.18	Times and machine use for the conventional aircraft production volume of 26 units.	57
4.19	Times and machine use for the joined wing production volume of 14 untis.	57
4.20	Cost distribution in the first analysis.	59
4.21	Times and machine use for the conventional aircraft production volume of 50 units.	61
4.22	Times and machine use for the joined wing production volume of 50 units.	61

4.23 Cost distribution in the second analysis.	63
4.24 New joined wing parts' weight.	64
4.25 Times and machine use for the new joined wing (production volume of 14 units).	65
4.26 Times and machine use for the new joined wing (production volume of 50 units).	67
4.27 Jet fuel burned in quilograms.	69
4.28 Net present value of the first analysis.	70
4.29 Net present value of the second analysis.	70
A.1 Cycle times and allocations for conventional aircraft skins	80
A.2 Cycle times and allocations for conventional aircraft spars	81
A.3 Cycle times and allocations for joined wing skins	82
A.4 Cycle times and allocations for joined wing spars	83
B.1 Conventional aircraft parts' weight.	85
B.2 Joined wing parts' weight.	86

List of Figures

2.1	Design process.	7
2.2	Distribution of materials applied to Boeing 787.	16
2.3	Novel aircraft configurations.	19
3.1	Processes of the manufacturing method.	24
3.2	Process block.	25
3.3	Process details.	27
3.4	Technical Scrap.	28
3.5	Production line.	29
3.6	Airfoil nomenclature.	30
3.7	Wing section.	31
3.8	Thickness in relation to wingspan.	32
3.9	Skin thicknesses.	32
3.10	Segmented airfoil approach.	33
3.11	Example of an upper skin.	34
3.12	Example of a spar.	34
3.13	Linear interpolation between two points.	35
3.14	Technical scrap according to different tape orientations.	37
3.15	ATL lay-up rate.	38
4.1	Part example.	52
4.2	Production costs of the first analysis.	58
4.3	Cost distribution in percentage in the first analysis.	60
4.4	Production costs of the second analysis.	62
4.5	Cost distribution in percentage in the second analysis.	63
4.6	Production costs of both joined wing regarding the first analysis.	66
4.7	Production costs of both joined wing regarding the second analysis.	67
4.8	Mission profile.	68

Nomenclature

Roman symbols

c Airfoil chord.

C_t Cash flow of period t .

H Trapezoid height.

h Spar height.

n Number of periods.

r Interest rate.

t_s Wing-box skin thickness.

t_s/t_{max} Wing-box skin thickness in maximum airfoil thickness percentage.

t_w Wing-box web thickness.

t_w/c Wing-box web thickness in airfoil chord percentage.

t_{max} Airfoil maximum thickness.

t_{max}/c Maximum airfoil thickness in airfoil chord percentage.

Subscripts

i, j, k Computational indexes.

l_i Distance between two points.

N_{seg} Number of segments.

X, Y, Z Cartesian components.

x, y, z Dimensionless cartesian components.

Glossary

ACCA	Advanced Composite Cargo Aircraft.
AC	Advisory Circular.
AD	Airworthiness Directive.
AFP	Automated Fiber Placement.
AFRA	Aircraft Fleet Recycling Association.
AFRL	Air Force Research Laboratory.
ATL	Automated Tape Laying.
BWB	Blended Wing Body.
CAD	Computer-Aided Design.
CAI	Composites Affordability Initiative.
CER	Cost Estimation Relationship.
CNC	Computer Numerical Control.
CTC	Countor Tape Layer.
CeRAS	Central Reference Aircraft data System.
DOC	Direct Operating Costs.
EASA	European Aviation Safety Agency.
EPA	Environmental Protection Agency.
FAA	Federal Aviation Administration.
FAR	Federal Aviation Regulation.
FC	Flight Cycle.
FH	Flight Hour.
FTI	Flight Test Installation.
FTL	Flat Tape Layer.
FV	Future Value.
HFC	Hydrofluorocarbon.
ICAO	Internacional Civil Aviation Organization.
IOC	Indirect Operating Costs.
IRR	Internal Rate of Return.
IST	Instituto Superior Técnico.
JAR	Joint Aviation Requirement.

LCC	Life Cycle Costing.
LMAS	Lockheed Martin Aeronautical Systems.
MDO	Multidisciplinary Design Optimization.
MPD	Maintenance Planning Document or Data.
MRO	Maintenance, Repair and Overhaul.
NPV	Net Present Value.
PAMELA	Process for Advanced Management of End-of-Life Aircraft.
PAP	Posted Airfield Price.
PBCM	Process Based Cost Model.
PFC	Perfluorocarbon.
PV	Present Value.
SBW	Strut Braced Wing.
TBW	Truss Braced Wing.
TOGW	Take Off Gross Weight.
TVM	Time Value Money.
WBS	Work Breakdown Structure.
WEEE	Waste Electrical and Economic Equipments.

Chapter 1

Introduction

The aerospace industry is constantly facing multiple and different challenges. The growth of air travelling flow is one of them and an increase on passenger traffic, air freight and mail transport has been registered. According to Eurostat [1], the total number of air passengers travelling in the European Union increased 4.7% in 2015 compared to 2014, and the air cargo transport grew by 7.2% and 1.3% in international intra Europe and extra Europe flights, respectively. The Heathrow Airport, in London, was considered the busiest European airport with respect to passenger traffic and the Charles de Gaulle Airport, in Paris, the freight and mail largest airport in Europe.

With the global economic crisis between 2007 and 2008, the crude oil price reached almost US\$140.00, corresponding approximately to an inflation of 100% at that time [2]. Currently, the price continues to float and it is unpredictable. Another challenge to the aerospace manufacturers are the government regulations to lower emissions of greenhouse gases exhaust from aircraft's engines. According to the U.S. Environmental Protection Agency (EPA), gases that came from engines used on commercial jets, as carbon dioxide (CO₂), methane (CH₄), nitrous oxide (N₂O), hydrofluorocarbons (HFCs), perfluorocarbons (PFCs) and sulfur hexafluoride (SF₆), impair the public health and the environment [3]. One of the latest agreements to mitigate the greenhouse gases effects was the Paris Climate Agreement [4], with the participation of 195 countries. The International Civil Aviation Organization (ICAO) also predicts that carbon emissions will grow 50% in 2050 and calls for a 4% reduction in fuel consumption from next generation commercial aircraft in production [5].

Conventional aircraft are also said to be at the end of its technical life cycle. Only minor improvements and few applications are currently made, thus requiring the implementation of new techniques and novel aircraft configurations to gain a sustainable competitive advantage in the global market [6]. Some of them are the joined wing and the struct braced wing aircraft that are going to be discussed later.

Therefore, with all these permanent challenges, aerospace manufacturers are obligated to improve aircraft flight performance, having capacity, speed, fuel and cost efficiency as a priority to the future aircraft. Innovative designs and new configurations are necessary to replace the conventional aircraft configuration at the end of its technical life. However, designers have to be sensitive to costs and must assume responsibility for life cycle engineering, therefore cost should always be taken into account as

one of the objectives when designing a new aircraft. The design phase is when products are projected, decisions are made and solutions are achieved, being important to take into consideration all the costs associated since the design phase until the end of the product's life [6]. This, called the Life Cycle Costing, will lead to a more economical production of aircraft, being helpful to validate investments and compare alternatives.

1.1 Topic Overview

The development of a cost model of an aircraft is a work for a team of engineers and designers of a company. This work of costs' estimation is complex due to the amount of relevant information and the preliminary phase of the prediction [7]. It is on the design phase that all costs associated to the life cycle of the product should be estimated, being important the reliability of them. Production costs, operating costs and maintenance costs are some crucial costs that companies must have detailed in order to proceed with businesses, making suitable and affordable offers to their clients, the aviation companies.

This care about costs is important not only to manufacturers, but also to the aviation companies that, apart from lower acquisition prices of aircraft, could do a better financial management of the company. Knowing the operating and maintenance costs, aviation companies will know how much each aircraft will consume and spend per flight and could also predict the maintenance cost. It is also interesting to mention the commercial agreements between manufacturers and aviation companies. The exclusivity contracts and the large amount of orders per aviation company make the acquisition price even cheaper and maintain the client in contact, offering the original quality of the producer's plant.

Cost models are usually based on several cost estimation relationships developed by using historical data of variables which could be for example the empty weight, speed, wing area, power and production quantity [8]. The difficulty of a traditional cost modeling is the prediction for unconventional aircraft, for which no historical data is available and there are no cost estimation relationships validated.

1.2 Objectives

This thesis consists in developing a cost model that predicts essentially the production costs of conventional and unconventional aircrafts designed by the Multidisciplinary Design Optimization (MDO) framework developed by the IST Aerospace Group. The cost model is applied at a preliminary level, during the aircraft design, and should adequately account for the effects of changing configurations, including novel aircraft configurations. In the end of this thesis, two aircraft models, developed by the framework, will be applied in the cost model and compared in order to determine which of them is more suitable for a specific case.

1.3 Thesis Outline

This chapter initiates the work made throughout this thesis with an introduction to the subject followed by a brief overview of cost models and their relevance to companies.

In Chapter 2, state of the art and the background of cost models are presented. Life Cycle Costing (LCC) and investment appraisal are explained in detail, some cost estimation techniques are studied, aircraft production methods are discussed and novel aircraft configurations are observed.

In Chapter 3, the cost model implemented in this thesis is introduced. A process based cost model for Automated Tape Laying is studied in-depth and developed.

In Chapter 4, two aircraft models developed by the MDO framework are analysed: a conventional aircraft and a joined wing. All inputs, intermediate calculations and outputs are presented, compared and discussed. A sensitivity analysis through a reduction in the amount of material is also carried out on production costs. An investment appraisal which analyses the production costs of both aircraft studied is still discussed at the end of this chapter.

Finally, in Chapter 5, the work done throughout this thesis and conclusions of the developed cost model are summarized. It is also presented some suggestions for the future work.

Chapter 2

Background

The importance of the present chapter is to introduce the life cycle costing and costs estimation of a product, in this specific case of an aircraft. In life cycle cost analysis, all costs associated to the product should be pointed out since the design phase. That is how companies can make affordable and suitable offers to their clients and either engineers and designers should be aware of costs.

Subsequently, an approach to composite materials and their production methods is presented due to the growth that has been registered in the implementation of composites in the aerospace industry. Some novel aircraft configurations, such as blended wing body, joined wing and strut/truss braced wing, are also discussed and compared with conventional aircraft.

Finally, the investment appraisal is introduced, describing some evaluation methods, such as net present value, internal rate of return, payback period and discounted payback period.

2.1 Life Cycle Costing

In order to validate investments, an analysis to all associated costs with expenditures during the life span is necessary. This analysis is called Life Cycle Costing (LCC) and it is also particularly useful for economic comparison of alternatives, giving the required technical and economic considerations to every aspect of the life cycle [9]. From the initial design of the product, costs and all subsequent expected costs are included in the calculations, as well as disposal value and any other quantifiable benefits to be derived [10].

The LCC complexity varies from product to product, and it may be represented by a simple table that shows the expected annual costs or by a complex computerized model based on estimates and hypotheses about future costs drivers. Generally, a complex LCC analysis represents a greater ability to predict future costs and those costs will impact decision-making [11].

The LCC is a method that benefits both the manufacturer and the consumer, in this case the airlines whose products are aircraft. On the one hand, the higher the perception of the associated costs by the manufacturer, the higher the control over them, optimizing the production, thereby increasing the companies' profit. In the case of the design and production stage, for example, the main goal is to

reduce the average cost of producing one unit, by diminishing the costs per operation hour and the support [6]. On the other hand, on the customer's side, the LCC is used as an evaluation technique that summarizes costs and relevant information on which it can be based an informed decision about investment, contributing to a logic and wise decision [10]. The more information provided on the aircraft's life cycle, the easier it becomes for the operator to check if the aircraft fits his operational and economic strategy, as well as which methods may be better to operate it.

According to Curran et al. [12], the majority of the LCC costs are projected during the early stages of design and development. Around 70% of the LCC costs are established taking into account operational requirements, performance and effectiveness factors, number of items to be produced and logistics support, among other decisions. Given this, significant changes at later stages of the project are considered complicated and expensive [11].

LCC can be divided into four phases: design, production, utilization and disposal phases [13], which are going to be described below.

2.1.1 Design phase

The main differences between scientists and designers are that scientists' problems are solved by analysis and using "problem-focused strategies", unlike designers' problems, which are solved by synthesis and using "solution-focused strategies" [14].

At the design process, it can be seen that there is not an universal model of the process. There are several simplistic models that only describe the sequence of the different stages carried out, and others that, in addition to the sequence, specify and develop the activities within each phase [14].

However, the design process of an airplane consists on a sequence of several studies from different aerospace areas, in order to obtain a viable configuration for the pretended type of mission and that meets the requirements set out initially, such as performance, handling, manufacturing, certifiability, upgradability, maintenance, and many others [15]. This process is a commitment between conflicting goals and opposing constraints that must be understood and studied, to ensure that the project is well succeeded. Due to the amount of different areas and the influence of each one on the others, this project is considered a multidisciplinary one, that converges to the intended goal [16].

The design process may also be staged, as observed in Figure 2.1. Despite being iterative, the process stages may be simultaneous, all converging upon a solution [16].

Figure 2.1 represents an aircraft design process. The first stage is called conceptual design and begins when the project's goals are set out and the requirements for the aircraft are established. It is considered an important guide during the entire project since it becomes a comparative study of different aircraft with the same, or similar, type of mission. The conceptual design is also very important to determine the best configuration that shall be used for the aircraft, and it is, therefore, the first task to be carried out. Three aircraft's development possibilities emerge from this study: minor modifications needed to an existing aircraft; major modifications needed to an existing aircraft; or a total new design, which is, in most cases, the best solution to fulfill all the requirements and restrictions. It is also at this

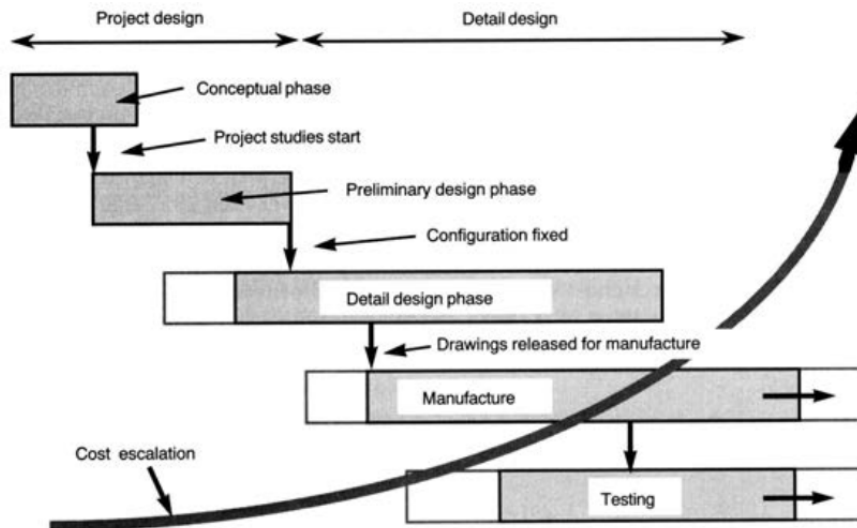


Figure 2.1: Design process [16].

stage that the first drawings, which help to compare different concepts, are developed. The designed aircraft are shaped and dimensioned. Hence, the final goal of this phase is to select the concept that best suits the requirements initially proposed, so it can be optimized through the next stages [16].

The preliminary design initiates when the project study starts. This is an iterative stage that optimizes the aircraft, concerning its definitions, such as dimensions, materials and structures. Analyses and computer simulations are conducted, with regard to aerodynamics, structure, propulsion, landing gear, control system, electrical system and hydraulic system, and the first physical models start to be developed and tested [16].

The last design stage, called the detailed design, precedes the production stage and prepares the aircraft for that stage with detailing draws, material lists and cost estimations. At this stage, there are no changes that can be done to the aircraft's configurations and all the parts are developed and detailed at real scale. At least one aircraft prototype is built to carry out real scale tests, in terms of components as well as systems: structure, mechanisms and simulations [16].

With regard to design costs, as observed in Figure 2.1, as the process is being detailed, the associated cost is increasing. These costs are called research and development costs and their growth are explained, not only due to the beginning of the production of parts for studies and tests, but also due to the increase in the number and detail of the conducted trials. It should also be pointed out that the studies and investigations in the search for new materials are included in these costs [16].

There is one platform that supports researchers and designers from all over the world. This project is developed by the Institute of Aerospace System, at RWTH Aachen University and is called CeRAS-Central Reference Aircraft data System. It consists of a database system of reference design data of commercial aircraft, intended to be used for research projects. Conceptual and preliminary design studies are integrated (at present, only for short range reference aircraft), as well as the parameter definitions and the calculating methods of the estimated costs, performance and fuel [17].

2.1.2 Production phase

The production phase, which proceeds the design process, begins with the production of each component of the aircraft, through all manufacturing and assembly processes, until the certification and delivery of the aircraft to the customer, ready to be used.

According to Airbus [18], and taking it as an example, the aircraft production is divided through different plants located in Europe. Parts, such as wings, vertical stabilizers and high-lift systems for the wings, are produced in different individual production plants, which are then transported to assembly lines. Many of the components are transported by ships and trucks. However, a large number of smaller sections, such as the nose section or the vertical fin, are transported by air through the Beluga Airbus fleet.

The production methods depend on dimensions of the part to be produced, the production volume, the part complexity and other factors that will be developed and presented in section 2.5. However, all associated costs, from the purchase of raw material to the tooling cost, including the depreciation of machinery too, are values that fall into this phase.

Continuing with the example of Airbus [18], after all the individual parts have been produced and transported to the assembly lines, aircraft's fuselage arrives to the assembly lines segmented in sections. After being joined, the complete fuselage is raised and, through automated robots, wings, horizontal and vertical stabilizers, engine pylons and landing gear are installed. Simultaneously, cabin installation is initiated and cabin side walls, overhead storage racks, carpets, floor surfaces and partitions are implemented.

Subsequently, the aircraft is taken to a ground test station, where its systems are subjected to mechanical, electrical and avionics tests, similar to flight conditions. At this station, the latest structural elements are also installed, such as the aircraft belly fairing, landing gear doors and wing leading edge. Internally, seats, their cabling and galley equipment are also installed, preparing everything for delivery to the customer.

Finally, the engines are installed and new tests of fuel and pressurization are realized. With their approval, painting, engine run-up and flight testing, certification and delivery to the customer are the following steps.

In the case of new aircraft productions, before the flight test, the new configuration is subject to some structural static tests. Flight Test Installation (FTI), calibration test, maximum wing bending at limit load, fuselage pressure test, fatigue tests and flight cycles simulation are some examples that test the aircraft structure on the limit, to see if any improvement, in terms of design, is required. As an example, fatigue tests recreate some flight phases (taxiing on the runway, take-off, cruising and landing) through a combination of controlled loads and test the aircraft's structure in terms of stress over long periods of time [19].

Thereafter, before starting a series production, the aircraft has to perform the flight tests and be certified by the airworthiness authorities. In terms of flight test, the aircraft is subjected to a rigorous flight, that evaluates the general handling qualities, operational performance, airfield noise emission and systems operation in both normal flight and extreme conditions (covering the entire flight envelope) or

failure scenarios [18]. Certification is mandatory for all types of aircraft, engines and propellers. The two largest certification authorities are the European Aviation Safety Agency (EASA) [20] and the U.S. Federal Aviation Administration (FAA) [21]. Each one is in charge of legal control of its geographic area. The main certification systems are the FAR25 regulations [22] in the USA, and the JAR25 regulations [23] in Europe.

At delivery, the aircraft is verified by the customer, who checks if the aircraft complies with all initial contractual requirements [18].

2.1.3 Utilization phase

At this phase, costs largely depend on the user, usually aviation companies. However, due to the manufacturer's guarantees, some of the costs may also fall on the manufacturer, during the first few years after the purchase of the aircraft.

During the utilization phase, costs are referred as operating costs and are classified into two types: Direct Operating Costs (DOCs) and Indirect Operating Costs (IOCs).

Direct Operating Costs are defined by ICAO [24] as the total of flight operating costs, maintenance and overhaul costs and market depreciation. In other words, DOCs include all dependent aircraft costs and all necessary costs to maintain the aircraft operational.

Some examples of flight operating costs are cabin crew salaries and benefits, usually fixed values; aircraft fuel and oils, which are variable values directly related to aircraft flight speed and load and to prices established by airports through Posted Airfield Prices (PAPs); aircraft insurances for both the aircraft itself and the flight itself, holding passengers and baggage; and other flight expenses [25].

In terms of maintenance and overhaul costs, this value is based on a man-hour to flight-hour ratio that varies according to aircraft type, model complexity, age, check cycle, operating environment, warranty status, utilization and general condition, and the experience of the maintenance, repair and overhaul (MRO) company, including all consumable parts during this process, the most common tires and brakes [25]. Regarding age, when it comes to a new aircraft, the maintenance costs are generally lower and assured by the manufacturers' warranty. As the aircraft reaches maturity, after around five years, the costs increase and reach a steady and predictable maintenance cost, which after around 15 years begins to rise again because of age. Regular maintenance is important because it ensures the airworthiness conditions in terms of structure, engines, systems and components. Planning is established through documents from manufacturers, such as the Airbus-Maintenance Planning Document (MPD) or the Boeing-Maintenance Planning Data (MPD) for example, which contain the minimum required maintenance tasks and how and when they should be executed. Other considerations to take into account in maintenance planning, are intervals between checks, which result from a combination of flight cycles (FC), flight hours (FH), calendar months, and the most appropriate moment for the maintenance, avoiding the high season of an airline, for example. Additional tasks, used for older aircraft near the end of their design life and that require more non-routine maintenance and corrosion prevention tasks, are issued by civil aviation regulatory authorities, such as EASA [20] and FAA [21], and presented as

Advisory Circulars (AC) and Airworthiness Directives (AD) [26].

Depreciation is also considered a fixed direct operating cost. Depending on market-based depreciation values, on how the aircraft will be used (such as regular or heavy operations) or on the number of hours or miles flown, the aircraft loses a fixed percentage of their original purchase price each year [27]. The simplest case of depreciation is the straight-line formula, where the depreciation of each year is the purchase price divided by the number of years over which depreciation is spread.

Indirect Operating Costs are also defined by ICAO [24] as the total user charges and airport expenses, passenger services costs, catering, security, general, administrative and other operating expenses. Landing fees based on aircraft weight, en-route facility and navigation charges, and handling expenses are some of these costs charged by airports, air traffic control agencies and airport management companies respectively.

2.1.4 Disposal phase

The disposal phase is the last phase of life cycle costing and is important not only in economical and social terms, but mainly in ecological and environmental terms. One of the main entities to control environment damage is the Environmental Protection Agency (EPA) [28].

For a few years, retired aircraft were being deployed in so-called aircraft graveyards, often located around airports or in deserts all over the world. With the increasing restrictions on imported 10 or 20 year old aircraft by developed countries, such as China and Russia, the number of aircraft to be dumped has increased significantly annually, contributing to a non-sustainable process [29].

In order to reduce environmental impact and to promote a circular economy, a so-called ReX strategy was created, an abbreviation for alternative end-of-life strategies of a product starting with the 'Re' prefix [30]. Reduce, reuse, repair, refurbish, remanufacture, recycle and recover are all measures or alternatives to be taken in the end-of-life process of a product according to this strategy and are presented and compared in the Table 2.1.

Table 2.1: End-of-life strategies [30].

ReX scenarios	Level of disassembly	Expected quality	Identity
ReDUCE	None	New	Original
ReUSE			
ReUse	None	'As-is'	Original
RePair	Product/down to faculty part	Working order	Retain
ReFurbish	Module	Specified level	Retain
ReManufacture	Part	'Like-new'	Retain
ReCYCLE	Material	Low-high	Lost
ReCOVER	Substance	Low-high	Lost

Nevertheless, the industry often continues to prefer more economical methods (landfilling and incineration) than the ecological ones [31].

In the case of aviation, there are many participants in this process, such as industry, legislators and even society. It should be noted that each end-of-life alternative has its consequence regarding the sustainability of the process: being beneficial and favorable to one participant according to one criterion, it ceases to be to another one, which could become a tendentious process [32].

An end-of-life aircraft has a residual value due to materials and parts that can still be recycled, which must be recovered. Therefore, recycling is required and can be defined as an operation to recover waste materials in new materials and products useful and equivalent to the original ones, leading to waste reduction and the decrease of the number of landfills sites. Although it does not include energy recovery, the production of recycled material requires less energy than the production of raw material, which leads to a reduction of pollutant emissions to air, water and land. With the recovery of some parts and their reuse, not only the natural resources are saved by the decrease in the production of new parts, but also less expensive will be the production, due to the reduced number of labor hours and the reduction of energy required [30].

In 2006, Airbus and Boeing initiated two alternatives to deal with end of life aircraft, improving the process in environmental terms and in a sustainable way. Airbus launched the Process for Advanced Management of End-of-Life Aircraft (PAMELA) project [33] and Boeing started the Aircraft Fleet Recycling Association (AFRA) [34] with other aviation companies, Bombardier, Embraer and Rolls-Royce.

Today, the AFRA's mission is to improve the performance of the industry and increase the commercial value of aircraft in end-of-service [34]. In the case of the PAMELA project [33], the main objective was to demonstrate in a real recycling process of an Airbus A300 aircraft that 85% of the weight of the aircraft would be recycled, re-used or recovered. This end-of-life process consisted of three steps: Decommissioning, Disassembly and Smart Dismantling, the so-called 3D approach. In the decommissioning phase, the aircraft was withdrawn from service. Subsequently, it was inspected, cleaned and decontaminated, removing all operational liquids that would be re-sold for direct reuse or only withdrawn for recovery channels. In this project, the aircraft did not re-enter in service and the disassembly phase was carried out, however, there could have been the possibility of repairing or recycling and coming into service again. At this stage, the aircraft deconstruction began according to a plan, parts were grouped in disassembly families and, in the end, some of them that could be reused were sold or stored. Finally, the smart dismantling phase was initiated, beginning with the identification of the various recovery channels. The materials were grouped after aircraft dismantling and were prepared for grinding, followed by sorting and shipping to the recovery channels. Types of aluminium alloy, titanium, austenitic nickel-based superalloys, stainless steel, waste electrical and electronic equipments (WEEE), wiring, tires and plastic were all cast. In the case of recycled metals, these were put in ingotes and returned to the aeronautical, mechanical or automotive markets [32].

In the case of composite materials, they are usually incinerated or even dumped into landfills because of the high cost of separating the fiber and resin for future reuse. The main methods are mechanical, thermal or chemical separation, however, it is still necessary to optimize processes in order to be an economically sustainable process that could also ensure the future quality of the fibers [35].

2.2 Design for Cost

Competitiveness is fundamental to the equilibrium of markets and the need and the demand for new techniques, developments and innovations must be constant between companies. However, the benefits of these improvements are not always achievable due to the high financial investment of the project, and therefore these initiatives are usually set aside [36].

Through manufacturing cost estimations and predictions, designers can realize and find solutions to the economic problems related with the product and design more cost-effective systems, which will subsequently influence the feasibility of the project [7]. Designers must have the knowledge and sensitivity of all product development processes, must understand economics, marketing and risk, and consider cost as a variable design of equal weight as other performance variables. Therefore, designers begin to have a responsibility for life cycle engineering, an area neglected until the 1990s in the design of aerospace systems [37].

As mentioned in the article [38], the definition of design for cost can be stated as "studying and developing methods and tools allowing the designer to calculate costs in the early design phase by managing the knowledge of production processes and, hence, costs incurred therein."

Due to the amount of information regarding the manufacturing process, such as related parameters, raw materials, size of production lot and number of labor hours, manufacturing cost estimation is a complex assignment [7]. However, cost models integrated in design, especially in conceptual and preliminary design, should not be so complex as they would become too time-consuming. In these design phases, the goal is to obtain cost models that provide approximate and rounded estimates, quickly and usefully, with a sufficient fidelity rate so that the different alternatives of a product can be compared. Generally, the cost estimate of a part focuses on features related to production, operations and support, then resorting to basic engineering economics to forecast costs, prices, rates of return and profitability indicators. In the case of more complex models, algorithms that simulate organizational learning and manufacturing processes are also used, complementing and making the results more accurate [6].

It is also important to note that it is through these estimations and predictions that the sales department is initially based on to make the first offerings to customers keeping them constantly informed of new products, new updates and new offers, ensuring competitiveness against competing companies.

An interesting tool referenced by Mengoni et al. [7], would be an automatic association of the part's costs of manufacturing through the 3D model drawn in CAD, thus generating the estimate of the final cost. In other words, the tool would associate manufacturing processes, discretized in a database, to each geometry, taking into account roughnesses, tolerances, materials and all other non-geometrical data. By relating all the information with the production cycles, the necessary operations, the number of units to be produced and the cost of each process, one would obtain the cost estimate of each unit. This example would facilitate a designer to develop a more cost-effective product with emphasis on a more competitive economy, also ensuring the economic viability of the same in the market.

2.3 Cost Estimation Techniques

Cost estimation is an important process in the design phase of aircraft production. Through this technique, a company is able to determine the selling price of its products and whether its investments are feasible or not. However, it is a difficult process due to the high amount of information used in the estimation models and the coverage of the required areas [39].

The costs of a product can then be generated by three methodologies [40]: analogical method, parametric method and process based model.

The analogical method is a technique based on costs of similar products previously produced, historical relations, among which the analyst compiles the maximum of similarities between the products generating the estimate. However, despite being fast, this technique fails in terms of accuracy in estimating the final cost [41].

The parametric method is a methodology that uses Cost Estimation Relationships (CERs) based on historical data. A CER is a fundamental technique in estimating costs that establishes a mathematical relationship between two variables, a dependent and an independent. The dependent variable is the case study, or in other words, the cost to be estimated, while the independent variable is the variable that predicts the other through a correlation between one or more parameters with a certain meaning [42]. Generally, the relationship is based and developed through historical data to which a statistical technique is applied later, such as linear regression for example [43].

In the case of independent variables, they should be considered according to the impact that their characteristics have on the cost of the product, in order to establish an accurate CER. These characteristics are called cost drivers [44]. Regarding to aviation, conventional cost drivers are usually related to performance and to the physical and technical characteristics of the aircraft, such as empty weight, speed, useful load, wing area, power, landing speed and production quantity [42],[45].

Statistical models, which generate independent variables, are enhanced by the provision of historical data. This data collection is meticulous, time-consuming and can not contain errors, nor influential factors that can take credibility to the CER [42]. The advantages of historical data collection are the guarantees that the data is real, objective and reliable. In addition, it has been proven over time that CERs have established good estimates and are good predictors. Though, regarding to disadvantages, CERs are based on historical facts to predict the future [46]. In the case of products that maintain the same structure and the same production method, cost predictions usually do not have any type of problem and are accurate. However, innovative configurations, new structures, new manufacturing techniques, new materials, they all lack any kind of documentation and historical basis so that a statistical model can be used and credible.

Rand Corporation was the first institution that, in partnership with the United States Department of Defense, initiated the development of CERs to predict the cost of aircraft. This development began after World War II in the military area and with historical evolution has become increasingly complete [47]. Later, NASA also began studies on CERs, launching the NASA RC Method, a cost estimation technique for costing based on weight as the most important parameter [48]. Nowadays, there are CERs

for all types of conventional aircraft, whether military or commercial, produced by aircraft companies themselves.

Finally, the last methodology is based on the decomposition of the production and manufacturing processes that will be executed in each component of the product through a Work Breakdown Structure (WBS), which has costs associated later, that when summed will generate the estimate of cost [45]. It is considered a process based cost model (PBCM) and the advantages of this method are the facility of analysing errors and identifying where the largest estimates deviations occur due to the separation of the final product into components and the facts that it does not require historical data and it is functional for both new or traditional technologies. This technique relates cost drivers directly to the processes involved in production and it is able to specify cost changes due to changes in product and process designs. However, the major disadvantage of this technique is the detailed information required for the various processes, such as number of labor hours, total material to be used, waste and others, which turn this technique time-consuming.

Some examples of cost estimating techniques are the Roskam [49] and Raymer [50] models, however, nowadays the aircraft companies have their own complete and detailed models.

2.4 Composites

Metals, more specifically aluminium alloys, have been the most widely used materials in the aerospace industry since the 1930s, particularly in structural parts. The experience and knowledge acquired over the years has decreased its cost of manufacturing and maintenance, which is an advantage in the choice of aluminium for the manufacture of aircraft [51],[52]. In addition, the levels of reliability and safety of the material are also high due to the historical use of aluminium alloys [53]. Features as excellent mechanical and thermal properties and being easily shaped in machining are other advantages of metals [54]. Also, with the appearance of composite materials, aluminium alloys have been increasingly studied to be able to compete. The most commonly alloys used are aluminium alloy with copper or lithium and also aluminium alloy with zinc [53],[55]. However, there are some disadvantages compared to composite materials, such as the weight increase for a part with the same tensile strength and the lower corrosion resistance.

The composite materials may be defined as a combination of two or more distinct materials, which results in a material with different mechanical properties when compared with the original properties of each initial material individually. Materials such as wood, bones, and teeth are considered some biological composite materials that contain complex internal structures suitable for the use and efforts to which they are subject [56].

Comparing with conventional materials, composites have highly appreciated properties in aircraft production. The high strength-to-weight and stiffness-to-weight ratios, the capacity to handle tension, that minimizes the need for maintenance due to fatigue, the reduced number of parts and fasteners used in the product assembly, the corrosion resistance and the extended product life are the main advantages [57]. In addition, it is still possible to produce specific composites, with certain stiffness

and strength, suitable to withstand the stresses and tensions which part will be subjected to during its lifetime. The desired properties are achieved by the different orientations of the fibers, the number of plies and the percentage of resin used. Thus, it is possible not only to reduce the number of labor hours required for production and development, but also to ensure the reliability of the material [58]. The major disadvantages of composite materials are the cost of acquiring the raw material and the fact that it is considered a new material, which implies qualification and safety acceptance by the competent authorities [59].

Despite the benefits of composite materials, the aircraft industry remained reluctant in its implementation due to the high costs when compared to metals and due to the novelty of the material. In 1996, the Air Force Research Laboratory (AFRL) launched the Composites Affordability Initiative (CAI) to mitigate concerns and make composites more affordable and widely used in aircraft production [60],[61]. The main conclusion of this initiative was the reduction of assembly costs through the integrated and bonding structures of composites. With the reduction of drilling holes and installing fasteners, the labor and rework in aircraft structures reduced from 50% to 80% compared to typical fastened structure, resulting in assembly cost savings of 20% to 50%. In cooperation with the FAA, the CAI team certified the structures, as well as all CAI-developed analysis tools and bonding process controls, which led to an increase in the reliability of composite materials.

Later, in 2006, the CAI team had the opportunity to build an aircraft mainly in composite material, to apply the processes and tools developed and to prove the reduction of production costs. The Advanced Composite Cargo Aircraft (ACCA) or the X-55 was the name assigned to the aircraft, built in partnership with Lockheed Martin [57],[62]. The project consisted in the production of a conventional high-wing transport aircraft, the Fairchild Dornier 328J (DO-328J), using advanced composite materials in the fuselage and vertical tail. Some modifications to the aircraft were also necessary to meet the military requirements and 40% of the total vehicle structure was replaced by large integrated and bonded composite structures. Through CAI technologies, the number of parts for assembly was reduced and achieved 90% and 80% reduction in fuselage and vertical tail, respectively, compared to the original DO-328J aircraft.

Other examples of the use of composite materials in the case of commercial aircraft, are the Boeing 787 Dreamliner and the Airbus A350 XWB. In the case of Boeing, the 787 Dreamliner is comprised of 50% composite material in its structure's weight (fuselage and wing), as observed in Figure 2.2 [63]. The high strength-to-weight ratio of composites was one of the main reasons for the introduction of composite material into the aircraft structure, which led to the reduction of thousands of fasteners that would be used in the assembly, about 80% reduction. For an efficient structures production, Boeing has resorted to the use of fiber placement machines, which will be presented in section 2.5. In the case of Airbus, the new A350 XWB was launched and 53% of its constituents are composite materials, resulting in an aircraft with low fuel consumption and empty maintenance due to the high capacities of material to fatigue and corrosion, that will keep the aircraft operational for long periods of time [64].

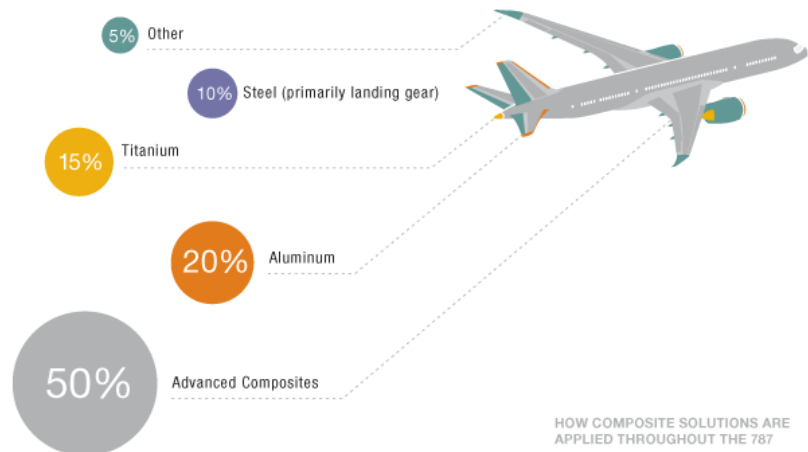


Figure 2.2: Distribution of materials applied to Boeing 787 [63].

2.5 Production Methods of Composites

In terms of production, composites can be manufactured by several methods, however, only three will be described in a comparative manner: hand lay-up of prepreg, automated taping lay-up (ATL) and automated fiber placement (AFP). In both cases preimpregnated fibers are used, which require care not to lose their properties. Due to the resin that involves the fibers, the prepreps must be packed in a refrigerated place and whenever removed to room temperatures, time should be documented. Another care to take into account is moisture condensation. Air-conditioned and humidity controlled rooms must be used for prepreg lay-up operations, as well as whenever the prepreps are removed from the freezer, they must reach the room temperature and only after that the protective wrapping material should be removed, avoiding the appearance of voids or porosity in the heating process for cure. To prevent the presence of dust and dirt in rooms, they must also contain slightly positive pressure [65].

In the production process of an aerospace part in composite material, the application of glass fiber and copper is also a prevention, avoiding galvanic corrosion of the aluminium if fibers are in contact with the metal, and protecting the outer part of lightning strikes, respectively [66]. Then, the process begins with the application of glass fiber and copper in the part mold, followed by the fiber placement according to the lay-up method and, finally, it is applied glass fiber once again. After the procedure, the part is sealed in a vacuum bag with a bleeder and a breather materials inside to absorb the excess resin and facilitate the absorption of air respectively. The curing process in the aerospace industry is usually performed in an autoclave, which, with increasing temperature and pressure, promotes a better finish to the part in terms of quality. At the end of production, finishing processes are performed followed by non-destructive tests to ensure that there are no defects [65].

2.5.1 Hand Lay-up

The hand lay-up process of prepreg is a standard method in the manufacture of composites by the quality and high performance that can be acquired in the composites and by the adaptability of the process in the production of new parts [67]. It is an open molding method where specialized technicians manually lay layer by layer on the surface of the mold according to the orientation and sequence of the fibers up to the desired thickness. Between each layer deposition, a squeezing rooler is used to remove entrapped air between layers. After reaching the required thickness, the part is sealed in a vacuum bag and the process continues as described above. According to Hagnell and Åkermo [68], the lay-up rate varies between 0.9 to 1.5 *kg* of material per hour, depending on the complexity of the piece, the lay-up angles, and the worker's experience. It is a labor intensive method subject to human errors, which lowers the production rates, however the tooling investment is low and it is possible to produce parts with quite complexity, unlike the automatic processes [69]. With the increase in the production volume of parts in composite materials, which in turn has been being verified over the years, the manual lay-up process becomes an unsustainable option and it is necessary to resort to automatic processes, such as ATL or AFP [69],[70].

2.5.2 Automated Tape Laying

Both ATL and AFP are composite manufacturing processes throughout the addition of material course by course. Unlike metal machining, which removes material, these processes are designated as additive manufacturing or inverse machining [71]. In the case of ATL, the high productivity of large and flat parts is a consequence of the ability to lay-up large amount of material due to the width of the tape and the speed of the method. The lay-up rate varies between 10 to 150 *kg* of material per hour and depends on the size and the shape of the part [71]. In the case of small parts, the ATL process significantly decreases its efficiency because the machine has to accelerate and decelerate rapidly along the path, failing to reach and work at the ideal laying-up speed [68]. In turn, the material waste will also be higher given the amount of material placed in excess in each course performed. Compared to the hand lay-up method, ATL has high production rates and a decrease in the material quantity wasted on large parts, however it is quite limited in the production of complex parts and the initial investment is around 3.5M \$ [71],[72]. Compared to AFP, although the waste is larger, the cost of the material for the ATL machine is lower than the cost for the AFP machine, which has an impact on the total cost of production and is often the distinctive factor between these two methods [68]. Some examples of parts produced in ATL are wing skins, horizontal and vertical tails [72].

In the industry, there are two types of ATL machines: flat tape layers (FTL) and countor tape layers (CTL). The FTL machine is essentially used only for flat parts, while the CTL machine (the most common model), in addition to flat parts, can also do tape laying of parts with angles up to 15 degrees [72].

The laying process is controlled by a Computer Numerical Control (CNC) system that commands the machine head and makes the placement of tapes of preregs, thus eliminating the human errors observed in the hand lay-up process. In addition, the majority of ATL machines have tape detection

systems, which allow the machine to stop as soon as it finds a defect. The ATL system is constituted by a roll of material which is inserted into the machine head and, through feed rollers, guide chutes, a heating system, cutters and a silicon roller, is placed on the mold under pressure exerted by the roller. The tape heating system serves to improve the tack and the tape adhesion. The machine speeds up to the ideal lay-up speed and slows again as it approaches the end of the desired path, cutting the tape automatically and laying-up its remaining. The process is repeated by placing the tape next to each other without overlapping. When all the courses are finished, a new plie is placed and so on until the desired thickness is reached [72].

2.5.3 Automated Fiber Placement

The AFP process is very similar to ATL, however, the main differences are the widths of the tapes placed, that are smaller, the fact that the machine head can distribute between 12, 24 or 32 tows of material simultaneously and the possibility of the system to be integrated in a robot, increasing the affordability of the process [72]. This is a method that can produce curved, complex, contoured shapes and the variation of the number of tows of material depends on their complexity, which affects the productivity of the fiber placement. Two advantages about the distribution of material in different tows and the fact that each tow is independent to one another are its own production of complex parts and also the reduction of the amount of wasted material that varies between 2% and 5% [65],[72].

The speed of lay-up and acceleration of the AFP machine, both linear and rotational, are higher than the ATL machine, which makes the AFP process faster, achieving larger lay-up rates in large and flat plates. However, because the complexity of the parts is greater in the AFP processes, productivity decreases compared to the ATL process [72]. Still, given the versatility of the process for production of complex parts, AFP is widely used in the aerospace industry [73].

Regarding fiber placement, this can be held by using either impregnated tows as well as slit prepreg tape. Although the slit prepreg tape is more expensive, it has advantages in terms of productivity, reliability and product quality. The material is then supplied to the lay-up head through spools that exert a controlled tow tension to enable lay-up into the convex geometries. During the fiber placement, a compaction roller is used to press the prepreg and heat through infrared irradiation techniques is also provided, eliminating the presence of voids in the layers [72].

2.6 Novel Aircraft Configurations

Nowadays, and for several decades, the most used aircraft either commercially or militarily is, as its name suggests, the conventional aircraft. Generally, the most common configuration, observed in most commercial aircraft, is the low wing cantilever monoplane with swept back trapezoidal wings of moderate aspect ratio and positive dihedral. However, one can also easily find conventional aircraft with high wing or zero swept angles for example. The concept of conventional aircraft is basically the identification of an aircraft with a main wing, a cylindrical fuselage and a vertical and horizontal tails, a design

studied for years, that thanks to the evolution of technology and sophisticated computational models has become increasingly efficient [74].

Currently, and according to experts in academia, industry and leading aerospace agencies, without a design change, this configuration only achieves incremental improvements in performance, fuel consumption and operative costs, which is not feasible with globalization and with the increase of air traffic observed in recent years. A major design change is therefore essential, new configurations are required to achieve new requisites and at the same time to reduce emissions, pollution and noise, thus contributing to a more sustainable environment [74]. Some of novel aircraft configurations are shown in Figure 2.3.

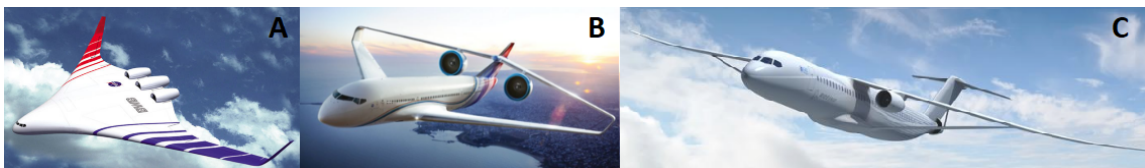


Figure 2.3: Novel aircraft configurations: a) Blended Wing Body [75]; b) Joined Wing [76]; c) Strut Braced Wing [77].

2.6.1 Blended Wing Body

The Blended Wing Body (BWB), represented in Figure 2.3 A, is an aircraft under development by NASA and the Boeing Company that aims at large commercial transport of the future [78]. This configuration is a combination of features from conventional aircraft and flying wing shape, which reveals performance advantages compared to the conventional configuration. The high fuel efficiency, the emissions and noise reductions, the large payload volume, the aerodynamics and structural efficiency are some of the advantages [79]. The wide airfoil-like body allows the fuselage itself to create lift and an effective span-wise lift distribution, also minimizing the total drag, which leads to a decrease in fuel consumption. This feature also makes the BWB having a large usable volume for the transport, which can be distributed along the central structure of the wings and body, reducing the structural stiffness required, which consequently decreases the weight of the aircraft. Two other characteristics of the BWB are the incorporation of the engines in the fuselage, which also contributes to the decrease of the total drag of the aircraft, and also the elimination of the conventional tail, being therefore necessary several control surfaces on the trailing edge [80].

However, one of the major problems in the development of the BWB's fuselage is its internal pressurization due to the appearance of nonlinear tensions. Some solutions have been presented, such as separated pressure shell, integrated skin or multi-bubble fuselage, but even today this problem is still being studied [80].

With this configuration, it is possible to achieve a reduction in fuel consumption of 27%, the take off and the operating empty weights decrease by 15% and 12% respectively, the total required thrust decreases by 27% and it is also possible an increase of 20% in lift/drag ratio. These results lead to the conclusion that BWB has a clear advantage over conventional aircraft [81].

2.6.2 Joined Wing

The joined wing (Figure 2.3 B) is another novel aircraft configuration that is still being studied and under development. Its main characteristic is the connection of two wings and is based on the concept of Best Wing System introduced by Prandtl a century ago [74]. The concept showed that a wing with a rectangular path seen from the frontal view guaranteed the lowest induced drag when compared to any other type of conventional wings with the same wingspan, total height and lift [82]. This new design is more structural and aerodynamically efficient and reaches the best range and the longest endurance in relation to any other type of configurations [74]. With its optimization, today the structural connection between the wings is made with the rear wing that has its root attached on the top of the vertical tail and the tip that sweeps forward to join the trailing edge of the main wing. The rear wing is used for pitch control and also as a structural support of the forward wing, reducing the wing bending moments [83].

The two major difficulties in designing this configuration are the takeoff field length and the rear wing buckling. Due to the unusual structural load paths on the leading and trailing edges, compressive and tensile pairs are formed, which will react with non linear behavior in a vertical gust. One solution to deal with buckling is strengthening the structure, however this would imply a weight gain that is not desired [74],[83].

A few studies evaluate the aircraft performance, presenting results as reductions of induce drag between 5% and 11%, as well as reductions of DOC between 2% and 5% compared to conventional aircraft, however they are not referred as detailed studies, being too early to conclude that joined wing configuration is an alternative to conventional aircraft [84].

2.6.3 Strut/Truss Braced Wing

The Strut/Truss Braced Wing (Figure 2.3 C) is the most similar configuration to conventional aircraft and therefore, the concept with more favorable reactions from the public compared to the joined wing or the BWB, which have a different appearance and may cause some apprehension [85]. The main modification is the incorporation of a support under the wing, which allows larger wingspans without an increase in wing weight or thickness. In the case of Strut Braced Wing (SBW) only one support is applied, and in the case of Truss Braced Wing (TBW), two ore more supports are applied, minimizing the buckling problems, but introducing penalties in aerodynamic drag [74].

The modification makes the aircraft more aerodynamic and structurally efficient, as it reduces wing loading and achieves higher lift coefficients and aspect ratios while minimizing induced drag. In addition, it is also possible to reduce the chord lenght that favors the laminar flow (reduction of Reynolds number) and allows a reduction of the parasite drag. With these characteristics, the aircraft performance is increased and the engine size can be reduced, which leads to reductions in fuel consumption and emissions of gases and noise. These advantages are even more evident when the range increases, which leads to the conclusion that this configuration is indicated for large and long-range transports [86].

A study from Lockheed Martin Aeronautical Systems (LMAS) and Virginia Tech shows that SBW burns 16.2 - 19.3% less fuel, requires 21.5 - 31.6% smaller engines and costs 3.8 - 7.2% less than an

equivalent conventional aircraft [74]. However, a recent study with a modified Lockheed Martin C-130J with a cruise Mach number of 0.60, 1800 nm range and a maximum payload of 40000 lbs compared the differences between conventional aircraft, SBW and TBW. The results obtained conclude that the SBW allows 10.7% reduction with a take off gross weight (TOGW) penalty of 4.2% and the TBW achieves 4.5% decrease in fuel weight but also an increase in TOGW by 11% compared with conventional configuration. The difference can be explained by the increase in drag associated with the introduction of one more support to the structure [87].

2.7 Investment Appraisal

Investment appraisal is an evaluation of the attractiveness of an investment. It is an assessment of the viability of the project and the value it generates. This assessment can incorporate several factors, such as financial, generally the most evaluated and only applied when there are financial returns of investment; legal, evaluated when current or future legislation requirements may interfere with investment; environmental, used when environmental impact is considered a distinctive factor, being increasingly used; social, used in terms of responsibility towards city; operational, including for example competitive advantage, product quality and also its life cycle; and risk, associated to all operational uncertainties and probabilities. It is therefore necessary to take stock of financial and non-financial factors to make the decision of an investment [88].

The net value present (NPV), the internal rate of return (IRR) and the payback period are some of the methods used to evaluate an investment.

However, before defining the methods, it is important to highlight that the present value of the money is not the same as the future value, there is a time value money (TVM) due to the potential earning capacity. In other words, receiving an amount today, is equivalent to receiving a larger amount tomorrow and receiving an amount tomorrow is equivalent to receiving a smaller amount today. The relation between present and future values is presented in equation 2.1.

$$PV = \frac{FV}{(1 + r)^n} \quad (2.1)$$

where PV is the present value, FV is the future value, n is the number of periods and r is the interest rate.

The equation 2.1 is derived from the theory of compound interest, which says that to each period is added an amount of interest proportional to the value already accumulated, that is, the interest rate falls on the accumulated value, which increases each period [89]. Thereby, the value of interest for each period is always increasing.

Focusing on methods, net present value (NPV) is the sum of all discounted cash flows associated to a time period at a given discount rate, as shown in the equation 2.2 [89]. Discounted cash flows are the current cash flows in the present value, noting that the investment is considered a cash flow, simply negative and usually done in year zero.

$$NPV = \sum_{t=0}^n \frac{C_t}{(1+r)^t} \cdot \quad (2.2)$$

where C is the cash flow of period t , n is number of periods and r is the interest rate, the rate that updates the future value in the present value.

The main objective in the realization of an investment is to obtain a positive NPV, which means that it was feasible, the initial investment was covered by the profits generated and there is no loss of money. Consequently, the higher the NPV value, the higher the yield. The discount rate, as can be seen in the equation 2.2, is inversely proportional to the NPV and shows how the value of money decreases with time.

Another method of investment appraisal is the internal rate of return (IRR), the discount rate for which the NPV of all cash flows has zero value, and which measures the efficiency of the capital investment [89]. In order to calculate the IRR, the equation 2.2 is used by equating the value of NPV with zero and deriving the value of the discount rate, through non-analytical calculations. Regarding its value, the higher the IRR value, the better and more profitable the investment will be.

Finally, the latter methods are called payback period and discounted payback period. The payback period is considered the time required to obtain the return on the initial investment. From that moment, the investment becomes profitable and it is desired that this time be minimized. The payback period occurs in the period of time in which the result of the cumulative sum of the cash flows becomes positive. However, this method is not widely used because it does not take into account the present value of cash flows. In this regard, the discounted payback period is more correct, because although it is calculated in the same way, it uses the values of the updated cash flows [89].

Chapter 3

Cost Model Development

This chapter presents the cost model developed and implemented within this thesis. After studying the various cost estimation techniques, materials and some production methods, a process based cost model (PBCM) of automated tape laying (ATL) for novel aircraft configurations was developed.

Thereafter, the cost model is described, starting with the decomposition of the manufacturing method and detailing all processes that incorporate it. Subsequently, all inputs required for the model are presented, as well as some of the intermediate calculations used by the model. Finally, the outputs of the model, which are divided into several types of costs, are shown. When all of them are added, the production cost estimate is finally achieved.

It should be noted that this cost model returns a preliminary estimate of production costs. With this, it is meant that only production phases are analysed and studied, excluding any type of previous or later phases, such as assembly. Likewise, outputs should be considered as approximate results, although these estimates can be very accurate. Cost models are not accounting tools, but engineering tools, used to make engineering decisions and it is only necessary that they are sensitive to the variables that influence the decision.

3.1 Process Based Cost Model

Before starting to develop the cost model, some assumptions had to be made. The type of material to be used, its production method and which cost estimation technique suits the production of novel aircraft configurations are some examples of these choices, previously studied in Chapter 2. Thereafter, it is explained how these assumptions were made.

Although the most used material in the aerospace industry is aluminium due to its advantages in terms of mechanical and thermal properties, wide experience and good machinability, composite materials have become increasingly appreciated in the sector. Their advantages in terms of strength-to-weight and stiffness-to-weight ratios, corrosion resistance, capacity to handle tensions, the reduced number of parts and fasteners used in the product assembly and the extended product life make composites a viable option for the future, and consequently, they are the type of material implemented in this production

model.

From the three composite production methods described in Section 2.5, ATL is the method selected for this model, not only for its advantages of high productivity of large and flat parts (due to the high deposition of material) but also due to the cost of material used by ATL machine which is lower when compared with the one used in the AFP machine. The hand lay-up and AFP methods are then discarded.

As referred in Section 2.3, with regard to estimation techniques, analogical and parametric methods are fundamentally based on historical data to develop cost estimations, which makes it impossible to estimate novel aircraft configurations' costs. A process based cost model (PBCM) is then developed through the decomposition of the necessary processes for the production of parts using ATL. The cost estimate is generated associating all costs related to each process. The advantages of this process are that it does not require historical data and it is a functional method for both novel and conventional aircraft configurations.

The model is developed in Excel and composed by processes which are detailed in the following section.

3.2 Processes

The PBCM is developed by decomposing the manufacturing method, as shown in Figure 3.1. This method can be divided into seven phases, which individually correspond to a particular production process. The assembly phase, as already mentioned, is not included in the cost model, since this is a preliminary model of production costs. Any kind of prior and/or post-production costs are not included in this template.

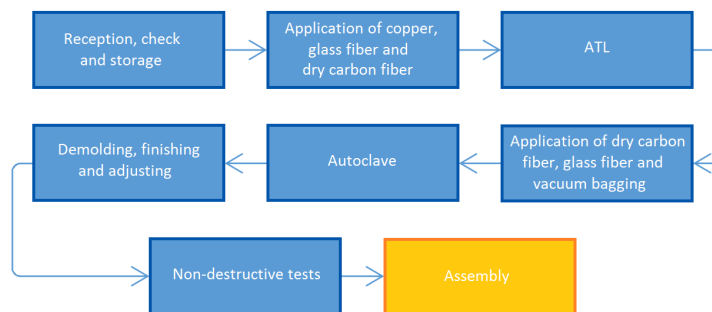


Figure 3.1: Processes of the manufacturing method.

The seven processes that incorporate the manufacturing method are:

1. **Reception:** When the material arrives at the plant, it is listed and stored in a refrigerated place so that there is no loss of properties, especially of the prepregs. Subsequently, for the production of parts, it is necessary to remove the material from the refrigerating chambers previously, so that it thaws and it is ready to be used in the following phases.
2. **Application of copper, glass fiber and dry carbon fiber:** In this phase, the first layers of material are placed in the mold. First, a copper layer is applied followed by a glass fiber layer, that protects

against lightning strikes and prevents the part from galvanic corrosion, respectively. Then, a dry layer of carbon fiber is deposited, which will initiate the next phase of fiber placement. For model simplification, these layers, placed by hand lay-up, do not contribute to the thickness of the part.

3. **Fiber Placement:** The deposition of material over the desired area is performed by the ATL machine, until it reaches the intended thickness. The material used in this process is the prepreg.
4. **Application of dry carbon fiber, glass fiber and vacuum bagging:** To finish the deposition of material, it is placed one last dry layer of carbon fiber and another of glass fiber to prevent, once again, the part from galvanic corrosion. The part is sealed inside a vacuum bagging with a bleeder and a breather material inside to absorb the excess resin and facilitate the absorption of air during the cure, respectively.
5. **Autoclave:** The part is transported to the autoclave, where it is cured with increasing temperature and pressure, which makes the process faster and promotes a better finish to the part in terms of quality.
6. **Demolding, finishing and adjusting:** After the cure, the molds are removed and last finishes are made, for example, the burr is removed from the entire perimeter of the part.
7. **Non destructive tests:** Finally, the part is submitted to non destructive tests to ensure that there are no defects.

In the developed cost model, each process of the manufacturing method receives a set of inputs and returns the outputs, as shown in Figure 3.2. The outputs of each phase are the costs of the process, that when finally added, lead to the production cost estimate of the part.

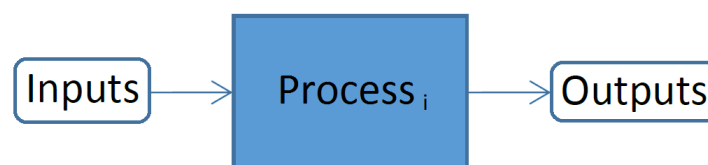


Figure 3.2: Process block.

It is presented below the various types of inputs of the developed cost model.

3.3 Inputs

In order to develop the cost model, it is necessary to introduce several types of inputs. For better understanding, it is decided to divide them into four groups: exogenous, material, process and part data. In the following sections, within each group, the input variables and respective physical quantities are presented. Later, in Chapter 4, the values for each variable will be assigned. These values were obtained from the aerospace industry, from the MDO framework developed by IST and also from own calculations.

3.3.1 Exogenous Data

The first group of inputs presented, named exogenous data, are common inputs for all phases that are dependent on the operation and organization of the company. In Table 3.1, the inputs referring to the company and their associated physical quantities are presented.

Table 3.1: Exogenous Data.

Exogenous Data	
Days per Year	<i>days/year</i>
Wage (including benefits)	<i>€/h</i>
Energy Unit Cost	<i>€/kWh</i>
Interest Rate	<i>%</i>
Building Unit Cost	<i>€/m²</i>
Equipment Life	<i>years</i>
Building Life	<i>years</i>
Production Period	<i>years</i>
Idle Space	<i>%</i>

Table 3.1 shows the number of days that a company works per year, the employees' payment per hour including the respective benefits, the energy cost per kilowatt hour (*kWh*), the interest rate at which the investment is annualized, the price invested in the building per square meter, the equipment and the building life which represents the mean duration of these items, the production period and finally the percentage of idle space available inside the building.

3.3.2 Material Data

In this group of inputs, called material data, the variables are dependent on the type of material used in the deposition phases. Four types of materials are defined: copper, glass fiber, dry carbon fiber (these three used in the second and fourth phase) and prepreg carbon fiber (used in the fiber placement by ATL machine, which corresponds to the third phase). Inputs related to the material data are presented in Table 3.2 with the respective physical quantities mentioned.

Table 3.2: Material Data.

Material Data	
Density	<i>g/m²</i>
Cost per <i>m²</i>	<i>€/m²</i>
Scrap Price	<i>€/kg</i>
Layer Height	<i>mm</i>

For each material used, it is required one set of inputs like those presented in Table 3.2: material density, material cost per square meter (*m²*), scrap price per kilogram of material and layer height after the cure.

3.3.3 Process Data

The specific inputs of each of the seven processes, which vary in value according to the characteristics and needs of each of them, are presented in Tables 3.3 and 3.4. These tables also show their respective physical quantities.

In Table 3.3, inputs related to the characteristics of the process, that define its quality, are presented.

Table 3.3: Manufacturing Process Data.

Manufacturing Process Data	
Technical Scrap	%
Pass	%
Rework	%
Non-Quality Scrap	%
Rework Pass	%
Rework Scrap	%
Material required in Rework	%

As can be seen in Figure 3.3, the process is characterized by percentages of *pass* and *rework pass*, which represent the number of parts that verify the quality requirements to go through the next process. The difference between these two inputs is that the first represents the number of parts that are finalized in the first pass of the process and the second represents the number of parts that are finalized after rework of the process. In turn, the percentage of *rework* represents the number of defective parts that can be reworked and corrected. The percentages of *non-quality scrap* and *rework scrap* are also presented. They reflect the number of parts that do not check the quality levels to move on to the next process (after the first pass and after rework, respectively). The percentage of *material required for rework* represents the amount of material needed for the correction of defects during rework. Finally, the percentage of *technical scrap* represents the wasted material during the process and that can not be avoided, as seen in Figure 3.4.

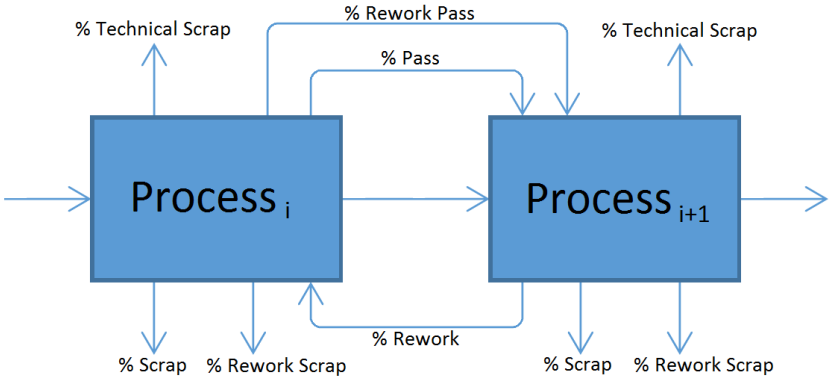


Figure 3.3: Process details.

Through Figure 3.3, it is verified that when there is loss of number of parts, the number of parts inserted at the beginning of the process is not the same as the obtained at the end. Therefore, there is a need to produce a larger volume of parts so that the desired number of units can be obtained in the end.

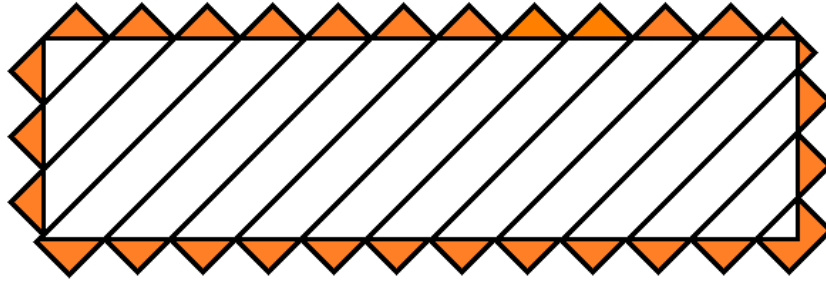


Figure 3.4: Technical scrap.

Consequently, it is introduced a new variable, the actual production volume, which will be discussed later in Section 3.4.

Other inputs related to the process are presented in Table 3.4, as well as their physical quantities.

Table 3.4: Infrastructure-related Process Data.

Infrastructure-related Process Data	
Workers	<i>units/machine</i>
% Dedication	%
Floor Space	<i>m²/machine</i>
Number of Machines	<i>units</i>
Acquisition Cost	<i>€/machine</i>
Energy Consumption	<i>kWh</i>
Setup Time	<i>h</i>
Machine Time	<i>h</i>
% Maintenance	%
% Overheads	%
% Allocation	%

Table 3.4 presents variables, such as the number of workers per machine, the percentage of workers' dedication to the process, the space used per machine or workstation, the number of machines needed for production and their individual cost, and also the energy consumption per hour of each machine. The setup time and the machine time, which represent the preparation time required before machining and the time the machine takes to perform the process, respectively, are also inserted in the model. The percentage of maintenance related to machine investment and the percentage of overheads related to labor cost, used for the cost estimation (that will be defined later) are presented in this table too. The percentage of allocation is another inserted variable, which represents the time required in the production line for the production of one type of parts.

Note that machine time is a variable that depends on the area and perimeter of the part under analysis, although, it is considered as an input to the cost model. Part allocation is also considered as a process-specific input despite varying with cycle times, in case the machine is not solely and exclusively dedicated to the production of one type of parts. If the process is dedicated to the production of only one type of parts and there is no idle time, the allocation percentage of that type is 100%. These variables are demonstrated in Section 3.4, since they require calculations to obtain their values.

There are also the consumables used in the production method. In the case of ATL, the only consumables considered are the molds used in the production of the parts, exclusive inputs of the fiber placement process. As shown in Table 3.5, in the fiber placement process it is necessary to enter the number of molds used, the acquisition price of each one, the preparation time of the mold and also the consumables cost used per square meter. These inputs, as will be seen when presenting the costs in Section 3.5, have an impact on material costs, labor cost and tooling costs of the fiber placement process exclusively.

Table 3.5: Consumables data.

Consumables Data	
Number of Molds	<i>units</i>
Mold Cost	€/unit
Mold preparation	<i>h</i>
Consumables	€/m ²

Finally, inputs related to the downtime information of the production line are presented, such as the worker unpaid and paid breaks, the on-shift maintenance and the unplanned downtime. These concepts will be explained below. In Figure 3.5, it can be observed all the periods of a production line.

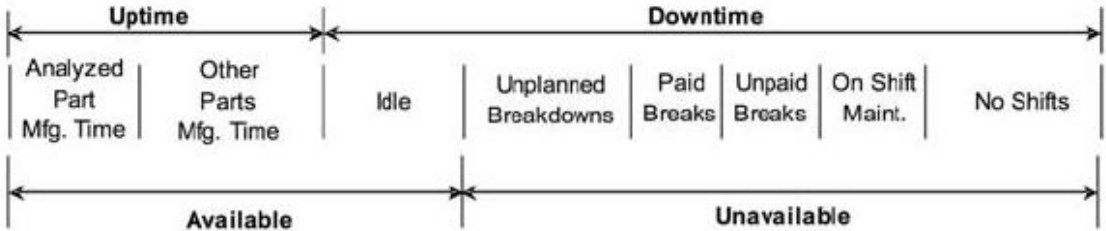


Figure 3.5: Production line.

The operating period of a production line can be divided into available and unavailable time. The available time is the sum of the uptime with idle time. In turn, the uptime represents the line’s production time and the idle time represents the time that the line could be in operation if there were more production volume. The unavailable time is the period used for maintenance, no shifts and all type of breaks. The downtime is obtained by summing the unavailable time with the idle time, and it corresponds to the non-productive time.

It should be noted that, in a production line, the main objective of the companies is to decrease the value of downtime. In order to do this, all types of time breaks must be reduced, maintenance times should not be focused on high production periods and, above all, idle time should be minimized. An ideal production line is one whose uptime is equivalent to the available time, or in other words, an idle time equals to zero. Maximizing the production volume of the number of machines in the process, it is possible to obtain the lowest value of idle time and achieve the best yield of the production line, as can be seen in the cases studied in Chapter 4. It is concluded that the production volume and the number of machines are two inputs mutually dependent: on one hand, a production volume can be fixed and

the number of machines needed for that volume can be determined; and on the other hand, the number of machines can be limited and the maximum production volume for the best line performance can be determined.

3.3.4 Part Data

Finally, inputs related to the parts are shown, namely geometric characteristics of parts and their production volumes.

To facilitate the reader’s understanding, the nomenclature of an airfoil is shown in Figure 3.6.

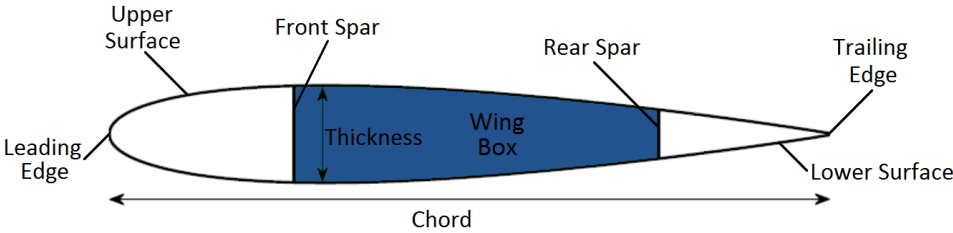


Figure 3.6: Airfoil nomenclature.

As shown, an airfoil has two surfaces: the upper surface, also called suction surface, which is associated to high velocities and a lower static pressure; and the lower surface, also called pressure surface, which has a higher static pressure. This pressure gradient between the two surfaces contributes to the airfoil lift force. In Figure 3.6, it is also observed the leading edge, the point where the airflow is separated, and the trailing edge, the point where the airflow separated by the leading edge reunites. It is depicted the chord (the line that joins the leading and trailing edges) and the thickness, which is the distance between suction and pressure surface. Lastly, the figure shows two structural reinforcement bars that limit the wing box, designated front and rear spars, respectively, also known as webs.

The cost model should receive as inputs the thickness, the perimeter and the area of each part that will be produced. However, the data that is provided by MDO framework developed by the IST Aerospace Group arrives through coordinates of points, dimensionless relations and percentages, as indicated in Table 3.6. In Chapter 4, it is verified that each data line of Table 3.6 provides information about a given airfoil. It is through linear interpolation of the coordinates of these same airfoils that geometries of surfaces are obtained. These data must be inserted in the cost model, as it will be seen later.

Table 3.6: Geometry Data.

Leading Edge Position			Chord (m)	Airfoil File	Spar Position		t_w/c	t_s/t_{max}
X (m)	Y (m)	Z (m)			Front (%)	Rear (%)		
...	

As can be seen in the Table 3.6, the coordinates X , Y and Z of the airfoils leading edge are given. It is also provided the chord (c) and the type of each airfoil, which generally vary along the wingspan. It should be noted that the type of airfoil assigned corresponds to a set of dimensionless values that need

to be sized to generate the geometries of the parts that will be produced. Thereafter, the percentages related to the chord, regarding the positioning of front and rear spars, are also provided. Finally, the dimensionless thicknesses of spars (t_w/c) and skins (t_s/t_{max}) referred to the wing box are indicated. These factors can be dimensioned by the chord and the maximum thickness (t_{max}) of the airfoil, respectively. Note that the data provided by the MDO framework also presents characteristics about the aircraft fuselage, although, and as it will be seen in Chapter 4, this thesis only addresses the lifting surfaces (main wing and rear wing) and the tail (vertical and horizontal).

In this thesis, the only components of wings to be analysed are spars and skins, since their information is the only data that can be extracted from the MDO framework. During model development, it is considered that the wing is divided according to the number of airfoils and, subsequently, through linear interpolation between equivalent points of two consecutive airfoils, it is possible to represent a surface, as shown in Figure 3.7.

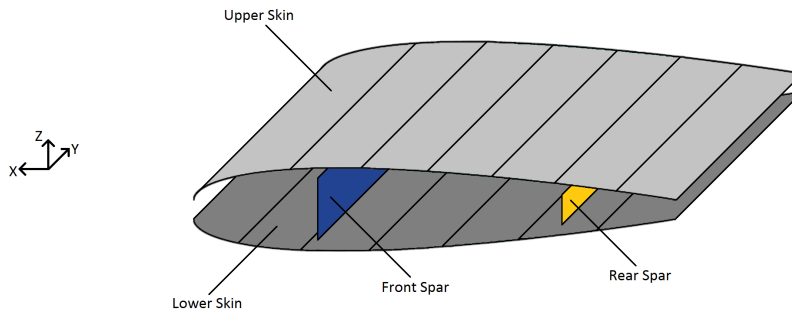


Figure 3.7: Wing section.

The analysed surfaces are thus divided into sections comprised between two airfoils. Also, in order to simplify data handling, it is assumed that each section is divided into four parts: two skins, the upper and the lower skins, and two spars, the front and the rear spars.

Thereafter, the necessary steps for the conversion of data in the respective inputs of the cost model are demonstrated: thicknesses, perimeters and areas of parts.

In order to calculate thicknesses of spars and skins, the following Equations 3.1 and 3.2 must be used, respectively.

$$t_w = \frac{t_w}{c} \cdot c. \quad (3.1)$$

$$t_s = \frac{t_s}{t_{max}} \cdot \frac{t_{max}}{c} \cdot c. \quad (3.2)$$

In Equation 3.1, t_w/c is the dimensionless thickness of the spar and c is the airfoil chord. In equation 3.2, t_s/t_{max} is the dimensionless thickness of the skin, t_{max}/c represents the relative position of the maximum thickness in the airfoil chord c .

In both spars and skins, the thickness varies linearly with the wingspan from the root to the tip of the wing. Since it is a composite material and the production of parts is carried out through deposition layer by layer, the model is simplified considering that a wing can be divided into several parts, each one with

a constant thickness, as presented in Figure 3.8. With this, the thickness ceases to be continuous along the wingspan, but in order to comply the safety factors, a conservative approach is taken and the greater thickness, verified in the part, is always the chosen one. As can be seen in Figure 3.8, the thickness that varies linearly (which corresponds to the real values) is always below the several constant thicknesses.

Note that the greater the discretization along the span, the better the thickness approximation along the same span. However, the model assumes a discretization according to the number of airfoils that constitute a wing for two reasons. Firstly, despite the presented advantages, a high discretization considerably reduces the dimensions of parts that constitute the wing, which can make their production unfeasible through ATL. Secondly, there is a simplification in data handling, using only the input data from the MDO framework, without further point interpolation being required.

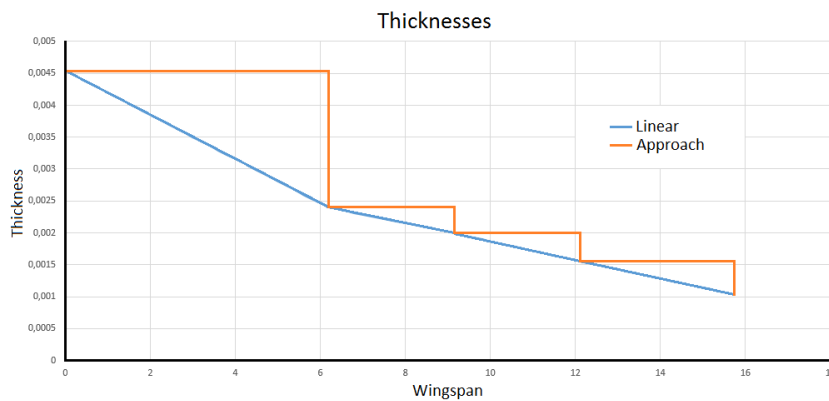


Figure 3.8: Thickness in relation to wingspan.

Another assumption to take into consideration are the skin thicknesses outside the wing box (highlighted in orange in Figure 3.9). Despite not being analysed by the MDO framework, they should be assigned with the same values of the skin thicknesses of the wing box.

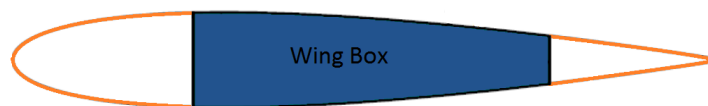


Figure 3.9: Skin thicknesses.

In order to calculate perimeters and areas of the several parts that constitute a wing, shown in Figure 3.7, airfoils need to be sized, as previously mentioned. To size one, the dimensionless coordinates must be multiplied by the chord and then summed with the position coordinates of the leading edge. In the case of sizing the lifting surfaces, such as the main wing, the horizontal tail and the rear wing, the Equations 3.3, shown below, must be used.

$$X = X_{LE} - x \cdot c. \quad (3.3a)$$

$$Y = Y_{LE}. \quad (3.3b)$$

$$Z = Z_{LE} + y \cdot c. \quad (3.3c)$$

In the case of sizing the vertical tail, Equations 3.4 must be used.

$$X = X_{LE} - x \cdot c. \quad (3.4a)$$

$$Y = Y_{LE} + y \cdot c. \quad (3.4b)$$

$$Z = Z_{LE}. \quad (3.4c)$$

These equations size the airfoil coordinates in X , Y and Z , respectively. The coordinates X_{LE} , Y_{LE} and Z_{LE} are the leading edge position coordinates, the coordinates x and y are the dimensionless coordinates of the airfoil (obtained through the airfoil files) and c is the chord value.

After sizing the airfoils, it is possible to calculate their perimeter. Using linear interpolation between two airfoil points, as can be seen in Figure 3.10, the distance l_i between these two points can be calculated. Equation 3.5 demonstrates how to calculate the distance between two points through their coordinates.

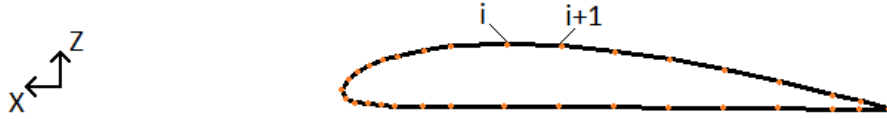


Figure 3.10: Segmented airfoil approach.

$$l_i = \sqrt{(X_{i+1} - X_i)^2 + (Z_{i+1} - Z_i)^2}. \quad (3.5)$$

In Equation 3.5, X_i and Z_i are the coordinates of a point and X_{i+1} and Z_{i+1} are the coordinates of the consecutive point.

After the distances l_i between all airfoil points had been calculated, the perimeter of the airfoil can be quantified through the sum of l_i of all N segments (N_{seg}), as the following equation presents.

$$AirfoilPerimeter = \sum_{i=1}^{N_{seg}} l_i. \quad (3.6)$$

As shown in Figure 3.7, a skin is bounded by two airfoils. Its perimeter is the sum of the perimeters of the two surfaces that limit it (upper surfaces, in the case of the perimeter of the upper skin, or lower surfaces, in the case of the perimeter of the lower skin) with the distance between the leading edges and the distance between the trailing edges of the same airfoils. Figure 3.11 exemplifies the necessary measures to calculate the upper skin perimeter.

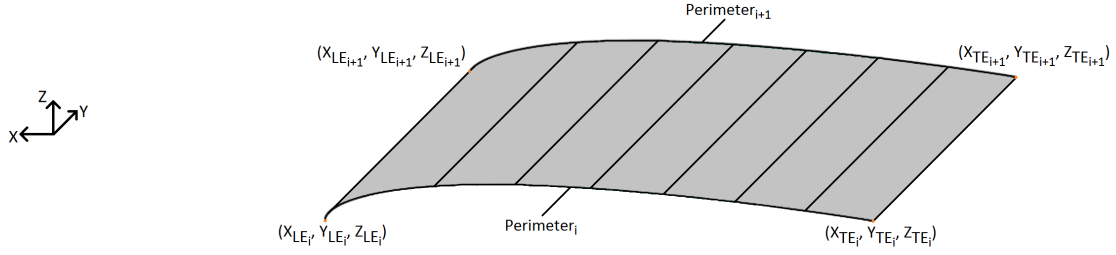


Figure 3.11: Example of an upper skin.

Equation 3.7 shows how to calculate the perimeter of a skin.

$$\begin{aligned} \text{Skin Perimeter} = & \text{Perimeter}_i + \text{Perimeter}_{i+1} + \\ & \sqrt{(X_{LE_{i+1}} - X_{LE_i})^2 + (Y_{LE_{i+1}} - Y_{LE_i})^2 + (Z_{LE_{i+1}} - Z_{LE_i})^2} + \\ & \sqrt{(X_{TE_{i+1}} - X_{TE_i})^2 + (Y_{TE_{i+1}} - Y_{TE_i})^2 + (Z_{TE_{i+1}} - Z_{TE_i})^2}. \quad (3.7) \end{aligned}$$

In equation 3.7, X_{LE} , Y_{LE} and Z_{LE} represent the coordinates of the leading edges of airfoils and X_{TE} , Y_{TE} and Z_{TE} the coordinates of the trailing edges of the same airfoils.

In the case of spars, the perimeter is given by the sum of the spar heights in airfoils (h_k and h_{k+1}) with the distances that separate them (distances between the coordinates of points i and $i+1$ and points j and $j+1$), as shown in Figure 3.12.

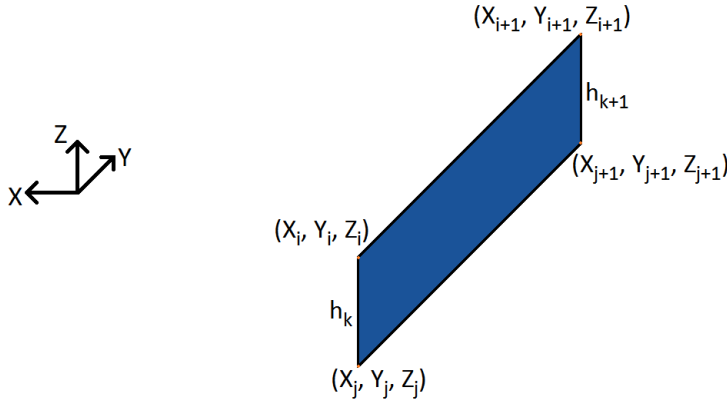


Figure 3.12: Example of a spar.

The perimeter of a spar is calculated using Equation 3.8, shown below.

$$\begin{aligned} \text{Spar Perimeter} = & h_k + h_{k+1} + \\ & \sqrt{(X_{i+1} - X_i)^2 + (Y_{i+1} - Y_i)^2 + (Z_{i+1} - Z_i)^2} + \\ & \sqrt{(X_{j+1} - X_j)^2 + (Y_{j+1} - Y_j)^2 + (Z_{j+1} - Z_j)^2}. \quad (3.8) \end{aligned}$$

In this equation, the square roots represent the distance calculation between the points coordinates i with $i+1$ and j with $j+1$. The spar heights, represented by h_k and h_{k+1} , are obtained by Equation 3.9.

$$h = \left[\left(\frac{X_{spar} - X_m}{X_{m+1} - X_m} \cdot (Z_{m+1} - Z_m) + Z_m \right) - \left(\frac{X_{spar} - X_n}{X_{n+1} - X_n} \cdot (Z_{n+1} - Z_n) + Z_n \right) \right]. \quad (3.9)$$

The spar height in an airfoil is obtained by two linear interpolations between two points on the upper surface and two points on the lower surface, as shown in Figure 3.13. Through the spar position relative to the chord, and the interpolations between previous and consecutive points to this position, it is possible to calculate the spar height. In the equation referred above, X_{spar} is the X spar coordinate in airfoil, the coordinates (X_m, Z_m) and (X_n, Z_n) are the coordinates of the points that precede the X_{spar} in the upper and lower surface, respectively, and the coordinates (X_{m+1}, Z_{m+1}) and (X_{n+1}, Z_{n+1}) are the coordinates of the points that proceed the X_{spar} in the upper and lower surface, respectively.

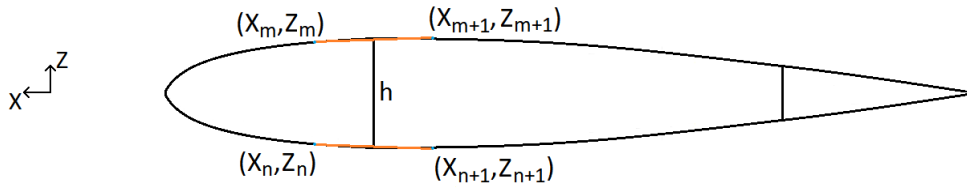


Figure 3.13: Linear interpolation between two points.

Regarding the areas, the fact that some parts have curvature makes it difficult to calculate their values. Thereby, and to simplify it, the skin is assumed to be a flat surface and the area of both skin and spar can be represented by the area of a trapezoid. It is known that the area of this geometric figure is given by Equation 3.10.

$$Trapezium\ Area = \frac{Base_1 + Base_2}{2} \cdot H. \quad (3.10)$$

In the equation, $Base_1$ and $Base_2$ are the bases and H is the height of the trapezoid.

Given this, Equations 3.11 are used to calculate the skin areas, where the bases of the trapezoid are given by the perimeters of the upper or lower surface of the airfoils, depending on the skin under analysis, and the height of the trapezoid is given by the difference of the coordinates that separate the airfoils. In the case of lifting surfaces, such as main wing, horizontal tail and rear wing, the height of the trapezoid is given by the difference between Y coordinates, represented in Equation 3.11a. In the case of vertical tail, the height of the trapezoid is given by the difference between Z coordinates, represented in Equation 3.11b.

$$Skin\ Area = \frac{Perimeter_i + Perimeter_{i+1}}{2} \cdot (Y_{i+1} - Y_i). \quad (3.11a)$$

$$Skin\ Area = \frac{Perimeter_i + Perimeter_{i+1}}{2} \cdot (Z_{i+1} - Z_i). \quad (3.11b)$$

The calculation of a spar area is identical. However, the trapezoid bases are given by the spar heights in the airfoils (see Equation 3.9) and the height of the trapezoid is the distance calculated through the square roots presented in Equations 3.12. In the case of lifting surfaces, such as main wing, horizontal

tail and rear wing, the height of the trapezoid is given by the distance between two points with coordinates in the Oxy referential, represented in Equation 3.12a. In the case of vertical tail, the height of the trapezoid is given by the distance between two points with coordinates in the Oxz referential, represented in Equation 3.12b.

$$S_{par\ Area} = \frac{h_i + h_{i+1}}{2} \cdot \sqrt{(X_{i+1} - X_i)^2 + (Y_{i+1} - Y_i)^2}. \quad (3.12a)$$

$$S_{par\ Area} = \frac{h_i + h_{i+1}}{2} \cdot \sqrt{(X_{i+1} - X_i)^2 + (Z_{i+1} - Z_i)^2}. \quad (3.12b)$$

After this procedure, thicknesses, perimeters and areas of the parts can be obtained, which are the last inputs necessary for the cost model.

3.4 Intermediate Calculations

This section demonstrate some intermediate calculations about material and time, two main cost drivers of this cost model. The presented variables are fundamental to cost analyses and important to the model development.

3.4.1 Material

As previously introduced in Section 3.3.3, the production processes are not ideal. There is a percentage of pass that causes a reduction of the number of parts obtained at the end of each production process when compared to the number of parts initially inserted. Thereby, it is necessary to produce a production volume greater than the desired volume at the end. It is a calculation based on the objective. The initial production volume decreases throughout the processes and the number of parts required in each process can be given by Equation 3.13.

$$Number\ of\ Parts_i = \frac{Number\ of\ Parts_{i+1}}{\% Pass_i + \% Rework_i \cdot \% Rework\ Pass_i}. \quad (3.13)$$

This equation demonstrates that the number of parts required in a process i is equal to the number of parts needed for the subsequent process $i+1$ divided by the percentages of pass, defined as process inputs.

Other important variable to the following equations is the part weight, given by Equation 3.14. In this equation, $Area$ represents the part surface area, $Layers$ represents the number of composite layers necessary to obtain the desired thickness (Equation 3.15) and $Density$ represents the density of the composite material given in kilograms per square meter (kg/m^2).

$$Part\ Weight = Area \cdot Layers \cdot Density. \quad (3.14)$$

$$Layers = \frac{Part\ Thickness}{Layer\ Height} . \quad (3.15)$$

In Equation 3.15, *Part Thickness* is the desired thickness given in millimeters (*mm*) and *Layer Height* is the layer height after the cure, also given in millimeters.

The final variable presented, related to the material, is the technical scrap percentage, previously introduced in Section 3.3.3, as an input. For most processes used in this cost model, this variable uses approximate constant values, obtained through the contact with industry technicians. However, for the ATL process, the percentage of technical scrap is calculated according to the aircraft structure (main wing, rear wing, horizontal and vertical tails) to be produced. Each part is produced by placing layers of carbon fiber that can be oriented in four directions: 0° , 90° , $+45^\circ$ e -45° , as shown in Figure 3.14.

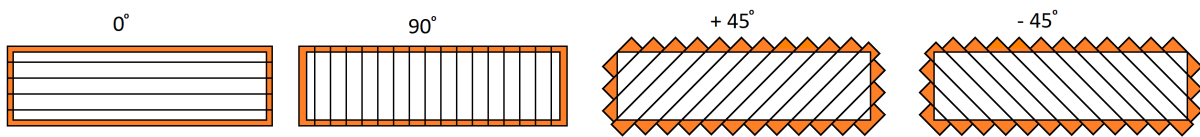


Figure 3.14: Technical scrap according to different tape orientations.

Thereby, the percentage of technical scrap of each component is achieved through the average of the percentages of technical scrap obtained in each direction, as presented in Equation 3.16.

$$\% Technical\ Scrap = \frac{\sum_{d \in \{-45^\circ, 0^\circ, +45^\circ, 90^\circ\}} \% Technical\ Scrap_d}{4} . \quad (3.16)$$

3.4.2 Time

Regarding this cost driver, cycle time is another important variable during the cost model and it is presented below.

$$Cycle\ Time = Setup\ Time + Machine\ Time . \quad (3.17)$$

In a process, the cycle time is given by the sum between setup time and machine time. The setup time, also referred in Section 3.3.3, represents the preparation time required before machining and it is a constant input, independent of the size of the part to be produced. The machine time is the time that the machine takes to carry out the process, being therefore a variable that depends on the part size and/or on the speed of the machine during the process. Machine time formulas used in each process are presented below.

In most processes of this cost model, the machine time is obtained through a relation with an area or a perimeter of the part to be produced. In the cases of processes that **precede** and **proceed the fiber placement** and in **non-destructive tests**, the machine time is given by an area relation. The machine time of a given part is obtained by comparing the machine time of a part previously produced on that same machine, as presented in the following Equation 3.18. One can note that the deposition rate is not a linear function, but this is a feasible approximation.

$$Machine\ Time_i = \frac{Machine\ Time}{Area} \cdot (Area_i). \quad (3.18)$$

In this equation, $Machine\ Time_i$ and $Area_i$ correspond to the part i under analysis, while $Machine\ Time$ and $Area$ correspond to values taken from a part example previously produced.

In the case of **demolding, finishing and adjusting** process, the procedure is exactly the same, except that the machine time relation is obtained through the perimeter, represented in Equation 3.19.

$$Machine\ Time_i = \frac{Machine\ Time}{Perimeter} \cdot (Perimeter_i). \quad (3.19)$$

In this equation, and similarly to the previous one, $Machine\ Time_i$ and $Perimeter_i$ correspond to the part i under analysis, while $Machine\ Time$ and $Perimeter$ correspond to the values taken from a part example previously produced.

Regarding the **fiber placement** process, the machine time is calculated through a lay-up rate obtained by Lukaszewicz [71]. A study of fiber placement was performed on flat parts with approximately rectangular geometry and different dimensions, and it was verified that the lay-up rate is related to the part size. The result of the study can be seen in Figure 3.15.

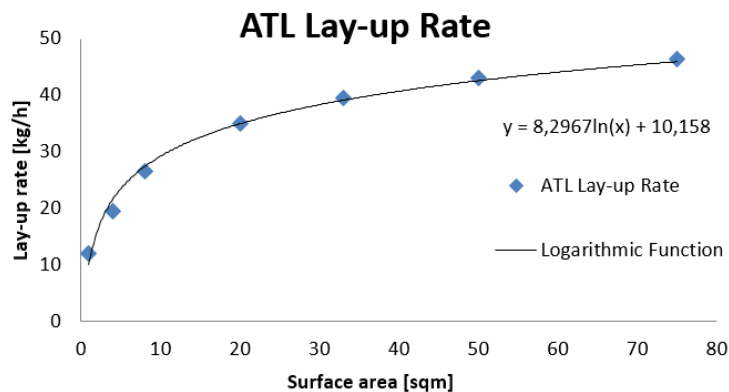


Figure 3.15: ATL lay-up rate [71].

Analyzing the graphic of Figure 3.15, it is verified that the lay-up rate increases logarithmically with the increase of the part surface area. A low lay-up rate is associated to small geometries because the optimum placement speed of the machine can not be reached. However, with the increasing of parts' area, the optimum speed of the machine is reached, increasing the lay-up rate, as can be seen in the graphic.

In the case of aircraft skins which have curvature along the chord, it is assumed that, due to their high dimensions, they can be considered as flat parts. Thus, the result of the study presented above can be used to calculate the machine time of the fiber placement. The curve which represents the lay-up rate as a function of the surface area is given by Equation 3.20.

$$Lay\ Up\ Rate = 8.2967 \cdot \ln(Area) + 10.158. \quad (3.20)$$

Once the lay-up rate is defined, the ATL machine time is calculated. Knowing that the lay-up rate is given in kilograms per hour (kg/h) by Equation 3.20, the ATL machine time can be given by Equation 3.21, dividing the weight of part in production (Equation 3.14) by lay-up rate.

$$Machine\ Time_{ATL} = \frac{Part\ Weight}{Lay\ Up\ Rate} \quad (3.21)$$

In the case of the **autoclave** process, the machine time represents the curing time of the part inside the autoclave and depends on the characteristics of the prepregs applied. Due to the large size of an autoclave, more than one part can be cured at the same time and, consequently, the machine time can be given by the following Equation 3.22.

$$Machine\ Time_{Autoclave} = \frac{Cure\ Time}{N} \quad (3.22)$$

In Equation 3.22, *Cure Time* represents the time the autoclave takes to cure parts, a constant value according to the prepregs placed, and *N* represents the number of parts that can be cured at the same time inside the autoclave.

In the case of the **reception, check and storage** process, the cycle time is considered constant and independent of part dimensions. The cycle time of this process starts with the arrival of material to the plant, continues with the storage time followed by the thawing time of material, and ends when the material is ready to be used in the following process. This value depends on the organization and operation mode of the plant and is obtained through the process duration.

With cycle times of each part and with the number of parts to be produced in each process, it is possible to calculate the time required for the production of all types of parts in each process, as can be seen in Equation 3.23.

$$Time\ Required_{ij} = Cycle\ Time_{ij} \cdot Number\ of\ Parts_{ij} \quad (3.23)$$

In Equation 3.23, *Cycle Time_{ij}* represents the time that a part of type *i* takes to be produced in the *j* process and *Number of Parts_{ij}* indicates the number of parts *i* to be produced in the *j* process. It is assumed a matrix, whose lines represent distinct types of parts and each column represents a process of this manufacturing method, as can be observed in the tables of Appendix A.

Through the times required for the production of different types of parts in each process, it is possible to determine the time it takes to produce all types of parts in each process, equivalent to the uptime of each process. This productive time can be calculated through Equation 3.24, a sum of the required times of the various types of parts in each process, where *t* represents the number of types of parts.

$$Uptime_j = \sum_{i=1}^t Time\ Required_{ij} \quad (3.24)$$

Knowing the times required for the production of each type of parts and the uptimes of each process, it is then possible to calculate the allocation of each type of parts in the production line through the following Equation 3.25.

$$Allocation_{ij} = \frac{Time\ Required_{ij}}{Uptime_j} . \quad (3.25)$$

The allocation of the production line in a process is the percentage of time required for the production of one type of parts in relation to the time required to produce all types of parts in that process. Note that if the sum of allocations is 100%, it means that the process is solely dedicated to the production of the various types of parts required, and there are no more parts to be produced.

Finally, it remains to be seen whether the number of machines in each process is sufficient for the production of all parts. Knowing the uptime in advance and then knowing that the available time can be given by Equation 3.26, it is possible to calculate idle time.

$$Available\ Time = 24h - (On\ shift\ maintenance + Worker\ Unpaid\ breaks + Worker\ Paid\ Breaks + Unplanned\ Downtime) . \quad (3.26)$$

The idle time, which represents the time that the line could be in operation if there were more production volume, is given by Equation 3.27.

$$Idle\ Time = Available\ Time - Uptime . \quad (3.27)$$

It should be noted that idle time can never be less than zero, otherwise it would mean that there is not enough time to produce all parts. In this case, either the production volume decreases or the number of machines increases, until the idle time returns to positive.

3.5 Costs

The cost model aims to analyse the production method and generate a cost associated with the process. The costs, detailed below, vary essentially according to the geometry of the part, its production volume and the size of the plant. In each process of this model, annual process costs are calculated, which are then converted into unit production costs, when divided by the annual production volume. The final production cost is obtained by the sum of all processes costs that compose the manufacturing method.

In each process, costs are divided into variable and fixed costs, presented in the following sections. The annual variable costs depend mainly on the production volume, however, these costs per part are approximately constant. Fixed costs are calculated by allocating an annual cost as an annuity of the investment and are constant as long as the plant structure does not vary. They are also constant costs on an annual scale and therefore, the larger the production volume, the lower the unit cost of production, provided that the allocation of the production line is not exceeded.

3.5.1 Variable Costs

As mentioned, variable costs are costs that depend essentially on the volume of production. These costs can be divided into material, scrap, labor, overhead and energy costs.

The **material cost** represents the value of the materials used in the production of parts. This cost takes into account the value of the materials required in both the production and necessary rework, and also the value of the consumables spent during the process. Equation 3.28 demonstrates how material costs can be calculated.

$$\text{Material Cost} = \text{Material Cost}_{\text{Production}} + \text{Material Cost}_{\text{Rework}} + \text{Consumables} . \quad (3.28)$$

The value of the material only used in production is given by Equation 3.29. The area and the number of layers of the part, the number of parts required in the process under analysis, the material cost per square meter and the percentages of rework, technical scrap and material required for rework are the necessary values to calculate this variable.

$$\begin{aligned} \text{Material Cost}_{\text{Production}} = & \text{Part Area} \cdot \text{Layers} \cdot \text{Number of Parts} \cdot \text{Cost per area} \\ & \cdot (1 + \% \text{Material}_{\text{Rework}} \cdot \% \text{Rework}) \cdot (1 + \% \text{Technical Scrap}) . \end{aligned} \quad (3.29)$$

In the case of the material value spent in rework, the cost is given by Equation 3.30, which multiplies the material cost per square meter with the area and number of layers of the part, the number of parts to be produced in the process and also with the percentages of rework and material required for rework relative to the same process.

$$\text{Material Cost}_{\text{Rework}} = \text{Cost per area} \cdot \text{Number of Parts} \cdot \% \text{Material}_{\text{Rework}} \cdot \text{Part Area} \cdot \text{Layers} \cdot \% \text{Rework} . \quad (3.30)$$

Finally, consumables are the last variable applied in Equation 3.28, only used in the fiber placement process. When calculating the material costs of all other production processes, this variable does not exist, as previously mentioned in Section 3.3.3. Molds, required to maintain the part shape during production, are some examples of consumables. In Equation 3.31 it is verified that this cost is given by multiplying the mold cost per area with the part area.

$$\text{Consumables} = \text{Cost per area} \cdot \text{Part Area} . \quad (3.31)$$

Scrap cost is another variable cost and it represents the amount spent to remove the wasted material. Unlike metals, the composite material is very difficult to be recycled due to the high costs of chemical separation. Thus, wasted material is converted into a cost to be dumped. The scrap cost is given by Equation 3.32.

$$Scrap Cost = Part Area \cdot Layers \cdot Material Density \cdot 10^{-3} \cdot Material Scrap Cost \cdot Number of Parts \cdot (\%Tech Scrap + \%Scrap + \%Rework \cdot \%Rework Scrap). \quad (3.32)$$

Labor cost represents the payment of employees who work directly on the production line. This variable cost depends on the number of workers per machine, the number of parts to be produced, the hourly wage that includes the benefits, the percentage of workers dedication to the machine and also the cycle time that defines the number of work hours. In Equation 3.33 the labor cost is demonstrated.

$$Labor Cost = Cycle Time \cdot Number of Workers \cdot Wage \cdot \%Dedication \cdot Number of Parts. \quad (3.33)$$

Note that in the case of the fiber placement process, it is added to the cycle time the time required for mold preparation, indicated as an input in Section 3.3.3.

Overhead costs are also variable costs associated with workers. However, these workers are indirectly related to the product operation. They are usually from engineering, administration or support areas. This cost can be approximated by Equation 3.34, multiplying the percentage of overheads with the labor cost value.

$$Overhead = Labor Cost \cdot \%Overheads. \quad (3.34)$$

The last variable cost introduced in this model is the **energy cost**. This expense represents the amount of money spent in energy consumption during the process and depends on the cycle time of each part, the number of parts to be produced, the energy consumption of the machine and also the cost of the energy unit (€/kWh).

$$Energy Cost = Cycle Time \cdot Number of Parts \cdot Energy Consumption \cdot Energy Unit Cost. \quad (3.35)$$

3.5.2 Fixed Costs

Fixed costs, as previously mentioned, are calculated by allocating an annual cost as an annuity of the investment. Depending on the type of investment under study, fixed costs can be related to main machine, tooling, building and maintenance. Equation 3.36 demonstrates how to calculate any fixed cost type.

$$Fixed Cost_i = Investment_i \cdot \left[\frac{Interest}{1 - (1 + Interest)^{-Lifetime}} \right]. \quad (3.36)$$

In this equation, it is considered a fixed interest rate, given as an input, and also a lifetime that can be related to the equipment, buliding or the production period, according to the fixed cost that is being

analysed.

When the investment is relative to the main machine of the process under analysis, fixed costs are denominated as **main machine costs**. In this case, Equation 3.36 uses a lifetime associated to the equipment and an investment that is given by Equation 3.37.

$$Investment_{Main\ Machine} = Machine\ Cost \cdot Machine\ Units \cdot \%Allocation. \quad (3.37)$$

In this equation, *Machine Cost* is the acquisition price of one machine of the process under analysis, the *Machine Units* indicates the number of machines required in the same process and the *%Allocation* represents the percentage of time used on the production line.

In the case of **tooling costs**, Equation 3.36 uses a lifetime associated to the production period and an investment given by Equation 3.38.

$$Investment_{Tooling} = Mold\ Cost \cdot Number\ of\ Molds. \quad (3.38)$$

The required inputs are the number of molds needed and the cost of each unit. This cost is exclusive of fiber placement process because it is the only process where the molds are inserted (the only tools considered throughout this manufacturing method).

Relatively to **building costs**, Equation 3.36 uses the lifetime associated to the building and the investment is calculated through the space occupied by the production line of the process, as can be seen in Equation 3.39.

$$Investment_{Building} = Floor\ Space \cdot Machine\ Units \cdot (1 + Idle\ Space) \cdot Building\ Unit\ Cost \cdot \%Allocation. \quad (3.39)$$

In the presented equation, the *Floor Space* represents the space occupied by each machine used in the process, the *Machine Units* indicates the number of machines required, the *%Allocation* is the percentage of time used on the production line, *Idle Space* is the percentage of unoccupied plant space and the *Building Unit Cost* represents the price per square meter of building area.

Finally, the last fixed cost presented is the **maintenance cost**. In this case, the lifetime, used in Equation 3.36, is relative to the equipment and the investment is given by the following Equation 3.40, through a percentage of maintenance that falls on the investment of the main machine.

$$Investment_{Maintenance} = Main\ Machine\ Investment \cdot \%Maintenance. \quad (3.40)$$

Chapter 4

Test Cases and Results

In this chapter, two test cases are presented. Two aircraft configurations from the Multidisciplinary Design Optimization (MDO) framework developed by the IST Aerospace Group are integrated in the cost model, proposed in the Chapter 3. A conventional and a joined wing model are analysed and the final results are evaluated and compared.

Two analyses are addressed in the study of the two aircraft: in the first one, the size of the plant was limited by the use of one machine for each process; in the second one, an annual production volume of 50 aircraft is desired.

Afterwards, a sensitivity analysis in regard to thickness is also carried out. The number of composite layers of each part is reduced and the impact in the final cost of production of an aircraft is reviewed.

Finally, with the results of the production costs obtained for each aircraft, an investment appraisal is carried out.

4.1 Part Data

In order to carry out the test cases, two aircraft configurations for the regional segment were developed in the MDO framework from the IST Aerospace Group. The first configuration is based on a conventional aircraft model, a low wing cantilever monoplane with swept back trapezoidal wings of moderated aspect ratio and positive dihedral. The second configuration is based on a novel aircraft configuration, a joined wing, in which the rear swept forward high wing joined the front swept back low wing near its tip. Both of them were designed to achieve the same requirements and due to that, there are some similarities between them. Because the objective is a comparison of production costs, only different parts were assumed to be relevant for the study. The parts that are equal, such as engines and fuselage, are not integrated. Therefore, only the main wing, rear wing, horizontal tail a vertical tail will be evaluated for having different dimensions and thicknesses.

In Tables 4.1 and 4.2 are presented the aircraft dimensions relative to the conventional and the joined wing configurations, respectively. These inputs are given by the MDO framework and are converted by the model into thicknesses, perimeters and areas that will be translated in production costs later. It

should be noted that the results achieved using the MDO framework for both aircraft were considering aluminium and not composite. However, since composite materials are now becoming more widely used in aircraft [60] and the fact that the aim of this study is to compare the two aircraft configurations, composite material was chosen. It is assumed that all laminated parts are symmetric with respect to their midplane in order to maintain the dimensional stability of composite. The layers are unidirectional and alternate between orientations of 0° , 90° , $+45^\circ$ and -45° .

Looking at each table, the first three columns regard to the X , Y and Z position of the leading edge in relation to the aircraft's gravity centre. The fourth column refers to the airfoil chord and the fifth column specifies the airfoil in that position. The sixth and the seventh columns indicate the front and rear spars position, respectively, as a chord percentage. Finally, the last two columns are thicknesses values of spars and skin dimensionless by chord and maximum airfoil thickness, respectively. Relatively to the table lines, each one corresponds to an airfoil in a certain position. Lines are also agrupated in aircraft components, such as main wing, rear wing, horizontal and vertical tail.

In Table 4.1 is presented the input data of the conventional aircraft. The main wing is divided in 3 sections with 4 airfoils types along the wingspan, the horizontal tail is divided in 2 sections with 3 airfoils and the vertical tail in 3 sections with 4 airfoils.

Table 4.1: Geometry inputs for conventional aircraft

	Leading Edge Position			Chord (m)	Airfoil File	Spar Position		t_w/c	t_s/t_{max}
	X (m)	Y (m)	Z (m)			Front (%)	Rear (%)		
Main Wing	6.695	0.000	-0.577	7.573	EMB1	10.4	55.0	0.0010	0.0054
	3.966	6.181	-0.037	3.995	EMB2	17.2	61.0	0.0010	0.0054
	0.368	12.110	0.482	2.588	EMB3	23.9	68.3	0.0010	0.0054
	-1.522	15.727	0.799	1.727	EMB4	33.3	68.3	0.0010	0.0054
Horizontal Tail	-12.874	0.000	0.500	3.543	EMB HT	20.0	70.0	0.0010	0.0054
	-13.831	1.500	0.684	2.987	EMB HT	20.0	70.0	0.0010	0.0054
	-16.830	5.833	1.216	1.382	EMB HT	20.0	70.0	0.0010	0.0054
Vertical Tail	-10.281	0.000	1.000	5.630	EMB VT	13.0	69.0	0.0010	0.0054
	-11.942	0.000	1.920	5.050	EMB VT	13.0	69.0	0.0010	0.0054
	-13.023	0.000	4.495	3.426	EMB VT	13.0	69.0	0.0010	0.0054
	-15.405	0.000	7.370	1.614	EMB VT	13.0	69.0	0.0010	0.0054

In Table 4.2 is presented the joined wing configuration. The main wing is divided in 4 sections with 5 airfoil types along the wingspan, the rear wing is divided in 3 sections with 4 airfoils and the vertical tail, as for the reference model, in 3 sections with 4 airfoils.

It can be already noted that the vertical tails of the two aircraft have the same leading edge coordinates, the same chords and the same airfoil files, so it can be concluded that the perimeters and the areas of the parts that make up the sections will be the same. However, thicknesses of both aircraft have different dimensionless ratios. It can be concluded that the vertical tail thickness of the joined wing is greater when compared to the vertical tail thickness of the conventional aircraft, because the first one has to support the weight of the rear wing, which joins the main wing to the vertical tail.

Table 4.2: Geometry inputs for joined wing

	Leading Edge Position			Chord (<i>m</i>)	Airfoil File	Spar Position		t_w/c	t_s/t_{max}
	<i>X</i> (<i>m</i>)	<i>Y</i> (<i>m</i>)	<i>Z</i> (<i>m</i>)			Front (%)	Rear (%)		
Main Wing	6.695	0.000	-0.577	3.787	EMB1	10.4	55.0	0.010	0.010
	3.966	6.181	-0.037	1.998	EMB2	17.2	61.0	0.010	0.010
	1.928	9.1455	0.223	1.665	EMBJW3	20.5	62.4	0.010	0.010
	0.368	12.110	0.482	1.294	EMB3	23.9	68.3	0.010	0.010
	-1.522	15.727	0.799	0.864	EMB4	33.3	68.3	0.010	0.010
Rear Wing	1.928	9.1455	0.223	1.000	EMBJW3	20.5	62.4	0.010	0.010
	0.058	8.6882	0.500	1.102	EMB HT JW	20.0	70.0	0.010	0.010
	-13.723	1.500	0.684	2.700	EMB HT JW	20.0	70.0	0.010	0.010
	-15.405	0.000	1.216	3.000	EMB VT	13.0	69.0	0.010	0.010
Vertical Tail	-10.281	0.000	1.000	5.630	EMB VT	13.0	69.0	0.010	0.010
	-11.942	0.000	1.920	5.050	EMB VT	13.0	69.0	0.010	0.010
	-13.023	0.000	4.495	3.426	EMB VT	13.0	69.0	0.010	0.010
	-15.405	0.000	7.370	1.614	EMB VT	13.0	69.0	0.010	0.010

As previously stated, the cost model is based on thicknesses, perimeters and areas, being necessary to convert the geometry data of each part. Through Equations 3.1 and 3.2, presented in Chapter 3, it is possible to obtain the spars and skins thicknesses, respectively, of all sections. For the calculation of skins thickness, it is assumed a maximum airfoil thickness at 12% of the chord, an approximate value for the selected airfoils. In order to calculate parts' perimeters and areas, airfoils need to be sized by the Equations 3.3 and 3.4 relatively in *X*, *Y* and *Z*. Subsequently, Equations 3.7 and 3.8 are used to calculate skins and spars perimeters, respectively, and Equations 3.11 and 3.12 are used to calculate the areas of the same parts, respectively. In the following tables, the results obtained by applying these equations are shown. All skins and spars thicknesses, perimeters and areas of the various sections from the aircrafts' structures under study are presented. Tables 4.3 and 4.4 are relative to the conventional aircraft, and Tables 4.5 and 4.6 are relative to the joined wing configuration.

Table 4.3: Thicknesses, perimeters and areas of skins of conventional aircraft

		Skins					
		Upper			Lower		
		Thickness (<i>m</i>)	Perimeter (<i>m</i>)	Area (<i>m</i> ²)	Thickness (<i>m</i>)	Perimeter (<i>m</i>)	Area (<i>m</i> ²)
Main Wing	Section 1	0.0050	24.985	36.696	0.0050	25.024	36.817
	Section 2	0.0026	20.028	19.946	0.0026	20.003	19.874
	Section 3	0.0017	12.284	7.994	0.0017	12.262	7.954
Horizontal Tail	Section 1	0.0023	9.965	4.959	0.0023	10.090	5.053
	Section 2	0.0020	14.304	9.585	0.0020	14.387	9.766
Vertical Tail	Section 1	0.0037	14.165	4.990	0.0037	14.165	4.990
	Section 2	0.0033	14.033	11.083	0.0033	14.033	11.083
	Section 3	0.0023	11.783	7.358	0.0023	11.783	7.358

Table 4.4: Thicknesses, perimeters and areas of spars of conventional aircraft

		Spars					
		Front			Rear		
		Thickness (m)	Perimeter (m)	Area (m ²)	Thickness (m)	Perimeter (m)	Area (m ²)
Main Wing	Section 1	0.0076	14.789	4.320	0.0076	14.182	4.648
	Section 2	0.0040	14.541	2.413	0.0040	13.829	1.850
	Section 3	0.0026	8.652	1.026	0.0026	8.047	0.651
Horizontal Tail	Section 1	0.0036	4.226	0.655	0.0036	3.729	0.401
	Section 2	0.0030	10.757	1.297	0.0030	9.840	0.789
Vertical Tail	Section 1	0.0057	4.590	0.846	0.0057	3.883	0.594
	Section 2	0.0051	6.171	0.996	0.0051	5.756	0.778
	Section 3	0.0035	7.613	0.782	0.0035	6.540	0.555

Table 4.5: Thicknesses, perimeters and areas of skins of joined wing

		Skins					
		Upper			Lower		
		Thickness (m)	Perimeter (m)	Area (m ²)	Thickness (m)	Perimeter (m)	Area (m ²)
Main Wing	Section 1	0.0046	19.020	18.348	0.0046	19.040	18.409
	Section 2	0.0024	10.778	5.545	0.0024	10.764	5.526
	Section 3	0.0020	9.592	4.487	0.0020	9.579	4.468
	Section 4	0.0016	10.215	3.997	0.0016	10.204	3.977
Rear Wing	Section 1	0.0014	6.133	0.492	0.0014	6.126	0.490
	Section 2	0.0033	36.412	13.984	0.0033	36.403	13.950
	Section 3	0.0036	10.667	4.358	0.0036	10.661	4.353
Vertical Tail	Section 1	0.0068	14.165	4.990	0.0068	14.165	4.990
	Section 2	0.0061	14.033	11.083	0.0061	14.033	11.083
	Section 3	0.0042	11.783	7.358	0.0042	11.783	7.358

Table 4.6: Thicknesses, perimeters and areas of spars of joined wing

		Spars					
		Front			Rear		
		Thickness (m)	Perimeter (m)	Area (m ²)	Thickness (m)	Perimeter (m)	Area (m ²)
Main Wing	Section 1	0.0379	14.170	2.166	0.0379	13.749	2.396
	Section 2	0.0200	7.594	0.688	0.0200	7.345	0.573
	Section 3	0.0167	7.019	0.548	0.0167	6.833	0.411
	Section 4	0.0130	8.419	0.514	0.0130	8.099	0.335
Rear Wing	Section 1	0.0111	4.155	0.230	0.0111	4.340	0.180
	Section 2	0.0270	32.100	3.506	0.0270	33.380	2.405
	Section 3	0.0300	4.982	0.615	0.0300	5.313	0.503
Vertical Tail	Section 1	0.0563	4.590	0.846	0.0563	3.883	0.594
	Section 2	0.0505	6.171	0.996	0.0505	5.756	0.778
	Section 3	0.0343	7.613	0.782	0.0343	6.540	0.555

Comparing the two configurations through the data presented in the tables, it is verified that:

1. The upper and the lower skins of vertical tails of both aircraft have the same dimensions. Therefore, it can be concluded that the airfoils that make up this structure are symmetrical, ensuring that there are no asymmetries that might harm the yaw control of the aircraft.
2. By adding the skin areas of the main wings, it is verified that the main wing of the joined wing is smaller than the conventional aircraft main wing, due to the fact that joined wing presents a rear wing that also produces lift, and thus not requiring such a large main wing.
3. As previously mentioned, the vertical tail of joined wing has thicker spars compared to the vertical tail of conventional aircraft, due to the fact that the first one has to support the rear wing weight, thus requiring a more robust structure.
4. The rear wing is a larger and more robust structure compared to the horizontal tail.

4.2 Exogenous Data

Once the part data is integrated into the cost model, it is necessary to define and assume other input data, in this case regarding to the operation and organization of the plant. The exogenous data was obtained from aerospace companies and is presented in the Table 4.7.

Table 4.7: Exogenous Data.

Days per year	240 <i>days/year</i>
Wage (including benefits)	15.00 €/h
Energy unit cost	0.08 €/kWh
Interest rate	15%
Building unit cost	1 500.00 €/m ²
Equipment life	15 <i>years</i>
Building life	30 <i>years</i>
Production period	15 <i>years</i>
Idle space	20%

4.3 Material Data

Material data is another necessary set of inputs to the cost model. This data presents characteristics and information of the materials that are used in parts production, as can be observed in the Table 4.8.

As previously mentioned, in this model four types of materials are used. Copper, glass fiber and dry carbon fiber are materials used in the processes that precede and proceed the fiber placement process, and carbon fiber prepreg (Hexply M21 / 34% / UD194 / IM7-12K ¹, a high performance prepreg used in

¹ resin / resin content by weight (%) / fiber weight (gsm) / fiber type

Table 4.8: Material Data.

	Copper	Glass Fiber	Dry Carbon Fiber	Carbon Fiber Prepreg
Density	1600 g/m^2	800 g/m^2	300 g/m^2	300 g/m^2
Cost per m^2	45.00 $€/m^2$	5.00 $€/m^2$	30.00 $€/m^2$	24.30 $€/m^2$
Scrap price	5.00 $€/kg$	2.00 $€/kg$	3.50 $€/kg$	3.00 $€/kg$
Layer height	–	–	–	0.2 mm

primary aerospace structures [90]) is the material used by the ATL machine. It should be noted that the layer height values of copper, glass fiber and dry carbon fiber are not presented in Table 4.8, because the number of layers of these materials are neglected in the parts thickness.

4.4 Processes Data

Finally, the inputs related to the processes required for parts production are presented. As described in Chapter 3, the production method is divided into seven processes (Figure 3.1), each one with a set of three input groups: infrastructure-related process data, manufacturing quality data, and downtime information. The following tables present the values of these same inputs that will be introduced in each process of the developed cost model.

Most values were obtained through contact with aerospace industry technicians. However, there are some inputs that need to be determined, because they vary according to the parts dimensions or number of parts to be produced. This is the case of machine time and allocation percentage of each part, respectively, which are calculated through equations presented in Section 3.4. The number of machines in each process is another input that varies depending on the production analyses in study. This input is introduced later on, when different analyses are shown in Section 4.5.

Appendix A is a complement to this section. For conventional aircraft and joined wing, cycle times and allocation percentages of all parts are presented.

4.4.1 Reception, Check and Storage

The inputs related to the material reception, check and storage can be observed in Table 4.9.

An exception to this process is that setup time and machine time are not defined. As mentioned in Chapter 3, the cycle time of this process starts with the arrival of material to the plant, continues with the storage time followed by the thawing time of material, and ends when the material is ready to be used in the following process. Regarding this, it is assumed a constant cycle time, approximately 3.5h, which is independent from parts' dimensions.

Regarding manufacturing quality data, it is assumed that there is no restriction on parts' production, since this process is only material storage. A pass percentage of 100% is considered and there is also no scrap nor rework.

Table 4.9: Reception, check and storage data.

Infrastructure-related Process Data		Manufacturing Quality Data	
Workers	4 units/machine	Technical Scrap	0%
% Dedication	5%	Pass	100%
Floor Space	50 m ² /machine	Rework	0%
Number of Machines	(Section 4.5)	Non-Quality Scrap	0%
Acquisition Cost	300 000.00 €/machine	Rework Pass	0%
Energy Consumption	20.00 kWh	Rework Scrap	0%
Cycle Time	3.5 h	Material required in Rework	0%
% Maintenance	10%	Downtime Information	
% Overheads	160%	Worker Unpaid Breaks	1 h/day
% Allocation	(Appendix A)	Worker Paid Breaks	1 h/day
		On-Shift Maintenance	0.1 h/day
		Unplanned Downtime	0.1 h/day

4.4.2 Application of copper, glass fiber and dry carbon fiber

The inputs related to the application process of copper, glass fiber and dry carbon fiber are presented in Table 4.10.

Table 4.10: Application of copper, glass fiber and dry carbon fiber data.

Infrastructure-related Process Data		Manufacturing Quality Data	
Workers	4 units/machine	Technical Scrap	6%
% Dedication	50%	Pass	97%
Floor Space	8 m ² /machine	Rework	2%
Number of Machines	(Section 4.5)	Non-Quality Scrap	1%
Acquisition Cost	600.00 €/machine	Rework Pass	100%
Energy Consumption	20.00 kWh	Rework Scrap	0%
Setup Time	1 h	Material required in Rework	2%
Machine Time	(Equation 3.18)	Downtime Information	
% Maintenance	10%	Worker Unpaid Breaks	1 h/day
% Overheads	160%	Worker Paid Breaks	0.5 h/day
% Allocation	(Appendix A)	On-Shift Maintenance	0.05 h/day
		Unplanned Downtime	0.05 h/day

The machine time of this process is calculated through a relation of areas demonstrated in Equation 3.18. The example part, used for comparison, is represented in Figure 4.1, a square plate, with an area of 20 m² and with an application period of copper, glass fiber and dry carbon fiber of 5h.

The machine time results can be observed indirectly in Appendix A through the values obtained for cycle time, which is no more than the sum of setup time with machine time.

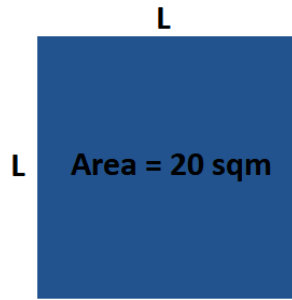


Figure 4.1: Part example.

4.4.3 ATL

In Table 4.11, it can be observed the inputs related to the ATL process.

Table 4.11: ATL Data.

Infrastructure-related Process Data		Manufacturing Quality Data	
Workers	<i>2 units/machine</i>	Technical Scrap	(Table 4.12)
% Dedication	100%	Pass	97%
Floor Space	<i>20 m²/machine</i>	Rework	2%
Number of Machines	(Section 4.5)	Non-Quality Scrap	1%
Acquisition Cost	1 000 000.00 €/machine	Rework Pass	99%
Energy Consumption	500.00 kWh	Rework Scrap	1%
Setup Time	2 h	Material required in Rework	20%
Machine Time	(Equation 3.21)		
% Maintenance	10%	Downtime Information	
% Overheads	160%	Worker Unpaid Breaks	1 h/day
% Allocation	(Appendix A)	Worker Paid Breaks	0.5 h/day
		On-Shift Maintenance	0.05 h/day
		Unplanned Downtime	0.05 h/day

In this process, the machine time is calculated through Equation 3.21. Part weights and layup rates required to this equation depend only on parts thicknesses and areas, indicated in Section 4.1. With this, it is possible to determine the machine time. Cycle times and allocation percentages of the ATL process can be observed in the Appendix A.

Regarding manufacturing quality data, the percentage of technical scrap is determined for each aircraft structure in production, as mentioned in Subsection 3.4.1. The fact that ATL process is the process where there is a greater deposition of material and the fact that there are different fiber orientations, make this analysis relevant. Table 4.12 presents the percentages of technical scrap for all structures of conventional aircraft and joined wing, taking into account the different fiber deposition orientations.

The fiber placement is carried out course by course and the technical scrap is determined by the amount of material placed in excess in each course performed, as observed in Figure 3.14. After percentages of technical scrap for each fiber orientation being defined, the percentage used for each aircraft structure is determined through the average of them.

Table 4.12: Percentages of technical scrap according to different tape orientations.

Fiber Orientation	Conventional Aircraft			Joined Wing		
	Main Wing	Horizontal Tail	Vertical Tail	Main Wing	Rear Wing	Vertical Tail
0°	10.8%	19.6%	21.5%	20.7%	37.0%	21.5%
90°	8.4%	16.0%	12.1%	16.9%	42.4%	12.1%
+45°	11.0%	19.4%	14.2%	18.8%	35.6%	14.2%
-45°	11.9%	21.7%	14.2%	21.7%	42.0%	14.2%
Average	10.5%	19.2%	15.5%	19.5%	39.3%	15.5%

The percentage of technical scrap in the production of trapezoidal parts by an ATL machine ranges approximately from 10 to 20%, according to industry technicians. Looking at Table 4.12, most of results are within the range presented, except for the rear wing, which has a percentage of 39.3%. Due to be a long and narrow structure, the ideal laying-up speed of ATL machine is not reached and a lot of fiber placement courses are required, which leads to several wastes of material.

The last inputs related to the ATL process are the consumables, presented in Table 4.13. The considered consumables are the molds used in the parts production, which have an impact on material, labor and tooling costs of the ATL process, exclusively.

Table 4.13: Consumables Data.

Number of Molds	1 <i>units</i>
Mold Cost	30 000.00 €/unit
Mold Preparation	5 <i>h</i>
Consumables	10.00 €/m ²

4.4.4 Application of glass fiber, dry carbon fiber and vacuum bagging

The inputs related to the application of glass fiber, dry carbon fiber and vacuum bagging are introduced in Table 4.14.

In this process, once again, the machine time is calculated through a relation of areas demonstrated by Equation 3.18. The example part used for comparison continues to be the plate represented in Figure 4.1, which has an application period of glass fiber, dry carbon fiber and vacuum bagging of 5*h*.

As previously mentioned, machine time results can be observed indirectly in Appendix A through the values obtained for cycle time.

Table 4.14: Application of glass fiber, dry carbon fiber and vacuum bagging data.

Infrastructure-related Process Data		Manufacturing Quality Data	
Workers	4 units/machine	Technical Scrap	3%
% Dedication	20%	Pass	95%
Floor Space	8 m ² /machine	Rework	4%
Number of Machines	(Section 4.5)	Non-Quality Scrap	1%
Acquisition Cost	600.00 €/machine	Rework Pass	90%
Energy Consumption	20.00 kWh	Rework Scrap	10%
Setup Time	1 h	Material required in Rework	20%
Machine Time	(Equation 3.18)	Downtime Information	
% Maintenance	10%	Worker Unpaid Breaks	1 h/day
% Overheads	160%	Worker Paid Breaks	0.5 h/day
% Allocation	(Appendix A)	On-Shift Maintenance	0.05 h/day
		Unplanned Downtime	0.05 h/day

4.4.5 Autoclave

The autoclave process has, as inputs, the values presented in Table 4.15.

Table 4.15: Autoclave data.

Infrastructure-related Process Data		Manufacturing Quality Data	
Workers	2 units/machine	Technical Scrap	0%
% Dedication	66%	Pass	99%
Floor Space	60 m ² /machine	Rework	0%
Number of Machines	(Section 4.5)	Non-Quality Scrap	1%
Acquisition Cost	2 000 000.00 €/machine	Rework Pass	0%
Energy Consumption	1 200.00 €/kWh	Rework Scrap	0%
Setup Time	4 h	Material required in Rework	0%
Machine Time	10 h	Downtime Information	
% Maintenance	10%	Worker Unpaid Breaks	1 h/day
% Overheads	160%	Worker Paid Breaks	0.5 h/day
% Allocation	(Appendix A)	On-Shift Maintenance	0.05 h/day
		Unplanned Downtime	0.05 h/day

In this process, the machine time is considered the curing time of the part inside the autoclave and depends on the characteristics of the applied preregs. According to the fibers used, presented in Section 4.3, the curing time is 10h [90]. However, due to the large size of the autoclave (a cylinder autoclave with 3.5m – 10m), it is assumed that four parts can be cured at the same time. Assuming a setup time of 4h and adding both values (machine and setup times) leads to a cycle time of 3.5h per part, according to Equation 3.22. In Appendix A, cycle times and percentages of allocations are presented.

It should be noted that the pass percentage is almost 100%, which means that there are not too many parts being wasted (1% scrap). In addition, since the autoclave process only cure parts, there is no need for rework, nor required material for that. Thus, it can be concluded that this process does not have material costs.

4.4.6 Demolding, Finishing and Adjusting

The inputs for the demolding, finishing and adjusting process are presented in Table 4.16.

Table 4.16: Demolding, adjusting and finishing data.

Infrastructure-related Process Data		Manufacturing Quality Data	
Workers	<i>2 units/machine</i>	Technical Scrap	3%
% Dedication	66%	Pass	97%
Floor Space	<i>10 m²/machine</i>	Rework	0%
Number of Machines	(Section 4.5)	Non-Quality Scrap	3%
Acquisition Cost	2 000 000.00 €/machine	Rework Pass	0%
Energy Consumption	400.00 kWh	Rework Scrap	0%
Setup Time	1 h	Material required in Rework	0%
Machine Time	(Equation 3.19)		
% Maintenance	10%	Downtime Information	
% Overheads	160%	Worker Unpaid Breaks	1 h/day
% Allocation	(Appendix A)	Worker Paid Breaks	0.5 h/day
		On-Shift Maintenance	0.05 h/day
		Unplanned Downtime	0.05 h/day

In this case, the machine time is not given by a relation of areas, but by a relation of perimeters (Equation 3.19). The example part remains the same as the one represented in Figure 4.1 and its machine time, in this process, is $4h$. Knowing that the plate is square and has an area of $20 m^2$, it is possible to calculate its perimeter through Equation 4.1, where L is the side of the square.

$$Perimeter = 4 \cdot L = 4 \cdot \sqrt{Area}. \quad (4.1)$$

With the parts perimeters introduced in Section 4.1, it is possible to determine the machine times, presented indirectly through the cycle times in Appendix A. In the same appendix, allocations of each part are also presented.

Regarding the manufacturing quality data, it is verified that, similarly to the previous process, there is no need for rework nor required material for that, and it can also be concluded that this process does not have material costs.

4.4.7 Non-Destructive Tests

The last process inputs are presented in Table 4.17 and are relative to non-destructive tests.

Table 4.17: Non-destructive tests data.

Infrastructure-related Process Data		Manufacturing Quality Data	
Workers	1 <i>units/machine</i>	Technical Scrap	0%
% Dedication	30%	Pass	98%
Floor Space	4 <i>m²/machine</i>	Rework	1%
Number of Machines	(Section 4.5)	Non-Quality Scrap	1%
Acquisition Cost	1 000 000.00 <i>€/machine</i>	Rework Pass	50%
Energy Consumption	20.00 <i>kWh</i>	Rework Scrap	50%
Setup Time	1 <i>h</i>	Material required in Rework	4%
Machine Time	(Equation 3.18)	Downtime Information	
% Maintenance	10%	Worker Unpaid Breaks	1 <i>h/day</i>
% Overheads	160%	Worker Paid Breaks	0.5 <i>h/day</i>
% Allocation	(Appendix A)	On-Shift Maintenance	0.05 <i>h/day</i>
		Unplanned Downtime	0.05 <i>h/day</i>

The machine time is once again obtained by the relation of areas through Equation 3.18. In this process, the example part of Figure 4.1 takes $5h$ to carry out the non-destructive tests. Machine time results can be observed indirectly in the Appendix A through the cycle times. The allocations of each part are also presented in this same appendix.

4.5 Costs

After the introduction of the required inputs for the cost model development, the results obtained for the production costs of the aircraft under study, the conventional aircraft and the joined wing dimensioned by the MDO framework, are presented in the following subsections.

Due to the advantages of the composite material previously shown, when producing a part in this type of material with the same strength of an aluminium part, it is verified that the thickness of the composite material part may be thinner than the corresponding part thickness in aluminium. In the case of the aircraft under study in this thesis, knowing that they were designed for aluminium and are being produced in composite material, it is verified that there is an over-sizing regarding the quantity of material necessary for the production of its parts.

In this thesis, two analyses are carried out to obtain costs. In the first analysis (Subsection 4.5.1), it is assumed that there is a plant with only one machine in each process. The objective is to determine the maximum annual production volume of each aircraft and compare the production costs of them. In the second analysis (Subsection 4.5.2), it is intended to obtain an annual production volume of 50 aircraft, being necessary to determine the number of machines required to that production. After sizing the plant,

the production costs are compared.

4.5.1 Production costs considering the production at maximum capacity

In this first analysis, the aim is to determine the maximum annual production volume that a plant can produce for the conventional and the joined wing aircraft. Afterwards, production costs of both aircraft are compared.

It is assumed that there is a plant equipped with a specific machine in each process and a reception, check and storage space of $150 m^3$, equivalent to three machines of this process, an exception justified by the need for sufficient space so that there is no problem with the amount of material storage.

With the number of machines defined, it is intended to determine the annual production volume of each aircraft. It is known that the production capacity in each process can not exceed 100%, otherwise, the machines would be overloaded and the production of all parts would not be possible. In that case, it would be necessary either to acquire one more machine for that process, or to reduce the production volume, or even through some process optimization to decrease the cycle time. This capacity problem can also be checked when idle time is less than zero.

In the Tables 4.18 and 4.19 are presented the uptimes, idle times and machine use percentages of each process, obtained for the maximum annual production volumes of conventional aircraft and joined wing, respectively. If only one machine were present in each process, as already mentioned, the results would be 26 units for conventional aircraft and 14 units for joined wing. These annual production volumes were obtained by maximizing the machine use.

Table 4.18: Times and machine use for the conventional aircraft production volume of 26 units.

	Reception	Aplication 1	ATL	Aplication 2	Autoclave	DFA	NDT
Number of Machines	3	1	1	1	1	1	1
Uptime	5178 h	4358 h	5187 h	4271 h	5003 h	5348 h	4044 h
Idle Time	10518 h	1018 h	189 h	1105 h	373 h	28 h	1332 h
% Machine Use	32.99%	81.07%	96.48%	79.44%	93.06%	99.48%	75.22%

Table 4.19: Times and machine use for the joined wing production volume of 14 untis.

	Reception	Aplication 1	ATL	Aplication 2	Autoclave	DFA	NDT
Number of Machines	3	1	1	1	1	1	1
Uptime	3646 h	2138 h	5185 h	2095 h	3523 h	3751 h	1984 h
Idle Time	12050 h	3238 h	191 h	3281 h	1853 h	1625 h	3392 h
% Machine Use	23.23%	39.77%	96.45%	38.97%	65.52%	69.77%	36.90%

As can be seen, for an annual production volume of 26 conventional aircraft (Table 4.18), the process that limits the production is the demolding, finishing and adjusting process, with the machine being used up to 99.48% of its capacity. In the case of joined wing (Table 4.19), for an annual production volume of 14 units, the process that limits the production is the ATL process, with an use of 96.45%. Using the tables in Appendix A, it can be justified the fact why processes that limit the production are different.

Adding the cycle times of the ATL process for both aircraft (Appendix A), it turns out that the joined wing takes approximately twice the time (211.49 h) of the conventional aircraft (110.53 h). The reason for this increase is that joined wing has thicker parts (Tables 4.5 and 4.6), which in turn require more material deposition that increases the uptime of the process and turns it into the limiting process. In the tables presented, it should also be noted that there is not any percentage greater than 100% or any idle time less than zero, which leads to the conclusion that all parts are produced.

After the annual production volumes being determined, aircraft production costs can be finally obtained, using the equations previously presented in Section 3.5. The results can be observed in Figure 4.2.

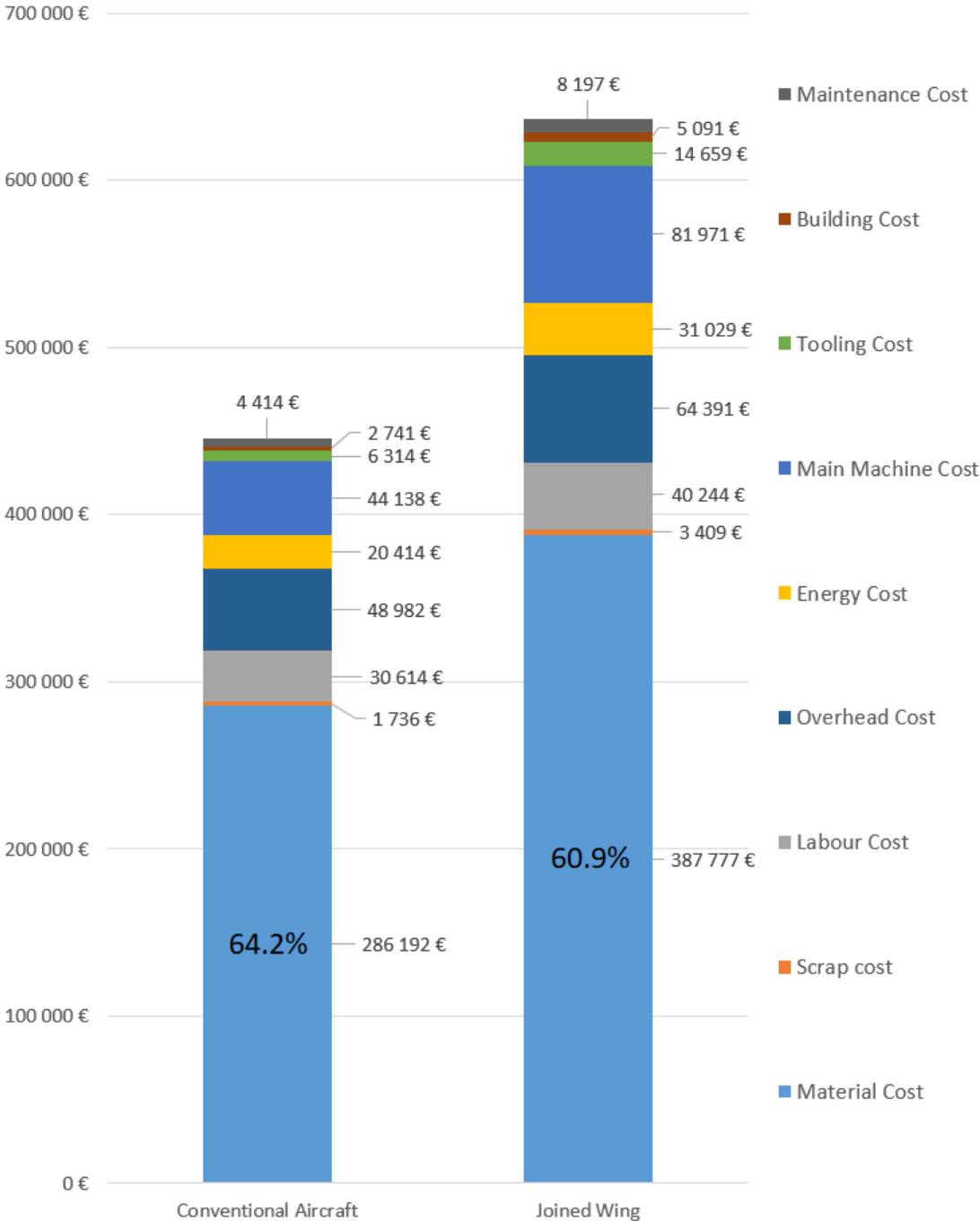


Figure 4.2: Production costs of the first analysis.

Analysing the results obtained, it is verified that the conventional aircraft has a production cost inferior to the production cost of the joined wing. By adding the different cost values presented, it is obtained a production cost of 445 548 € for conventional aircraft and 636 768 € for joined wing. The cost difference between both aircraft is 191 220 €.

Comparing the graphs, it is verified that the biggest difference is registered in the material cost (more than 100 000 €), which, as already explained, is due to the fact that joined wing requires more material for its parts production. The part weights of conventional and joined wing aircraft are shown in Appendix B. It is verified that joined wing is heavier than conventional aircraft. In addition, the scrap cost is also higher in the joined wing case for the same reason. If there is more material to be used during production, the greater the amount of scrap to be produced. Regarding labor, overhead and energy costs, with more material and more working hours being required for the production of joined wing, the higher the costs compared to the conventional aircraft.

Relatively to fixed costs, cost differences are subject to the fact that the annual cost is allocated according to the number of aircraft produced. Since the annual production volume of conventional aircraft is higher than joined wing, the fixed costs per unit are lower, with a constant ratio of 26 to 14 units if main machine, building and maintenance costs are compared. In the case of tooling costs, the same does not happen because the joined wing needs more parts molds for its production. Looking once again to the tables of Appendix A, 32 different parts can be counted for the production of conventional aircraft, while for the joined wing are required 40 parts. This reason prevents the same ratio between the annual tooling costs of the two aircraft.

Looking at Figure 4.2, it is also verified that the highest cost is observed in material cost. Approximately, percentages of 64% for the conventional aircraft and 61% for the joined wing are obtained, which are values considered realistic according to industry technicians, proving that material is one of the most relevant parameters in this analysis.

Despite the observed differences, it can be seen that the graphs of both aircraft are similar, which proves the consistency and accuracy of the cost model in data handling.

Finally, it can be observed in Table 4.20 and in Figure 4.3 the differences in the distribution of costs for the aircraft structures under study: main wing, rear wing, horizontal and vertical tails.

Table 4.20: Cost distribution in the first analysis.

	Conventional Aircraft		Joined Wing
Main wing	302 989 €	Main wing	281 366 €
Horizontal tail	73 944 €	Rear wing	223 760 €
Vertical tail	68 615 €	Vertical tail	131 642 €

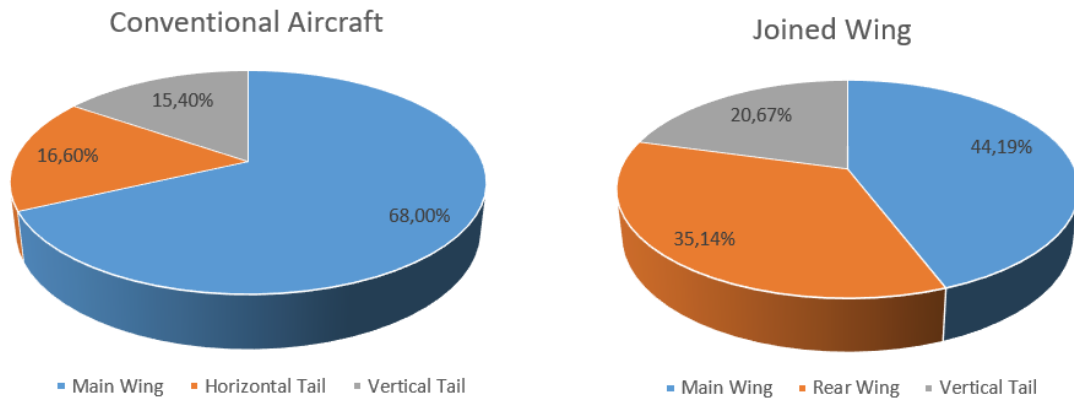


Figure 4.3: Cost distribution in percentage in the first analysis.

It can be verified that the distribution of costs is quite different. While in conventional aircraft most of the costs are attributed to the main wing production (68%), in the joined wing the costs distribution is more uniform. The reasons are given below:

1. The thicknesses increase in the vertical tail of the joined wing (in order to support the rear wing) almost doubles its production cost, comparing to the vertical tail cost of the conventional aircraft.
2. The reduction of the main wing area in the joined wing diminishes the production cost about 20 000 € in relation to the production cost of the conventional aircraft main wing.
3. Finally, the fact that the rear wing is larger and requires more material for its production, compared to the horizontal tail of conventional aircraft, increases its production cost to more than double the cost of horizontal tail. Another point which also contributes to the increase in the production cost of the rear wing is the several wastes of material produced during the ATL process, due to be a long and narrow structure, as already mentioned in Subsection 4.4.3.

In this way, the distribution of production costs in the joined wing becomes more uniform than the distribution of costs in the conventional aircraft, as shown in Figure 4.3.

4.5.2 Production costs considering an annual production volume of 50 aircraft

In this second analysis, it is assumed that the plant has an annual production volume of 50 aircraft, a value based on the annual production of an aircraft used for regional flights, such as the aircraft of this study. Taking this as a premise, it is necessary to determine the number of machines per process, to obtain the production costs of conventional aircraft and joined wing. Afterwards, a comparison of costs between the two aircraft is made.

Regarding the number of machines per process, this was determined by taking into account their production capacity. Knowing that this capacity can not exceed 100% (or that the idle time can not be less than zero), machines have been added until the capacity percentage is immediately less than 100% (or that the idle time is equal to or greater than zero). In the case of reception, check and storage

process, it was, once again, assumed a space of $150m^3$, equivalent to three machines of this process, so that there is no problem regarding the lack of space for material storage.

Tables 4.21 and 4.22 show the obtained results for the number of machines required for conventional aircraft and joined wing productions, respectively. The uptimes, idle times and the machine use percentages of each process are also presented.

Table 4.21: Times and machine use for the conventional aircraft production volume of 50 units.

	Reception	Aplication 1	ATL	Aplication 2	Autoclave	DFA	NDT
Number of Machines	3	2	2	2	2	2	2
Uptime	9957 h	8382 h	9974 h	8213 h	9621 h	10285 h	7777 h
Idle Time	5739 h	2370 h	778 h	2539 h	1131 h	467 h	2975 h
% Machine Use	63.44%	77.95%	92.77%	76.39%	89.48%	95.65%	72.33%

Table 4.22: Times and machine use for the joined wing production volume of 50 units.

	Reception	Aplication 1	ATL	Aplication 2	Autoclave	DFA	NDT
Number of Machines	3	2	4	2	3	3	2
Uptime	13021 h	7636 h	18519 h	7483 h	12581 h	13396 h	7085 h
Idle Time	2675 h	3116 h	2985 h	3269 h	3547 h	2732 h	3667 h
% Machine Use	82.96%	71.02%	86.12%	69.60%	78.01%	83.06%	65.90%

As can be seen, there is no machine use percentages above 100%, so it can be concluded that the number of machines determined is sufficient for the production of 50 units, for conventional aircraft and also for joined wing. In the case of conventional aircraft, two machines are required in each process (excluding the reception, check and storage process), and in the case of joined wing, it is verified that the number of machines in some processes must be greater than two to ensure the production volume. Regarding the processes that limit the production of the aircraft, they continue to be the same as the previous analysis, which reveals the model coherence. In the case of conventional aircraft, the process which limits the production is the demolding, finishing and adjusting process, with a use of 95.65%, and in the case of joined wing is the ATL process with machines being used up to 86.12% of its capacity.

With the production volumes and the number of machines per process defined, the production costs of the aircraft can be determined (shown in Figure 4.4).

As can be observed in Figure 4.4, it is concluded, once again, that the production cost of the conventional aircraft is lower than the production cost of the joined wing. According to the obtained results, it is achieved a production cost of 438 286 € for the conventional aircraft and a production cost of 595 978 € for the joined wing. The difference between both production costs is 157 692 €.

Similar to the first analysis, it is verified that the variable costs of the joined wing are superior to those of the conventional aircraft. Both material and scrap costs are higher because the joined wing needs more material for its production. The labor, overhead and energy costs are also higher due to the increase in the number of working hours.

In regard to fixed costs, since the annual production volume is the same (50 aircraft), if both plants had the same number of machines, the costs would be similar. However, it is verified in Tables 4.21 and

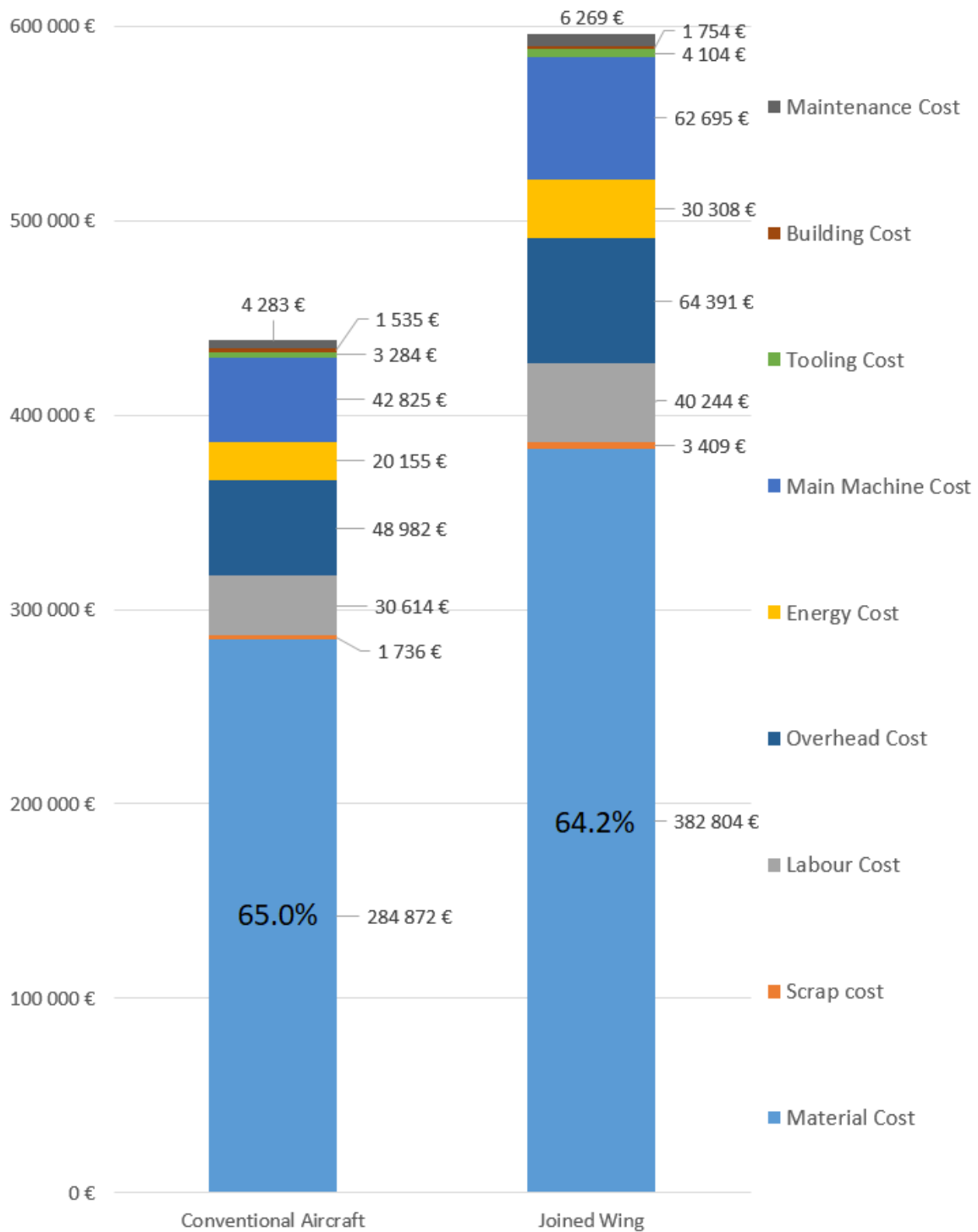


Figure 4.4: Production costs of the second analysis.

4.22 that the number of machines required to produce the 50 joined wings is higher than the number of machines required to produce the 50 conventional aircraft. Thus, as can be seen in Figure 4.4, all fixed costs of the joined wing are higher than the fixed costs of the conventional aircraft.

Comparing the values obtained in this analysis with the values obtained in the previous one (Sub-section 4.5.1), it can be seen that the production costs of both aircraft are lower in this second analysis. Analysing the results, it can be seen that the variable costs per aircraft are very similar and that the

fixed costs are the ones that decrease the total production cost of the aircraft. Although in the second analysis there is a larger number of machines per process, the annual production volume is also higher, significantly reducing the fixed costs per aircraft, which leads to lower total production costs in this second analysis. This is equivalent to what happens in an economy of scale: the larger the number of units to be produced, the lower the unit production cost.

As can be seen in Figure 4.4, the graphics of the two aircraft are once again quite identical, which reveals the consistency and accuracy of the cost model once more. This similarity also seems to demonstrate a certain tendency in the percentage distribution of costs, however, this can not be taken as a conclusion, since more test cases would be necessary to justify it. Once more, the figure also shows that the highest percentage of costs is the material cost, about 65% of the production costs in both aircraft, which, as previously mentioned, is a realistic value according to industry.

Finally, it can be observed in the Table 4.23 and in Figure 4.5 the differences in the distribution of costs for the aircraft structures under study: main wing, rear wing, horizontal and vertical tails.

Table 4.23: Cost distribution in the second analysis.

	Conventional Aircraft		Joined Wing
Main wing	300 295 €	Main wing	263 120 €
Horizontal tail	72 111 €	Rear wing	209 919 €
Vertical tail	65 880 €	Vertical tail	122 939 €

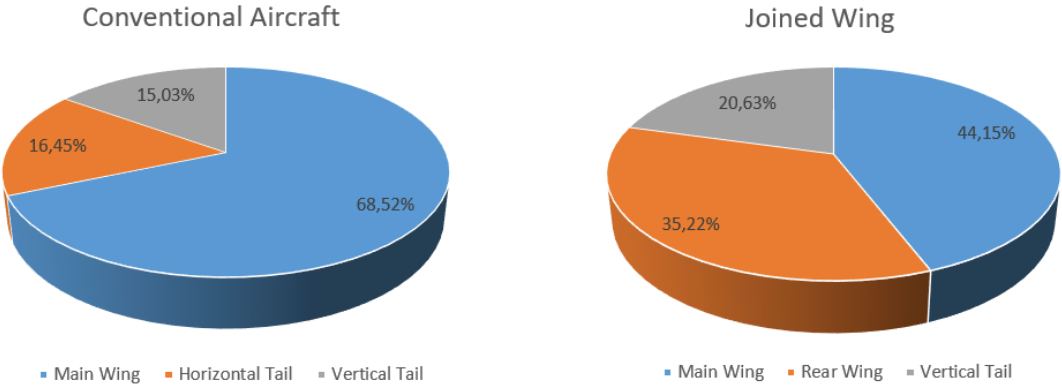


Figure 4.5: Cost distribution in percentage in the second analysis.

As in the first analysis, it is again verified that the costs distribution is quite different. While in conventional aircraft most of the costs are attributed to the main wing production (68%), in the joined wing the costs' distribution is more uniform. The reasons for standardizing the distribution of costs of joined wing are the same as those presented previously in Subsection 4.5.1, such as the thicknesses increase in the vertical tail, the reduction in the main wing area and the fact that the rear wing is larger and requires more material for its production than the horizontal tail.

4.6 Sensitivity Analysis

In this section, a sensitivity analysis of the production cost is carried out with respect to the thickness of the parts that constitute the aircraft. The objective is to analyse the impact that a reduction in the number of layers of composite material has on the final production cost of an aircraft.

According to the IST Aerospace Group, the MDO framework (program which develops the aircraft configurations under study in this thesis) designs the structures in aluminium. However, since composite material has high strength-to-weight and stiffness-to-weight ratios besides the increase trend to use it in aerospace applications, it was assumed that this would be the material used in this cost model. Thus, in order to simplify the test cases and the fact that the results are only for comparative analyses between them, the configurations from the MDO framework were maintained, as previously mentioned.

In the case of the aircraft under study in this thesis, knowing that they were designed for aluminium and are being produced in composite material and that, as mentioned in Chapter 3, it was considered that parts constituting the aircraft structures have a conservative and constant thickness in order to comply with the safety factors, it is verified that there is an over sizing regarding the quantity of material necessary for the production of its parts. Given these reasons, it is decided to make this sensitivity analysis through a reduction in the number of layers of composite material.

For this analysis, the example used is the joined wing. It is decided to remove two layers of composite material on all aircraft parts, since if only one layer of material were removed, symmetry problems could occur and the material properties would be altered.

In this way, the new parts weights of the aircraft are shown in Table 4.24. The total weights of the main wing, rear wing and vertical tail are also presented in Table 4.24. Values are given in kilograms (*kg*). It should also be noted that the total weights of the main and rear wings already contemplate the left wing and the right wing weights.

Table 4.24: New joined wing parts' weight.

		Skins		Spars		Total Weight
		Upper	Lower	Front	Rear	
Main Wing	Section 1	121.10 kg	121.50 kg	122.19 kg	135.15 kg	1291.86 kg
	Section 2	16.63 kg	16.58 kg	20.22 kg	16.85 kg	
	Section 3	10.77 kg	10.72 kg	13.48 kg	10.10 kg	
	Section 4	7.19 kg	7.16 kg	9.87 kg	6.42 kg	
Rear Wing	Section 1	0.88 kg	0.88 kg	3.72 kg	2.91 kg	943.18 kg
	Section 2	67.12 kg	66.96 kg	140.96 kg	96.70 kg	
	Section 3	20.92 kg	20.89 kg	27.33 kg	22.31 kg	
Vertical Tail	Section 1	47.90 kg	47.90 kg	71.10 kg	49.90 kg	706.90 kg
	Section 2	99.75 kg	99.75 kg	75.31 kg	58.81 kg	
	Section 3	44.15 kg	44.15 kg	39.87 kg	28.30 kg	

Adding the total weights of each structure, it is determined a total structural weight of 2941.94 *kg*. Comparing this value with the result obtained previously for the joined wing, in the Appendix B, it is verified a reduction of 171.79 *kg* in composite material.

However, this reduction does not only diminish the material cost. Reducing the number of layers of composite material also decreases the number of hours required to produce the parts. For this reason, the production costs of the new joined wing are recalculated, similarly to what was presented previously in Subsections 4.5.1 and 4.5.2, first and second analyses, respectively.

Taking into account the first analysis, where it is assumed that there is a plant equipped with only one specific machine in each process and with a space for reception, check and storage of 150 *m*³, the obtained results for the new uptimes, idle times and machine use percentages of each process are presented in Table 4.25. The maximum annual production volume is equal to the one achieved in Subsection 4.5.1, of 14 aircraft.

Table 4.25: Times and machine use for the new joined wing (production volume of 14 units).

	Reception	Aplication 1	ATL	Aplication 2	Autoclave	DFA	NDT
Number of Machines	3	1	1	1	1	1	1
Uptime	3646 h	2138 h	5068 h	2095 h	3523 h	3751 h	1984 h
Idle Time	12050 h	3238 h	308 h	3281 h	1853 h	1625 h	3392 h
% Machine Use	23.23%	39.77%	94.27%	38.97%	65.52%	69.77%	36.90%

It should be noted that the removal of two layers of composite material does not change the annual production volume. However, comparing these results with those of Table 4.19, there is a decrease in the uptime of the ATL process (the only process which cycle time depends on the number of layers of composite material). Therefore, the machine use percentage in this process also decreases. It is concluded that there is a reduction in the number of working hours which, consequently, has resulted in a decrease in production costs.

With the annual production volume and the number of machines in each process defined, the production costs of the new joined wing can be determined. In Figure 4.6, it is presented the graphs of the production costs of both joined wings.

As can be seen, the production cost of the new joined wing is lower than the one in the first analysis. The removal of two layers of composite material results in a reduction of 20 602 €. Analysing the graphs, it can be seen that the fixed costs are exactly the same and there is only a reduction in the variable costs. The fixed costs are maintained by the fact that there is no change in the number of machines or the annual production volume. Thus, the variable costs are the responsible factors for the reduction of the production cost of the aircraft: a decrease in the amount of material used, resulting in a saving of 19 437 €, which is practically the total difference of costs between the two joined wings; and there is also a decrease in the number of hours required for the production of this new aircraft.

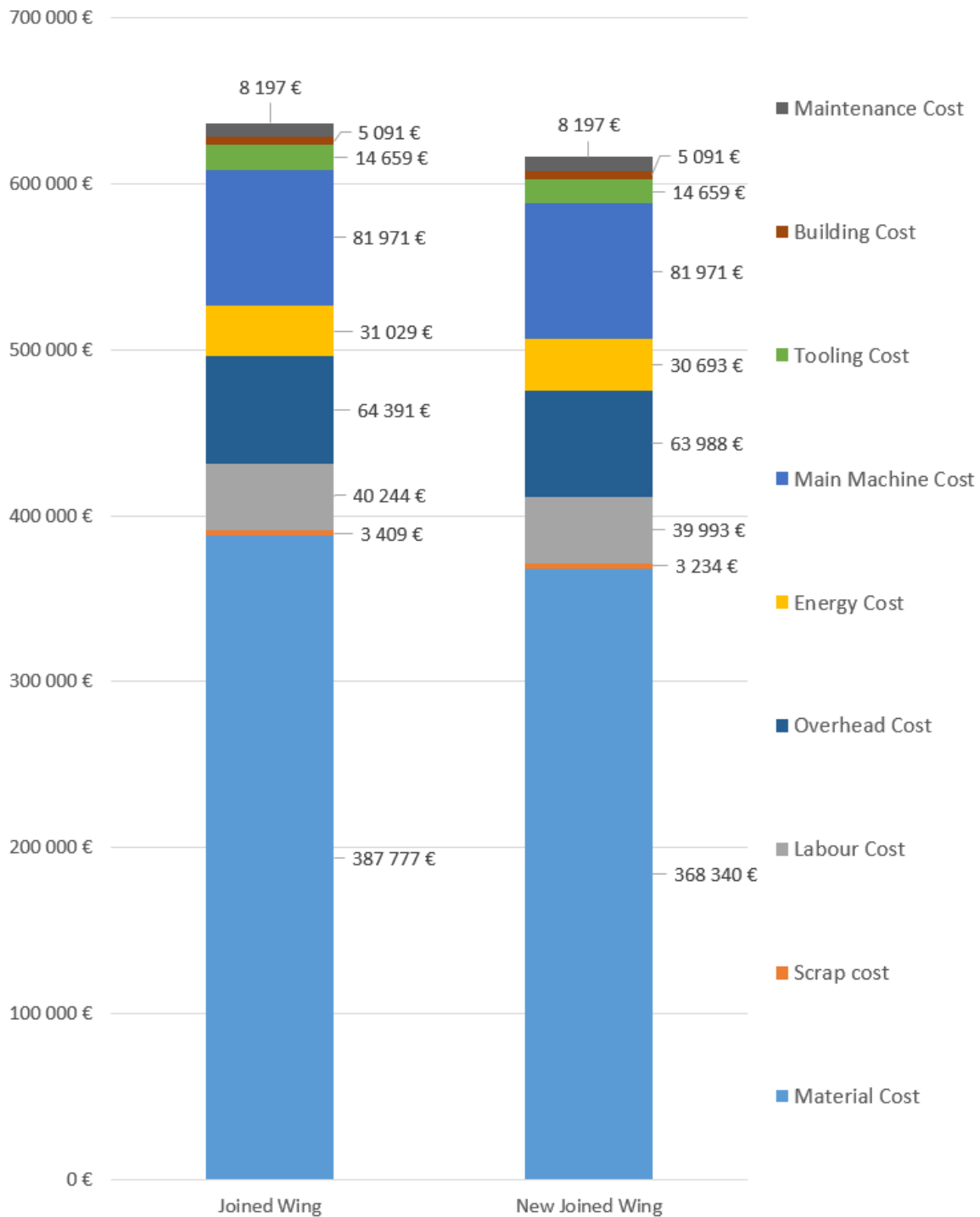


Figure 4.6: Production costs of both joined wing regarding the first analysis.

Regarding the second analysis, where an annual production volume of 50 units is assumed, the results obtained for the required number of machines for this production, uptimes, idle times and machine use percentages of each process are presented in Table 4.26.

Once more, comparing the obtained results with those in Table 4.22, it is verified that the removal of two layers of composite material, in all parts of the joined wing, does not cause changes in the number of machines per process, decreasing only the uptime value of the ATL process (the only process whose cycle time depends on the number of layers of composite material), which consequently decreases the

Table 4.26: Times and machine use for the new joined wing (production volume of 50 units).

	Reception	Application 1	ATL	Application 2	Autoclave	DFA	NDT
Number of Machines	3	2	4	2	3	3	2
Uptime	13021 h	7636 h	18100 h	7483 h	12581 h	13396 h	7085 h
Idle Time	2675 h	3116 h	3404 h	3269 h	3547 h	2732 h	3667 h
% Machine Use	82.96%	71.02%	84.17%	69.60%	78.01%	83.06%	65.90%

percentage of machine use in that process. This reduction in the number of working hours translates into a reduction of costs.

With the annual production volume and the number of machines in each process defined, the production costs of the joined wing are once again determined. In Figure 4.7, the graphs of the production costs of the joined wings (one from the second analysis and the other the new joined wing) are presented.

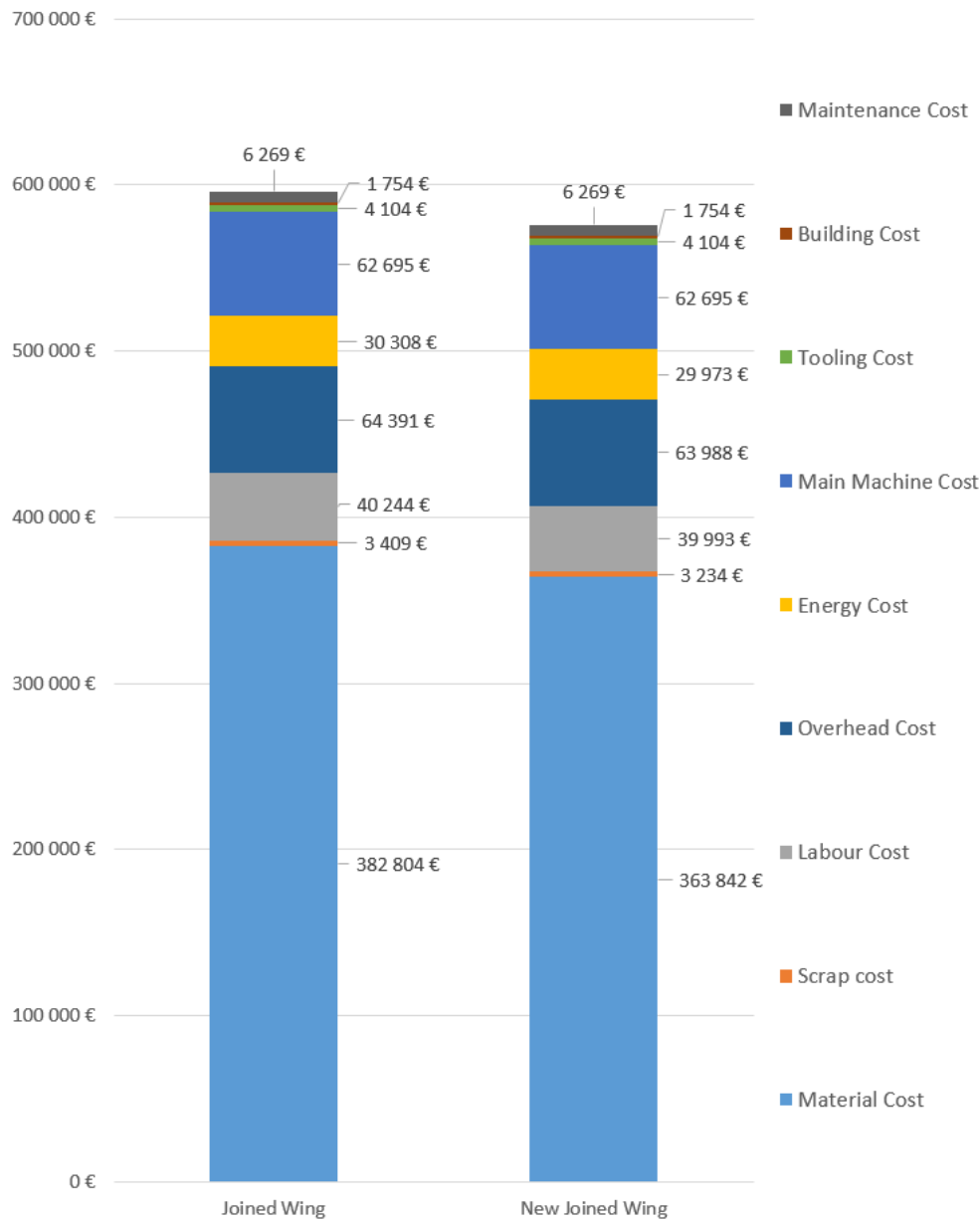


Figure 4.7: Production costs of both joined wing regarding the second analysis.

It is verified that the production cost of the new joined wing is, once again, lower when compared to the joined wing of the second analysis. The removal of two layers of composite material results in a reduction of 20 126 €. As in Figure 4.6, it is also observed in this one that fixed costs remain constant because there is no change in the number of machines or the annual production volume. In regard to variable costs, their reduction is implicit in the amount of material decrease, which results in a saving of 18 962 € (practically the total difference of costs between the two joined wings) and in a reduction of the number of working hours required.

As can be seen, a removal in the number of layers of composite material causes a reduction in production costs, not only in terms of material cost but also at all of the other types of variable costs. The decrease in the number of working hours is essential for the reduction of labor, overhead and energy costs.

It can be concluded that if the number of layers of composite material to be removed was higher, it could be observed either a reduction in the number of machines required for the ATL process or an increase in the annual production volume. In that case, it would be possible to achieve a reduction in fixed costs.

4.7 Investment Appraisal

After the determination of the production costs of the conventional aircraft and the joined wing, an investment appraisal is carried out in this section.

Assuming that an airline intends to invest in an aircraft and exists the possibility to choose between a conventional aircraft or a joined wing, through this assessment it is possible to verify the moment from which one investment becomes profitable when compared to the other.

The desired aircraft will be used for regional flights with a range of 1400 *km* and with a mission profile equal to the one shown in Figure 4.8. In addition, the aircraft is expected to perform two daily flights, 300 days a year, equivalent to a total of 600 flights per year.

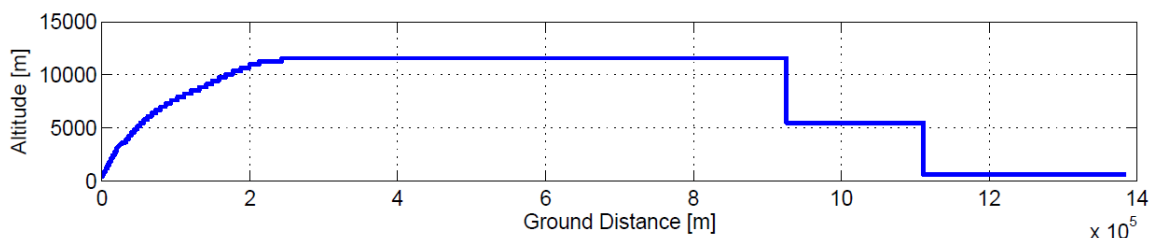


Figure 4.8: Mission profile [91].

Observing the figure, it is verified that this mission profile is divided into six segments: climb, cruise, first descent, alternate, second descent and hold. Note that the descent phases were assumed to be negligible in terms of fuel consumption.

The factors taken into account in this investment appraisal are the differences in production costs and jet fuel consumption of each aircraft.

From the MDO framework, it is obtained the consumptions of jet fuel per segment, in kilograms (*kg*), which are presented in Table 4.27.

Table 4.27: Jet fuel burned in quilograms.

	Conventional Aircraft	Joined Wing
Climb	458 kg	414 kg
Cruise	775 kg	598 kg
Alternate	239 kg	172 kg
Hold	500 kg	529 kg
TOTAL	1972 kg	1713 kg

As can be seen, the joined wing consumes less fuel than the conventional aircraft. The fact that the joined wing is heavier causes a higher angle of attack during its mission, which results in a drag increase. However, this problem is compensated by the reduction in induced drag due to the reduced wing area that produces lift (aspect ratio increase), associated to the wings of the joined wing, which reduces fuel consumption. When the aircraft is flying at lower speeds, as in the hold segment, the drag reduction is not so significant, leading to an increase in fuel consumption during this segment, as shown in the table.

The average price of jet fuel per gallon in 2017 was about 1.42 \$/gal [92]. Assuming that a gallon is 3.785 L, the jet fuel density is 0.81 kg/L and the conversion from dollar to euro is 0.89 (average of 2017), the price of jet fuel per kilogram is 0.520 €/kg. Multiplying this value by the kilograms of burned fuel, it is obtained a fuel cost per flight of 1025 € for conventional aircraft and 890 € for joined wing. The difference in fuel cost per flight between both aircraft is 135 €.

Regarding the differences in aircraft production costs, according to the first analysis (Subsection 4.5.1), it is verified that the conventional aircraft costs 191 229 € less than the joined wing, and according to the second analysis (Subsection 4.5.2), the difference is 157 692 € less. It is decided to carry out an investment appraisal for each analysis.

As mentioned in Chapter 2, the NPV is the sum of all discounted cash flows associated to a time period at a given discount rate, calculated by Equation 2.2. For this equation, it is used an interest rate of 6%, an assumed value in the aerospace sector, according to Tomás [93]. The initial cash flow ($t = 0$) is the difference in production costs between both aircraft, considered negative, since it is an initial expense that will be subsequently discounted by the following cash flows, which results from savings in fuel consumption. Assuming that 600 flights are performed per year, and knowing that the savings in each flight is 135 €, cash flows of 81 000 € are obtained per year.

In the following tables, the obtained results for the NPV over the years are presented. Table 4.28 refers to the first analysis between the conventional aircraft and the joined wing, while Table 4.29 presents the results for the second cost analysis.

As can be seen in the tables, in both analyses, the payback periods are short, between the second and third years. It is concluded that despite having to spend more money on the joined wing production,

Table 4.28: Net present value of the first analysis.

Years	0	1	2	3	4	5
Cash Flows	- 191 220 €	81 000 €	81 000 €	81 000 €	81 000 €	81 000 €
TOTAL	- 191 220 €	- 114 805 €	- 42 715 €	25 294 €	89 454 €	149 981 €

Table 4.29: Net present value of the second analysis.

Years	0	1	2	3	4	5
Cash Flows	- 157 692 €	81 000 €	81 000 €	81 000 €	81 000 €	81 000 €
TOTAL	- 157 692 €	- 81 277 €	- 9 187 €	58 822 €	122 982 €	183 509 €

in a few years the return of this investment is recovered.

In this investment appraisal, as mentioned above, the only factors considered are the differences between the production costs and the fuel consumptions of the aircraft. However, there are other factors that could have entered into this assessment, such as aircraft maintenance and overhaul costs, other flight operating costs and environmental costs. The first factor referred would benefit the choice of conventional aircraft, since this one is the most used today, and there is a greater maintenance experience, implying lower maintenance costs. On the other hand, environmental costs would benefit the choice of joined wing since the economic costs at this level (regulations, standards) are lower compared to conventional aircraft.

It should also be noted that the differences between the production costs of the aircraft studied in this thesis are only due to the production costs of some structural parts, wings and tails. As mentioned in Section 3.3.4, only different parts were assumed to be relevant for the study. The equal parts in both aircraft, such as engines and fuselage, were not integrated, since their costs are the same and therefore have no value in a comparative analysis.

It should also be taken into account that this is a preliminary analysis. The considered structures in this cost model were simplified, highlighting the use of skins and spars (wing box layout) as the only constituent parts of these structures, disregarding others, such as ribs and stringers.

Chapter 5

Conclusions and Future work

In the aerospace sector there is a growing demand for new aircraft configurations and new materials. Nowadays, only minor improvements can be made to the most used aircraft configuration. Moreover, composite materials are increasingly sought after by their advantages over aluminium and, therefore, their implementation in this sector is growing.

Consequently, the development of novel configurations is a necessary reality, as well as costs estimate at a preliminary design stage, so that decisions can be made on the financial viability of the investment. When developing a conventional aircraft, the parameters used in its cost estimate come from historical data. However, in the case of novel configurations, these parameters do not exist, being required the development of a new method for estimating costs.

The aim of this thesis was to develop a process based cost model of automated tape laying (ATL) for novel aircraft configurations. It is concluded that this model is versatile since it can also give an estimate of the production costs of conventional aircraft, since model inputs are entered in the form of parts' geometry. The model can also be adapted to different annual production volumes or to the capacity of the existing machines in a plant. The cost estimate obtained presents the fixed and variable costs of an aircraft production.

From the test cases analysed in this thesis, it is concluded that the joined wing has higher production costs than the conventional aircraft. Costs related to the rear wing and vertical tail are higher than the costs of horizontal and vertical tails of conventional aircraft. The fact that the rear wing is larger and requires more material in its production, and the fact that this structure is long and narrow, which leads to several wastes of material during the ATL process, contribute to the increase in the joined wing production cost. In relation to its vertical tail, it needs a more robust structure due to have to support the rear wing weight, which implies a greater deposition of material and consequently an increase of its cost. Unlike these structures, the cost of the main wing in the joined wing is lower: this main wing has smaller area due to the fact that the rear wing also produces lift.

In the test cases, aircraft fuselage and engines were not contemplated, since these structures are the same for both aircraft and, therefore, their costs have no impact on the comparative analyses performed.

It has also been found that the majority of the production costs, about 60 to 65% of the total value,

comes from the material costs, material which was used in the production of the parts.

Through an investment appraisal, it was observed that the difference in the production cost of the joined wing when compared to conventional aircraft can be compensated after two to three years, taking into account only the fuel consumption, which in this configuration (joined wing) is lower.

A sensitivity analysis of production costs was also carried out by reducing the number of layers of composite material applied to the aircraft. This removal has led to a reduction in these costs, not only in terms of material cost, but at all types of variable costs (scrap, labor, overhead and energy costs), since the removal of layers diminishes the number of working hours. It can further be concluded that if the number of layers of composite material to be removed was higher, the number of machines required could decrease or the annual production volume could increase, leading to a reduction in fixed costs.

A few suggestions for future work are proposed below.

The cost model developed in this thesis is a versatile and flexible model, allowing variety in the type of inputs introduced. Thus, it is possible that this model can be applied in a financial analysis of several types of configurations, and not only in the two test cases in this thesis (conventional aircraft and joined wing). However, the model is limited with respect to the production method, allowing only the use of composite material and ATL.

It should be taken into account that this cost model still requires the insertion of inputs manually, which makes their use time-consuming. This can be one of the points to improve in the future, making this process more automatic and easy to handle.

Worth to note that this is a preliminary model of production costs, excluding any previous or subsequent phases, such as the assembly phase. Thus, the model can be developed, making it comprehensible to the other phases mentioned.

In addition, in the test cases, only production costs of wings and tails are considered, and the production costs of an entire aircraft are not accounted. In this way, there is the possibility of carrying out a more reliable financial analysis taking into account the higher possible number of parts of an aircraft.

In this thesis, some approaches were made in order to determine inputs of the cost model: the MDO framework designs the configurations' structures in aluminium, although it was assumed to be composite material; machine times were determined according to an unique example part that served as a comparison. An analysis with more accuracy than the one carried out in this thesis can be obtained, being more rigorous in these determinations.

Through variations in the number of machines in each process and the annual production volume, an optimization can be performed to maximize the production, so that its costs can be decreased.

Observing the results obtained in the test cases, the model appears to show a trend in the percentage distribution of costs, however, further analysis are required to confirm this trend.

It is also suggested that more sensitivity analyses should be performed, varying new parameters, in order to understand how the model will react, analysing the impact on final costs.

Finally, it is suggested that a more comprehensive investment appraisal should be carried out, including other types of costs, such as maintenance and overhaul costs, other flight operation costs and environmental costs, allowing a more accurate and reliable analysis of the investment.

Bibliography

- [1] Eurostat. Air transport statistics. Online, April 2017. http://ec.europa.eu/eurostat/statistics-explained/index.php/Air_transport_statistics.
- [2] Investing.com. Brent oil futures. Online, April 2017. <https://www.investing.com/commodities/brent-oil-streaming-chart>.
- [3] U. S. Environmental Protection Agency. EPA determines that aircraft emissions contribute to climate change endangering public health and the environment. Online, July 2016. <https://www.epa.gov/newsreleases/epa-determines-aircraft-emissions-contribute-climate-change-endangering-public-health>.
- [4] United Nations. Paris Climate Agreement, December 2015.
- [5] International Civil Aviation Organization. ICAO Environmental Report 2016. Technical report, International Civil Aviation Organization, 2016.
- [6] W. Marx, D. Mavris, and D. Schrage. A hierarchical aircraft life cycle cost analysis model. In *Aircraft Engineering, Technology and Operations Congress*, Los Angeles, USA, 1995.
- [7] M. Mengoni, M. Mandolini, M. Matteucci, and M. Germani. A scalable “Design for Costing” platform: a practical case in ball valves industry. *Procedia CIRP*, 50:311–317, 2016.
- [8] J. D. Ritschel. A comparative analysis of the cost estimating error risk associated with flyaway costs versus individual components of aircraft. Master’s thesis, Air Force Institute of Technology, March 2003.
- [9] L. I. Keys. System life cycle engineering and DF’X’. *IEEE Transactions on Components, Hybrids and Manufacturing Technology*, 13(1):83–93, March 1990.
- [10] K. Okano. Life cycle costing - An approach to life cycle cost management: A consideration from historical development. *Asia Pacific Management Review*, 6(3):317–341, 2001.
- [11] Water Environment Research Foundation: Sustainable Infrastructure Management Program Learning Environment. Overview: What is Life Cycle Costing? Online, May 2017. <http://simple.werf.org/simple/media/LCCT/index.html>.

- [12] R. Curran, S. Raghunathan, and M. Price. Review of aerospace engineering cost modelling: The genetic causal approach. *Progress in Aerospace Sciences*, 40(8):487–534, November 2004.
- [13] Y. Asiedu and P. Gu. Product life cycle cost analysis: State of the art review. *International Journal of Production Research*, 36(4):883–908, 1998.
- [14] N. Cross. *Engineering Design Methods: Strategies for Product Design*. John Wiley & Sons, LTD, Third edition, June 2005.
- [15] S. Gudmundsson. *General Aviation Aircraft Design: Applied Methods and Procedures*, chapter 1, pages 1–32. Butterworth-Heinemann, 2014.
- [16] Projecto Aeroespacial - Instituto Superior Técnico. Lecture 1: Introduction to Aircraft Design, 2016.
- [17] Institut für Luft- und Raumfahrtssysteme: RWTH Aachen University. Centre Reference Aircraft data System. Online, May 2017. <http://ceras.ilr.rwth-aachen.de/>.
- [18] Airbus. How is an aircraft built? Online, May 2017. <http://www.aircraft.airbus.com/market/how-is-an-aircraft-built/>.
- [19] A. S. H. Makhoulf and M. Aliofkhaezai. *Handbook of Materials Failure Analysis with Case Studies from the Aerospace and Automotive Industries*, chapter 13, pages 261–277. Butterworth-Heinemann, 2015.
- [20] European Aviation Safety Agency. Online, May 2017. <https://www.easa.europa.eu/>.
- [21] Federal Aviation Administration. Online, May 2017. <https://www.faa.gov/>.
- [22] Federal Aviation Administration. Federal Aviation Regulations Part 25: Airworthiness Standards: Transport Category, 1964.
- [23] Joint Aviation Requirements JAR-25: Large Aeroplanes, 1994.
- [24] International Civil Aviation Organization. Online, May 2017. <https://www.icao.int/Pages/default.aspx>.
- [25] Air Fleet: Private Client Aviation Solutions. Costs. Online, May 2017. <http://www.airfleetops.com/aviation/costs/>.
- [26] Transport Studies Group. Innovative Cooperative Actions of Research & Development in EURO-CONTROL Programme CARE INO III: Dynamic Cost Indexing. Technical report, University of Westminster, June 2008.
- [27] Gellman Research Associates Incorporated. Section 4 - Aircraft Operating Costs. In *Economic Values for FAA Investment and Regulatory Decisions Guide*. Federal Aviation Administration, 2015.
- [28] U. S. Environmental Protection Agency. Online, May 2017. <https://www.epa.gov/>.
- [29] B. James. How to make money with older equipment. *Airfinance Journal*, (335):48, 2010.

- [30] S. Sihvonena and T. Ritola. Conceptualizing ReX for aggregating end-of-life strategies in product development. *Procedia CIRP*, 29:639–644, 2015.
- [31] J. Duflou, G. Seliger, S. Kara, Y. Umeda, A. Ometto, and B. Willems. Efficiency and feasibility of product disassembly: A case-based study. *CIRP Annals - Manufacturing Technology*, 57:583–600, 2008.
- [32] J. S. Ribeiro and J. de Oliveira Gomes. Proposed framework for End-Of-Life aircraft recycling. *Procedia CIRP*, 26:311–316, 2015.
- [33] Airbus. PAMELA - Process for Advanced Management of End-of-Life of Aircraft. Company publication, 2008.
- [34] Aircraft Fleet Recycling Association. Online, May 2017. <https://afraassociation.org/about-us/afra-mission/>.
- [35] Y. Liu, M. Farnsworth, and A. Tiwari. A review of optimisation techniques used in the composite recycling area: State-of-the-art and steps towards a research agenda. *Journal of Cleaner Production*, 140:1775–1781, 2017.
- [36] A. L. Velocci. Profit wave uncovers nagging paradoxes. *Aviation Week and Space Technology*, May 1995.
- [37] Defense Manufacturing Council (DMC) Executive Group off-site meeting notes, January 1995.
- [38] M. Hundal. Design to cost. Concurrent Engineering. *Chapman&Hall*, pages 329–351, 1993.
- [39] S. O. L. Zijp. Development of a life cycle cost model for conventional and unconventional aircraft. Master's thesis, Delft University of Technology, June 2014.
- [40] S. Castagne, R. Curran, A. Rothwell, M. Price, E. Benard, and S. Raghunathan. A generic tool for cost estimating in aircraft design. *Research in Engineering Design*, 18(4):149–162, 2008.
- [41] A. N. et al. Product Cost Estimation: Technique Classification and Methodology Review. *Journal of Manufacturing Science and Engineering*, 128:563–575, May 2006.
- [42] Air Force Institute of Technology and Federal Acquisition Institute. Contract Pricing Reference Guides: Quantitative Techniques for Contract Pricing, March 1997.
- [43] O. Younossi, M. Kennedy, and J. Graser. *Military Airframe Costs: The Effects of Advanced Materials and Manufacturing Processes*. Monograph Reports. Rand Corporation, 2001.
- [44] J. Long. Parametric Cost Estimating in the New Millennium. *ISPA SCEA Joint International Conference Papers*, 2000.
- [45] U.S. Air Forces Systems Command. AFSC Cost Estimating Handbook Series, 1986.
- [46] Institute for Defense Analysis. Cost Estimating for Next Generation Aircraft, 2000.

- [47] G. S. Levenson, H. E. Boren, D. P. Tihansky, and F. Timson. Cost-Estimating Relationships for Aircraft Airframes. Technical report, Rand Corporation, February 1972.
- [48] M. N. Beltramo, D. L. Trapp, B. W. Kimoto, and D. P. Marsh. Parametric Study of Transport Aircraft Systems Cost and Weight. Technical report, NASA, April 1977.
- [49] J. Roskam. *Airplane Design*, chapter Part VIII: Airplane Cost Estimation: Design, Development, Manufacturing and Operating. Design, Analysis and Research Corporation, 2015.
- [50] D. P. Raymer. *Aircraft Design: A Conceptual Approach*, chapter 18, pages 501–518. AIAA, 1992.
- [51] C. Soutis. Carbon fiber reinforced plastics in aircraft construction. *Materials Science and Engineering*, 412(1–2):171–176, 2005.
- [52] G. Marsh. Composites flying high. *Reinforced Plastics*, 58(3):14–18, 2014.
- [53] T. Dursun and C. Soutis. Recent developments in advanced aircraft aluminium alloys. *Materials and Design*, 56:862–871, 2014.
- [54] V. Songmene, R. Khettabi, I. Zaghbani, J. Kouam, and A. Djebara. *Aluminium Alloys, Theory and Applications: Machining and Machinability of Aluminum Alloys*, chapter 18, pages 377–400. InTech, 2011.
- [55] J. P. Immarigeon, R. T. Holt, A. K. Koul, L. Zhao, W. Wallace, and J. C. Beddoes. Lightweight materials for aircraft applications. *Materials Characterization*, 35(1):41–67, 1995.
- [56] D. B. Lambert. Composite aircraft life cycle cost estimating model. Master's thesis, Air Force Institute of Technology, March 2011.
- [57] Lockheed Martin. Advanced Composite Cargo Aircraft (ACCA). Online, May 2017. <https://lockheedmartin.com/us/products/acca.html>.
- [58] Hexcel. *HexPly Prepreg - Technology*, January 2013.
- [59] G. Marsh. Aerospace composites - the story so far. *Reinforced Plastics*, 40:44–48, 1996.
- [60] J. Russell. Market Trends: The Composites Affordability Initiative, Part I. Online, June 2007. <https://www.compositesworld.com/columns/market-trends-the-composites-affordability-initiative-part-i>.
- [61] J. Russell. Market Trends: Composites Affordability Initiative, Part II. Online, June 2007. <https://www.compositesworld.com/columns/market-trends-composites-affordability-initiative-part-ii>.
- [62] J. Russell. Advanced Composite Cargo Aircraft proves large structure practicality. Online, June 2009. <https://www.compositesworld.com/columns/advanced-composite-cargo-aircraft-proves-large-structure-practicality>.

- [63] J. Hale. Boeing 787 from the Ground Up. Boeing Aeromagazine, 2008.
- [64] Airbus. A350 XWB. Online, July 2017. <http://www.aircraft.airbus.com/aircraftfamilies/passengeraircraft/a350xwbfamily/>.
- [65] U. K. Singh and M. Dwivedi. *Manufacturing processes*. New Age, 2009.
- [66] S. Black. Lightning strike protection strategies for composite aircraft. Online, July 2017. <http://www.compositesworld.com/articles/lightning-strike-protection-strategies-for-composite-aircraft>.
- [67] J. Hinrichsen and C. Bautista. The challenge of reducing both airframe weight and manufacturing cost. *Air & Space Europe*, 3:119–121, 2001.
- [68] M. Hagnell and M. Åkermo. A composite cost model for the aeronautical industry: Methodology and case study. *Composites: Part B*, 79:254–261, 2015.
- [69] J. Sloan. Taking the hand out of hand layup. Online, July 2017. <https://www.compositesworld.com/articles/taking-the-hand-out-of-hand-layup>.
- [70] J. Sloan. ATL and AFP: Defining the megatrends in composite aerostructures. Online, July 2017. <http://www.compositesworld.com/articles/atl-and-afp-defining-the-megatrends-in-composite-aerostructures>.
- [71] D. H.-J. A. Lukaszewicz. *Optimisation of high-speed automated layup of thermoset carbon-fibre preimpregnates*. PhD thesis, University of Bristol, 2011.
- [72] D. H.-J. A. Lukaszewicz, C. Ward, and K. D. Potter. The engineering aspects of automated prepreg layup: History, present and future. *Composites: Part B*, 43:997–1009, 2012.
- [73] Airbus orders six MAG fiber placement machines for A350 fuselage. Online, July 2017. <http://www.compositesworld.com/news/airbus-orders-six-mag-fiber-placement-machines-for-a350-fuselage>.
- [74] R. Cavallaro and L. Demasi. Challenges, Ideas, and Innovations of Joined-Wing Configurations: A Concept from the Past, an Opportunity for the Future. *Progress in Aerospace Sciences*, 87:1–93, 2016.
- [75] NASA. Blended Wing Body - A potential new aircraft design. Online, May 2017. <https://www.nasa.gov/centers/langley/news/factsheets/FS-2003-11-81-LaRC.html>.
- [76] Lockheed Martin. NASA Environmentally Responsible Aviation. Online, May 2017. <https://www.lockheedmartin.com/en-us/index.html>.
- [77] Boeing. Environment Report - Future Flight. Online, May 2017. http://www.boeing.com/aboutus/environment/environment_report_14/2.3_future_flight.html.

- [78] E. Ordoukhanian and A. M. Madni. Blended Wing Body Architecting and Design: Current Status and Future Prospects. *Procedia Computer Science*, 28:619–625, 2014.
- [79] NASA. Past Projects: X-48B Blended Wing Body. Online, August 2017. <https://www.nasa.gov/centers/dryden/research/X-48B/index.html>.
- [80] R. Liebeck. Design of the Blended Wing Body Subsonic Transport. *Journal of Aircraft*, 41(1):10–25, 2004.
- [81] R. Liebeck, M. Page, and B. Rawdon. Blended-wing-body subsonic commercial transport. In *36th AIAA Aerospace Sciences Meeting and Exhibit*, Reno, USA, 1998.
- [82] L. Prandtl. Induced Drag of Multiplanes. Technical Report TN-182, National Advisory Committee for Aeronautics, 1924.
- [83] J. W. Gallman, S. C. Smith, and I. M. Kroo. Optimization of Joined-Wing Aircraft. *Journal of Aircraft*, 30(6):897–905, December 1993.
- [84] I. Kroo, J. Gallmant, and S. Smith. Aerodynamic and Structural Studies of Joined-Wing Aircraft. *Journal of Aircraft*, 28(1):74–81, January 1991.
- [85] F. H. Gern, A. Ko, E. Sulaeman, J. F. Gundlach, R. K. Kapania, and R. T. Haftka. Multidisciplinary Design Optimization of a Transonic Commercial Transport with Strut-Braced Wing. *Journal of Aircraft*, 38(6):1006–1014, 2001.
- [86] R. Turriziani, W. Lovell, G. Martin, J. Price, and E. S. G. Washburn. Preliminary design characteristics of a subsonic business jet concept employing an aspect ratio 25 strut-braced wing. Technical Report CR-159361, NASA, 1980.
- [87] R. Gupta, W. Mallik, and R. Kapania. Multidisciplinary Design Optimization of Subsonic Truss-Braced Wing Cargo Aircraft. In *52nd Aerospace Sciences Meeting*, National Harbor, USA, 2014.
- [88] Association for Project Management. Investment appraisal. Online, October 2017. <https://www.apm.org.uk/body-of-knowledge/delivery/financial-cost-management/investment-appraisal/>.
- [89] R. Brealey, S. Myers, and F. Allen. *Principles of Corporate Finance*. McGraw-Hill, 10 edition, 2011.
- [90] Hexcel Corporation. Hexply M21 - Product Data Sheet, 2015.
- [91] J. Vale, F. Afonso, F. Lau, and A. Suleman. Performance Based MDO of a Joined-Wing Regional Transport Aircraft. In *56th AIAA/ASCE/AHS/ASC Structures, Structural Dynamics, and Materials Conference*, Kissimmee, USA, 2015.
- [92] Index Mundi. Jet Fuel. Online, April 2018. <https://www.indexmundi.com/commodities/?commodity=jet-fuel&months=60>.
- [93] D. Tomás. Melhoria do processo de controlo de qualidade na fuselagem central de uma aeronave militar. Master's thesis, Instituto Superior Técnico, April 2017.

Appendix A

Cycle Times and Allocations

In this appendix, cycle times and allocation percentages of each part produced in all processes are shown, complementing the section 4.4, where the inputs of the cost model are presented.

The cycle time is given by the sum of the machine time with the setup time, as demonstrated in Equation 3.17. Through the inputs presented in Section 4.4, the results obtained for the cycle times of all parts, for all processes, are observed in the tables below.

Regarding to the allocations of each part, these are calculated through Equation 3.25. With the cycle times achieved and knowing that the production of an aircraft requires one vertical tail structure, two main wing structures (right and left) and two horizontal tail structures or two rear wing structures (right and left), according to the production of a conventional aircraft or a joined wing respectively, the values corresponding to the allocations are also presented in the same tables.

Thus, according to the methodology described above, the results obtained are presented in four tables. Tables A.1 and A.2 present the cycle times and the skins and spars allocations, respectively, relative to the conventional aircraft. Tables A.3 and A.4 present the cycle times and the allocation percentages of skins and spars, respectively, relative to the joined wing.

As observed in these tables, both reception, check and storage process and autoclave process have constant cycle times, which are independent of the dimensions of the produced parts, as referred in Subsections 4.4.1 and 4.4.5, respectively. In the case of the allocation percentages of these same processes, knowing that the number of parts to be produced related to the vertical tail is always half the number of parts related to the main wing, rear wing or horizontal tail, the allocation percentage of each vertical tail's part will also be half of the other percentages.

As previously mentioned in Section 4.1, the vertical tails are composed of symmetrical airfoils. Thus, it is verified that the obtained values for skin parts of this structure are equal for both upper and lower surfaces.

It should also be noted that the sum of the skins and spars allocation percentages in each process is equal to 100%, for both conventional aircraft and joined wing, which means that each machine is exclusively allocated to the type of aircraft under analysis.

Table A.1: Cycle times and allocations for conventional aircraft skins

		Reception	Aplication	ATL	Aplication	Autoclave	DFA	NDT	
		Skins		Main Wing					
1 U	3.5h (3.85%)			10.17h (13.28%)	9.15h (9.93%)	10.17h (13.28%)	3.5h (3.85%)	6.59h (6.70%)	10.17h (13.28%)
1 L	3.5h (3.85%)			10.20h (13.32%)	9.17h (9.95%)	10.20h (13.32%)	3.5h (3.85%)	6.60h (6.71%)	10.20h (13.32%)
2 U	3.5h (3.85%)			5.99h (7.82%)	4.39h (4.77%)	5.99h (7.82%)	3.5h (3.85%)	5.48h (5.58%)	5.99h (7.82%)
2 L	3.5h (3.85%)			5.97h (7.79%)	4.39h (4.77%)	5.97h (7.79%)	3.5h (3.85%)	5.47h (5.57%)	5.97h (7.79%)
3 U	3.5h (3.85%)			3.00h (3.91%)	2.88h (3.12%)	3.00h (3.91%)	3.5h (3.85%)	3.75h (3.81%)	3.00h (3.91%)
3 L	3.5h (3.85%)			2.99h (3.90%)	2.87h (3.12%)	2.99h (3.90%)	3.5h (3.85%)	3.74h (3.81%)	2.99h (3.90%)
Horizontal Tail									
4 U	3.5h (3.85%)			2.24h (2.92%)	2.76h (3.00%)	2.24h (2.92%)	3.5h (3.85%)	3.23h (3.29%)	2.24h (2.92%)
4 L	3.5h (3.85%)			2.26h (2.95%)	2.77h (3.01%)	2.26h (2.95%)	3.5h (3.85%)	3.26h (3.31%)	2.26h (2.95%)
5 U	3.5h (3.85%)			3.40h (4.43%)	2.99h (3.25%)	3.40h (4.43%)	3.5h (3.85%)	4.20h (4.27%)	3.40h (4.43%)
5 L	3.5h (3.85%)			3.44h (4.49%)	3.01h (3.27%)	3.44h (4.49%)	3.5h (3.85%)	4.22h (4.29%)	3.44h (4.49%)
Vertical Tail									
6 U	3.5h (1.92%)			2.25h (1.47%)	3.27h (1.78%)	2.25h (1.47%)	3.5h (1.92%)	4.17h (2.12%)	2.25h (1.47%)
6 L	3.5h (1.92%)			2.25h (1.47%)	3.27h (1.78%)	2.25h (1.47%)	3.5h (1.92%)	4.17h (2.12%)	2.25h (1.47%)
7 U	3.5h (1.92%)			3.77h (2.46%)	3.99h (2.17%)	3.77h (2.46%)	3.5h (1.92%)	4.14h (2.11%)	3.77h (2.46%)
7 L	3.5h (1.92%)			3.77h (2.46%)	3.99h (2.17%)	3.77h (2.46%)	3.5h (1.92%)	4.14h (2.11%)	3.77h (2.46%)
8 U	3.5h (1.92%)			2.84h (1.85%)	2.99h (1.62%)	2.84h (1.85%)	3.5h (1.92%)	3.63h (1.85%)	2.84h (1.85%)
8 L	3.5h (1.92%)	2.84h (1.85%)	2.99h (1.62%)	2.84h (1.85%)	3.5h (1.92%)	3.63h (1.85%)	2.84h (1.85%)		

Table A.2: Cycle times and allocations for conventional aircraft spars

		Reception	Aplication	ATL	Aplication	Autoclave	DFA	NDT	
		Spars		Main Wing					
1 F	3.5h (3.85%)			2.08h (2.72%)	4.21h (4.57%)	2.08h (2.72%)	3.5h (3.85%)	4.31h (4.38%)	2.08h (2.72%)
1 R	3.5h (3.85%)			2.16h (2.82%)	4.31h (4.68%)	2.16h (2.82%)	3.5h (3.85%)	4.17h (4.24%)	2.16h (2.82%)
2 F	3.5h (3.85%)			1.60h (2.09%)	2.83h (3.07%)	1.60h (2.09%)	3.5h (3.85%)	4.25h (4.33%)	1.60h (2.09%)
2 R	3.5h (3.85%)			1.46h (1.91%)	2.73h (2.96%)	1.46h (1.91%)	3.5h (3.85%)	4.09h (4.16%)	1.46h (1.91%)
3 F	3.5h (3.85%)			1.26h (1.64%)	2.42h (2.62%)	1.26h (1.64%)	3.5h (3.85%)	2.93h (2.99%)	1.26h (1.64%)
3 R	3.5h (3.85%)			1.16h (1.52%)	2.41h (2.62%)	1.16h (1.52%)	3.5h (3.85%)	2.80h (2.85%)	1.16h (1.52%)
Horizontal Tail									
4 F	3.5h (3.85%)			1.16h (1.52%)	2.53h (2.75%)	1.16h (1.52%)	3.5h (3.85%)	1.95h (1.98%)	1.16h (1.52%)
4 R	3.5h (3.85%)			1.10h (1.44%)	2.84h (3.09%)	1.10h (1.44%)	3.5h (3.85%)	1.83h (1.87%)	1.10h (1.44%)
5 F	3.5h (3.85%)			1.32h (1.73%)	2.51h (2.72%)	1.32h (1.73%)	3.5h (3.85%)	3.41h (3.47%)	1.32h (1.73%)
5 R	3.5h (3.85%)			1.20h (1.56%)	2.46h (2.67%)	1.20h (1.56%)	3.5h (3.85%)	3.20h (3.26%)	1.20h (1.56%)
Vertical Tail									
6 F	3.5h (1.92%)			1.21h (0.79%)	2.87h (1.56%)	1.21h (0.79%)	3.5h (1.92%)	2.03h (1.03%)	1.21h (0.79%)
6 R	3.5h (1.92%)			1.15h (0.75%)	2.92h (1.58%)	1.15h (0.75%)	3.5h (1.92%)	1.87h (0.95%)	1.15h (0.75%)
7 F	3.5h (1.92%)			1.25h (0.82%)	2.77h (1.50%)	1.25h (0.82%)	3.5h (1.92%)	2.38h (1.21%)	1.25h (0.82%)
7 R	3.5h (1.92%)			1.19h (0.78%)	2.75h (1.49%)	1.19h (0.78%)	3.5h (1.92%)	2.29h (1.16%)	1.19h (0.78%)
8 F	3.5h (1.92%)			1.20h (0.78%)	2.52h (1.37%)	1.20h (0.78%)	3.5h (1.92%)	2.70h (1.37%)	1.20h (0.78%)
8 R	3.5h (1.92%)	1.14h (0.74%)	2.57h (1.39%)	1.14h (0.74%)	3.5h (1.92%)	2.46h (1.25%)	1.14h (0.74%)		

Table A.3: Cycle times and allocations for joined wing skins

		Reception	Application	ATL	Application	Autoclave	DFA	NDT	
Skins	Main Wing	1 S	3.5h (2.94%)	5.59h (8.01%)	5.85h (3.42%)	5.59h (8.01%)	3.5h (2.94%)	5.25h (4.10%)	5.59h (8.01%)
		1 L	3.5h (2.94%)	5.60h (8.03%)	5.86h (3.43%)	5.60h (8.03%)	3.5h (2.94%)	5.26h (4.11%)	5.60h (8.03%)
		2 S	3.5h (2.94%)	2.39h (3.42%)	2.82h (1.65%)	2.39h (3.42%)	3.5h (2.94%)	3.41h (2.66%)	2.39h (3.42%)
		2 L	3.5h (2.94%)	2.38h (3.41%)	2.82h (1.65%)	2.38h (3.41%)	3.5h (2.94%)	3.41h (2.66%)	2.38h (3.41%)
		3 S	3.5h (2.94%)	2.12h (3.04%)	2.60h (1.52%)	2.12h (3.04%)	3.5h (2.94%)	3.14h (2.46%)	2.12h (3.04%)
		3 L	3.5h (2.94%)	2.12h (3.03%)	2.59h (1.52%)	2.12h (3.03%)	3.5h (2.94%)	3.14h (2.45%)	2.12h (3.03%)
		4 S	3.5h (2.94%)	2.00h (2.86%)	2.44h (1.43%)	2.00h (2.86%)	3.5h (2.94%)	3.28h (2.57%)	2.00h (2.86%)
		4 L	3.5h (2.94%)	1.99h (2.86%)	2.44h (1.43%)	1.99h (2.86%)	3.5h (2.94%)	3.28h (2.56%)	1.99h (2.86%)
	Rear Wing	5 S	3.5h (2.94%)	1.12h (1.61%)	2.28h (1.33%)	1.12h (1.61%)	3.5h (2.94%)	2.37h (1.85%)	1.12h (1.61%)
		5 L	3.5h (2.94%)	1.12h (1.61%)	2.28h (1.33%)	1.12h (1.61%)	3.5h (2.94%)	2.37h (1.85%)	1.12h (1.61%)
		6 S	3.5h (2.94%)	4.50h (6.44%)	4.36h (2.55%)	4.50h (6.44%)	3.5h (2.94%)	9.14h (7.14%)	4.50h (6.44%)
		6 L	3.5h (2.94%)	4.49h (6.43%)	4.35h (2.55%)	4.49h (6.43%)	3.5h (2.94%)	9.14h (7.14%)	4.49h (6.43%)
		7 S	3.5h (2.94%)	2.09h (2.99%)	3.05h (1.79%)	2.09h (2.99%)	3.5h (2.94%)	3.39h (2.64%)	2.09h (2.99%)
		7 L	3.5h (2.94%)	2.09h (2.99%)	3.05h (1.78%)	2.09h (2.99%)	3.5h (2.94%)	3.38h (2.64%)	2.09h (2.99%)
	Vertical Tail	8 S	3.5h (1.47%)	2.25h (1.61%)	4.17h (1.22%)	2.25h (1.61%)	3.5h (1.47%)	4.17h (1.63%)	2.25h (1.61%)
		8 L	3.5h (1.47%)	2.25h (1.61%)	4.17h (1.22%)	2.25h (1.61%)	3.5h (1.47%)	4.17h (1.63%)	2.25h (1.61%)
		9 S	3.5h (1.47%)	3.77h (2.70%)	5.53h (1.62%)	3.77h (2.70%)	3.5h (1.47%)	4.14h (1.62%)	3.77h (2.70%)
		9 L	3.5h (1.47%)	3.77h (2.70%)	5.53h (1.62%)	3.77h (2.70%)	3.5h (1.47%)	4.14h (1.62%)	3.77h (2.70%)
10 S		3.5h (1.47%)	2.84h (2.03%)	3.82h (1.12%)	2.84h (2.03%)	3.5h (1.47%)	3.63h (1.42%)	2.84h (2.03%)	
10 L		3.5h (1.47%)	2.84h (2.03%)	3.82h (1.12%)	2.84h (2.03%)	3.5h (1.47%)	3.63h (1.42%)	2.84h (2.03%)	

Table A.4: Cycle times and allocations for joined wing spars

		Reception	Application	ATL	Application	Autoclave	DFA	NDT	
Spars	Main Wing	1 S	3.5h (2.94%)	1.54h (2.21%)	9.45h (5.53%)	1.54h (2.21%)	3.5h (2.94%)	4.17h (3.26%)	1.54h (2.21%)
		1 L	3.5h (2.94%)	1.60h (2.29%)	9.85h (5.76%)	1.60h (2.29%)	3.5h (2.94%)	4.07h (3.18%)	1.60h (2.29%)
		2 S	3.5h (2.94%)	1.17h (1.68%)	4.93h (2.88%)	1.17h (1.68%)	3.5h (2.94%)	2.70h (2.11%)	1.17h (1.68%)
		2 L	3.5h (2.94%)	1.14h (1.64%)	5.10h (2.99%)	1.14h (1.64%)	3.5h (2.94%)	2.64h (2.06%)	1.14h (1.64%)
		3 S	3.5h (2.94%)	1.14h (1.63%)	4.67h (2.73%)	1.14h (1.63%)	3.5h (2.94%)	2.57h (2.01%)	1.14h (1.63%)
		3 L	3.5h (2.94%)	1.10h (1.58%)	5.73h (3.35%)	1.10h (1.58%)	3.5h (2.94%)	2.53h (1.97%)	1.10h (1.58%)
		4 S	3.5h (2.94%)	1.13h (1.62%)	4.19h (2.45%)	1.13h (1.62%)	3.5h (2.94%)	2.88h (2.25%)	1.13h (1.62%)
		4 L	3.5h (2.94%)	1.08h (1.55%)	8.17h (4.78%)	1.08h (1.55%)	3.5h (2.94%)	2.81h (2.20%)	1.08h (1.55%)
	Rear Wing	5 S	3.5h (2.94%)	1.06h (1.52%)	0.11h (0.06%)	1.06h (1.52%)	3.5h (2.94%)	1.93h (1.51%)	1.06h (1.52%)
		5 L	3.5h (2.94%)	1.04h (1.50%)	1.26h (0.74%)	1.04h (1.50%)	3.5h (2.94%)	1.97h (1.54%)	1.04h (1.50%)
		6 S	3.5h (2.94%)	1.88h (2.69%)	8.96h (5.24%)	1.88h (2.69%)	3.5h (2.94%)	8.18h (6.39%)	1.88h (2.69%)
		6 L	3.5h (2.94%)	1.60h (2.29%)	7.63h (4.46%)	1.60h (2.29%)	3.5h (2.94%)	8.46h (6.61%)	1.60h (2.29%)
		7 S	3.5h (2.94%)	1.15h (1.65%)	6.52h (3.81%)	1.15h (1.65%)	3.5h (2.94%)	2.11h (1.65%)	1.15h (1.65%)
		7 L	3.5h (2.94%)	1.13h (1.61%)	7.08h (4.14%)	1.13h (1.61%)	3.5h (2.94%)	2.19h (1.71%)	1.13h (1.61%)
	Vertical Tail	8 S	3.5h (1.47%)	1.21h (0.87%)	10.16h (2.97%)	1.21h (0.87%)	3.5h (1.47%)	2.03h (0.79%)	1.21h (0.87%)
		8 L	3.5h (1.47%)	1.15h (0.82%)	10.61h (3.10%)	1.15h (0.82%)	3.5h (1.47%)	1.87h (0.73%)	1.15h (0.82%)
		9 S	3.5h (1.47%)	1.25h (0.89%)	9.50h (2.78%)	1.25h (0.89%)	3.5h (1.47%)	2.38h (0.93%)	1.25h (0.89%)
		9 L	3.5h (1.47%)	1.19h (0.86%)	9.34h (2.73%)	1.19h (0.86%)	3.5h (1.47%)	2.29h (0.89%)	1.19h (0.86%)
10 S		3.5h (1.47%)	1.20h (0.86%)	6.97h (2.04%)	1.20h (0.86%)	3.5h (1.47%)	2.70h (1.06%)	1.20h (0.86%)	
10 L		3.5h (1.47%)	1.14h (0.82%)	7.43h (2.17%)	1.14h (0.82%)	3.5h (1.47%)	2.46h (0.96%)	1.14h (0.82%)	

Appendix B

Weights

In this appendix, weights of conventional aircraft and joined wing are determined and compared.

Through the areas and thicknesses of each part, obtained in Section 4.1, and knowing that the carbon fiber prepreg density used in the parts production is 300 g/m^2 (Table 4.8) and that the cured layer height is 0.2 mm (Table 4.8), it is possible to determine the weight of each part according to Equation 3.14.

In the following tables, the parts' weights that constitute the conventional aircraft (Table B.1) and the joined wing (Table B.2) are shown. The total weights of each wing or tail structures are also presented. Values are expressed in kilograms (kg). It should be noted that the total weights of the main wings, rear wing and horizontal tail already contemplate the left and right wings' weights.

Table B.1: Conventional aircraft parts' weight.

		Skins		Spars		Total Weight
		Upper	Lower	Front	Rear	
Main Wing	Section 1	286.23 kg	287.18 kg	49.25 kg	52.99 kg	1846.70 kg
	Section 2	83.77 kg	83.47 kg	14.48 kg	11.10 kg	
	Section 3	23.98 kg	23.86 kg	4.31 kg	2.73 kg	
Horizontal Tail	Section 1	17.85 kg	18.19 kg	3.54 kg	2.16 kg	219.63 kg
	Section 2	28.76 kg	29.30 kg	6.23 kg	3.79 kg	
Vertical Tail	Section 1	29.94 kg	29.94 kg	7.62 kg	5.35 kg	266.57 kg
	Section 2	59.85 kg	59.85 kg	7.77 kg	6.07 kg	
	Section 3	26.49 kg	26.49 kg	4.22 kg	3.00 kg	

Observing the tables and summing the respective total weights of each aircraft, it is concluded that the joined wing is heavier than the conventional aircraft. The conventional aircraft has a total weight of 2333 kg and the joined wing has a total weight of 3114 kg , approximately.

It is also verified that although the joined wing has a lighter main wing, adapting a rear wing instead of a horizontal tail in this type of aircraft has consequences on its total weight. In the presented tables, it is observed that the main and rear wings set of the joined wing is heavier than the main wing and horizontal tail set of the conventional aircraft. This difference in weight is explained by the fact that the rear wing is larger and has a more reinforced structure when compared to the horizontal tail. This

Table B.2: Joined wing parts' weight.

		Skins		Spars		Total Weight
		Upper	Lower	Front	Rear	
Main Wing	Section 1	132.11 kg	132.54 kg	123.49 kg	136.59 kg	1378.72 kg
	Section 2	19.96 kg	19.89 kg	20.63 kg	17.19 kg	
	Section 3	13.46 kg	13.40 kg	13.80 kg	10.35 kg	
	Section 4	9.59 kg	9.55 kg	10.18 kg	6.62 kg	
Rear Wing	Section 1	1.18 kg	1.18 kg	3.86 kg	3.02 kg	997.26 kg
	Section 2	75.51 kg	75.33 kg	143.06 kg	98.14 kg	
	Section 3	23.53 kg	23.50 kg	27.69 kg	22.61 kg	
Vertical Tail	Section 1	50.89 kg	50.89 kg	71.61 kg	50.25 kg	737.75 kg
	Section 2	106.40 kg	106.40 kg	75.91 kg	59.28 kg	
	Section 3	48.56 kg	48.56 kg	40.34 kg	28.64 kg	

structural reinforcement avoids the possible buckling effects that can occur on the rear wing.

However, the main difference in weight is observed in the vertical tails of both aircraft, approximately 470 kg. The reason why the joined wing has a stronger vertical tail, when compared to the one of conventional aircraft, is due to the fact that it has to support the rear wing weight.